

KAUNAS UNIVERSITY OF TECHNOLOGY

VYTAUTAS ABROMAITIS

**METOPROLOL ADSORPTION,
DESORPTION AND BIODEGRADATION
DYNAMICS IN BIOLOGICAL ACTIVATED
CARBON SYSTEMS**

Doctoral Thesis
Technological Sciences, Chemical engineering (05T)

2018, Kaunas

This doctoral dissertation was prepared at Kaunas University of Technology, Faculty of Chemical technology, Department of Environmental technologies during the period of 2011–2017. The studies were supported by Wetsus, European Centre of Excellence for Sustainable Water Technology (Leeuwarden, the Netherlands).

Scientific Supervisor:

Assoc. Prof. Dr. Viktoras RAČYS (Kaunas University of Technology, Technological Sciences, Chemical engineering, 05T).

Scientific Advisor:

Assoc. Prof. Dr. Roel MEULEPAS („Wetsus“, European Centre of Excellence for Sustainable Water Technology, Technological Sciences, Environmental engineering, 04T).

Doctoral dissertation has been published in:

<http://ktu.edu>

Editor:

Armandas Rumšas (Publishing House “Technologija”)

© V. Abromaitis, 2018

ISBN 978-609-02-1409-1

The bibliographic information about the publication is available in the National Bibliographic Data Bank (NBDB) of the Martynas Mažvydas National Library of Lithuania

KAUNO TECHNOLOGIJOS UNIVERSITETAS

VYTAUTAS ABROMAITIS

METOPROLOLIO ADSORBCIJOS,
DESORBCIJOS IR BIODEGRADACIJOS
DINAMIKA BIOLOGIŠKAI AKTYVIŲ ANGLIŲ
SISTEMOSE

Daktaro disertacija
Technologijos mokslai, Chemijos inžinerija (05T)

2018, Kaunas

Disertacija rengta 2011–2017 metais Kauno technologijos universiteto Cheminės technologijos fakulteto Aplinkosaugos technologijos katedroje. Mokslinius tyrimus rėmė Europos darnių vandens technologijų kompetencijos centras „Wetsus“ (*European Centre of Excellence for Sustainable Water Technology*, Nyderlandai, Leuwardenas).

Mokslinis vadovas:

Doc. dr. Viktoras RAČYS (Kauno technologijos universitetas, technologijos mokslai, Chemijos inžinerija, 05T).

Mokslinis konsultantas:

Doc. dr. Roel MEULEPAS („Wetsus“, Europos darnių vandens technologijų kompetencijos centras, technologijos mokslai, aplinkos inžinerija, 04T).

Interneto svetainės, kurioje skelbiama disertacija, adresas:

<http://ktu.edu>

Redagavo:

Armandas Rumšas (leidykla „Technologija“)

© V. Abromaitis, 2018

ISBN 978-609-02-1409-1

Leidinio bibliografinė informacija pateikiama Lietuvos nacionalinės Martyno Mažvydo bibliotekos Nacionalinės bibliografijos duomenų banke (NBDB)

Acknowledgements

All the former PhD students know very well how hard it is to go through all this. Without any extra help and without nice and smart people around, it would have been impossible to finish the doctoral thesis; therefore, I would like to thank all the people who directly and indirectly helped me in this process.

First of all, I would like to thank Johannes Boonstra and Cees Buisman for the opportunity to become a part of *Wetsus*. The professional help, the well-equipped labs and the friendly people are the key strength of *Wetsus*! It was awesome to work there.

I would also like to express my gratitude to my Lithuanian PhD supervisor Viktoras Račys, for the fruitful discussions and systematic support during this hard period. I know that it was hard not only for me, but we have finally made it.

My special and biggest THANK YOU goes to Roel Meulepas, the best supervisor and the greatest ideas brain-minator. I know that I was not the easiest-going guy, but your optimism and enormously huge support helped me to take one of the most important steps in my life. Once again, thank you for all your help and brilliant ideas that turned the impossible into possible.

How about the *Wetsus* technical and analytical team? Thank you, Ton, for the intelligent discussions and the super-fast analyses. The same goes for the two nice ladies, Mieke and Marianne, and huge Zanger Rinus fan Jelmer. Harm, thank you for the kind heart, and for being on the spot every time I needed it. It was very pleasant to work with you. Grumpy Friesian Jan, thanks for the nice conversations and for the lavish sense of humour.

My beloved office mates Martijn W., Taina, Lena, Rik, Jaap, Ricardo and Pom, thank you for the nice chatting and support, it was phenomenal to stay in the office together with you.

I met a lot of people at *Wetsus* and became friends with some of them, too. Once again, thank you Jaap and Rik for your Dutch lessons and 'super' intelligent jokes. Pom, you were the best house mate. Thanks for the tasty Thai food you were warming up for me and the beer evenings. I will probably never meet such a cool Thai girl like you. Paweł, it was nice to meet a real soul buddy like you – Żubrola evenings and jokes that only we can understand made the way through the PhD far easier to go! Judita, thank you for the tasty *kugelis* and the crazy trips to Lithuania together. Dries, you were the perfect punching bag during kick-boxing workouts. Also thanks for bringing the best Belgian beers in the world. Gintaras, I highly appreciate your support, the *Youtube* videos you were sending me all the time and the great sense of humour making the dark days brighter.

I would also like to thank the entire group from the department of Environmental Technologies, Lithuania, and especially Dainius Martuzevičius, for the consultations and for pushing me daily to go further with my thesis.

Finally, I would like to sincerely thank my family for helping me to go through and for tolerating my behaviour. My wife dr. Lina, thank you for understanding and supporting me throughout all those situations, especially those when sometimes I was losing hope. You are the best that has ever happened in my life!

Table of Contents

List of tables	8
List of figures	9
Abbreviations	11
Introduction	12
1. Literature review.....	15
1.1. Biological activated carbon (BAC)	15
1.2. Underlying principles	15
1.3. Adsorption	16
1.3.1. Adsorbent types used for water treatment	17
1.3.2. Physisorption and chemisorption.....	17
1.3.3. Transport mechanisms.....	18
1.3.4. Single and multi-solute adsorption	20
1.4. Biodegradation of organic matter	20
1.5. AC bioregeneration.....	23
1.5.1. Mechanisms	23
1.5.2. Factors affecting bioregeneration	25
1.6. Operation phases of BAC reactor.....	29
1.7. Application of BAC.....	30
1.8. Summary of the literature review	33
2. Materials and methods.....	35
2.1. General materials and methods.....	37
2.1.1. Chemicals and biomass suspension	37
2.1.2. Analytical tools and methods	38
2.2. Materials and methods to investigate the interdependence between metoprolol biodegradation and adsorption-desorption hysteresis in presence of acetate	42
2.3. Materials and methods to investigate the effect of shear stress and carbon surface roughness on bioregeneration and performance of suspended versus attached biomass in metoprolol-loaded biological activated carbon systems.....	44
2.4. Materials and methods to investigate the correlation between activated carbon characteristics and adsorption-desorption hysteresis and the implications for the performance of BAC systems.....	49
3. Results and discussion	53
3.1. Interdependence between metoprolol biodegradation and adsorption-desorption hysteresis in presence of acetate	54
3.1.1. Metoprolol and acetate bisolute adsorption isotherm experiments	55
3.1.2. Metoprolol desorption isotherm experiments.....	56
3.1.3. Metoprolol adsorption-desorption hysteresis in the relation between adsorption capacity q_e and equilibrium concentration C_e	57
3.1.4. Metoprolol and acetate bisolute biodegradation experiments	58
3.1.5. Full-scale BAC filter at Nieuw Amsterdam	60
3.1.6. Summary of chapter interdependence between metoprolol biodegradation and adsorption-desorption hysteresis in presence of acetate.....	60
3.2. Effect of shear stress and carbon surface roughness on bioregeneration and performance of suspended versus attached biomass in metoprolol-loaded BAC.....	62

3.2.1. Metoprolol removal in blank and BAC reactors over time	63
3.2.2. Metoprolol peak loading experiment with blank and BAC reactors	65
3.2.3. Surface and porosity measurements of AC granules sampled from the blank and BAC reactors	67
3.2.4. Metoprolol adsorption isotherms of the AC granules sampled from the blank and BAC reactors	68
3.2.5. Morphology and concentration of the suspended biomass and biomass attached to the AC granules sampled from BAC reactors	69
3.2.6. Metoprolol biodegradation with suspended biomass sampled from BAC reactors	71
3.2.7. Phylogenetic composition of the suspended biomass and the biofilm on the AC granules sampled from three BAC reactors	72
3.2.8. Bioregeneration of metoprolol loaded carbons in BAC reactors.....	74
3.2.9. Effect of applied shear stress and carbon surface smoothness for metoprolol removal and bioregeneration of loaded carbons in BAC reactors.....	75
3.2.10. Summary of chapter effect of shear stress and carbon surface roughness on bioregeneration and performance of suspended versus attached biomass in metoprolol-loaded biological activated carbon systems.....	76
3.3. The correlation between activated carbon characteristics and adsorption-desorption hysteresis and the implications for the performance of BAC systems ...	77
3.3.1. Physical properties of AC granules used for adsorption-desorption experiments.....	78
3.3.2. Metoprolol adsorption capacity	78
3.3.3. Kinetics of metoprolol adsorption and desorption.....	80
3.3.4. Metoprolol adsorption-desorption hysteresis	85
3.3.5. Adsorbent selection for BAC reactor	88
3.3.6. Summary of chapter the correlation between activated carbon characteristics and adsorption-desorption hysteresis and the implications for the performance of BAC systems	90
4. General discussion and recommendations.....	91
4.1. Interdependence between metoprolol biodegradation and adsorption-desorption hysteresis in presence of acetate	91
4.2. Effect of shear stress and carbon surface roughness on bioregeneration and performance of suspended versus attached biomass in metoprolol loaded biological activated carbon systems	91
4.3. The correlation between activated carbon characteristics and adsorption-desorption hysteresis and the implications for the performance of BAC systems ...	92
4.4. BAC reactor design for the removal of slowly biodegradable pharmaceuticals from water	93
5. Conclusions	96
References	98
Publications	104
Appendices	107

List of Tables

Table 1.1. The main differences between the chemisorption and physisorption	18
Table 2.1. Properties of model organic compounds used for the experiments	37
Table 2.2. Langmuir and Freundlich adsorption models	40
Table 2.3. Physical characteristics of the virgin Mast and Norit ACs	45
Table 2.4. List of Mast carbon granules used for experiments	50
Table 2.5. List of Norit AC granules used for metoprolol adsorption and desorption experiments.....	50
Table 2.6. Pseudo first and pseudo second order kinetic models.....	52
Table 3.1. Freundlich constants for metoprolol adsorption on virgin Norit GAC, in presence of different concentrations of acetate, and for acetate adsorption on virgin Norit GAC, in presence of different concentrations of metoprolol	55
Table 3.2. Freundlich constants for metoprolol desorption from pre-loaded Norit GAC.....	56
Table 3.3. Effect of the initial metoprolol and acetate concentration on the acetate biodegradation rate	58
Table 3.4. Effect of the initial metoprolol and acetate concentration on the metoprolol biodegradation rate.....	59
Table 3.5. Physical characteristics of the virgin AC granules from Mast and Norit and the AC granules, sampled at the end of the reactor experiments	67
Table 3.6. Langmuir adsorption isotherms constants obtained with the virgin AC granules from Mast and Norit and the AC granules, sampled at the end of the reactor experiments.....	68

List of Figures

Figure 1.1. BAC working principle, including the change in substrate concentration from the bulk liquid to the AC surface	16
Figure 1.2. External and internal mass transport in liquid-solid (AC) system	19
Figure 1.3. Concentration profiles over BAC particle	24
Figure 1.4. 2-Chlorophenol desorption from four different 2-chlorophenol loaded activated carbons	26
Figure 1.5. The change in biofilm thickness from 15 to 300 μm in a reactor.....	29
Figure 1.6. Normalized pressure drop over the RO module with and without BAC	32
Figure 2.1. General and specific materials and methods used in this doctoral thesis	36
Figure 2.2. Chemical structure of metoprolol tartrate and sodium acetate.....	37
Figure 2.3. Metoprolol adsorption over time with 0.4 g/L Norit GAC	42
Figure 2.4. Metoprolol desorption over time from 0.4g/L loaded Norit GAC	43
Figure 2.5. Scanning electron microscopy images of virgin Mast and Norit AC granules	45
Figure 2.6. Scheme of metoprolol loaded BAC reactors.....	46
Figure 2.7. Optical profilometry images for the assessment of the surface roughness of virgin Mast AC and virgin Norit GAC 830 Plus AC granules.....	46
Figure 3.1. Metoprolol adsorption to virgin Norit GAC as a function of metoprolol concentration after reaching equilibrium for different acetate concentrations	56
Figure 3.2. Freundlich adsorption isotherms of metoprolol, obtained after adsorption and desorption on/from Norit GAC.....	57
Figure 3.3. Metoprolol and acetate removal over time in 3 incubations	59
Figure 3.4. The cumulative metoprolol load and the cumulative metoprolol wash-out from blank and BAC reactors, operated at different shear stress and filled with AC granules having different surface roughness	63
Figure 3.5. The cumulative acetate load and the cumulative acetate washout from the blank and BAC reactors, operated at different shear stress and filled with AC granules having different surface roughness	64
Figure 3.6. The concentration of suspended biomass over time, expressed as total nitrogen, in the BAC reactors	65
Figure 3.7. The metoprolol removal over time after spiking with 93 mg/L metoprolol in blank and BAC reactors, operated at different shear stress and filled with AC granules having different surface roughness	66
Figure 3.8. Estimation of the adsorption and biodegradation rates from the metoprolol removal over time, after a peak load of 93 mg/L.....	66
Figure 3.9. Relationship of adsorption capacity versus surface area and pore volume of virgin ACs and metoprolol loaded ACs from the reactors	69
Figure 3.10. Scanning electron microscopy images of the BAC granules sampled at the end of the reactor experiments.....	70
Figure 3.11. Optical microscopy images of the BAC granules, sampled at the end of the reactor experiments, from the BAC reactors	70

Figure 3.12. Metoprolol biodegradation by the suspended biomass sampled from the BAC reactors	71
Figure 3.13. Changes in suspended biomass concentration, expressed as total nitrogen, and metoprolol removal efficiency over time in the BAC reactors.....	72
Figure 3.14. The relative abundance of specific phylogenetic groups in the biomass suspension used for inoculation, the suspension from the BAC reactors and biofilm on the surface of the AC granules	73
Figure 3.15. Photos of the biomass suspension used to inoculate three lab-scale BAC reactors and the biomass suspension obtained from R2 BAC reactor at the end of the reactor runs	74
Figure 3.16. Micropore and mesopore volumes, obtained after the physical analysis of Mast and Norit AC granules.....	78
Figure 3.17. Metoprolol adsorption capacities Q_m , obtained from adsorption equilibrium experiments with Mast and Norit AC granules.....	79
Figure 3.18. Relationship between metoprolol adsorption capacities Q_m and micropore volumes, obtained from adsorption equilibrium experiments with Mast and Norit AC granules.....	80
Figure 3.19. Adsorption rates, obtained from metoprolol adsorption kinetic experiments with Mast and Norit AC granules	81
Figure 3.20. Diffusion rates, obtained from metoprolol adsorption kinetic experiments with Mast and Norit AC granules	83
Figure 3.21. Graphical representation of possible mechanisms for metoprolol adsorption onto AC.....	84
Figure 3.22. Desorption rates, obtained from single cycle desorption experiments with metoprolol loaded Mast and Norit AC granules.....	85
Figure 3.23. Metoprolol adsorption and desorption isotherms of spherical Mast AC granules S0.25+, calculated based on natural logarithm model, at 93 mg/L equilibrium concentration.....	86
Figure 3.24. Adsorption-desorption hysteresis indexes, calculated at 93 mg/L metoprolol equilibrium concentration, for Mast and Norit AC granules	87
Figure 3.25. Difference in metoprolol sorption capacities after adsorption and desorption, calculated at equilibrium concentration of 93 mg/L, for Mast and Norit AC granules.....	88
Figure 3.26. Regeneration values of metoprolol loaded Mast and Norit AC granules	89
Figure 4.1. Single cycle sequential batch reactor operation stages.....	94
Figure 4.2. The proposed BAC reactor design, to treat wastewater polluted with slowly biodegradable pharmaceuticals.....	95

Abbreviations

AC – activated carbon

BAC – biological activated carbon

BOD – biochemical oxygen demand

COD – chemical oxygen demand

GAC – granular activated carbon

HI – hysteresis index

PAC – powdered activated carbon

PBS – phosphate buffered saline

SEM – scanning electron microscopy

Introduction

BAC technology has been used for drinking water production and wastewater treatment for over 40 years (Matovic 2013). However, the present guidelines and manuals on the operation of AC systems hardly ever consider, or, actually, do not consider at all, the active biomass in such systems, most likely because the net effect of the physicochemical adsorption and the biological degradation is difficult to predict (Ö. Aktaş and Çeçen 2007b). Therefore, the biodegradation and adsorption-desorption processes have to be evaluated properly, especially for BAC systems used to remove slowly biodegradable organics, e.g. pharmaceuticals and pesticides (Rattier et al. 2012).

A crucial step in the engineering of BAC systems is the selection of the adsorbent. Physical characteristics of the adsorbent, like granular size, porosity, surface active groups etc., will not only affect the adsorption of pollutants itself, but may indirectly also affect the bioregeneration of AC. The evaluation of adsorption-desorption hysteresis for different ACs can provide additional information about the bioregeneration possibilities; ACs showing a high level of adsorption-desorption hysteresis are more favourable for bioregeneration. Unfortunately, few BAC studies considering both the adsorption and desorption isotherms (Berhane et al. 2016).

Next to the adsorption and desorption processes, the biodegradation of slowly biodegradable organic compounds provides information about the ability of microbial biomass to regenerate AC. Another consideration is that, i.e. though co-metabolism, easy biodegradable compounds present in a system might be able to enhance the biodegradation process (Hess, Silverstein, and Schmidt 1993). In order to accurately quantify the different processes, experiments need to be done in a well-defined matrix with a limited amount of components, model compounds can be chosen to represent different types of constituents in real water treated in BAC systems.

The advantage of biofilm formation on the AC surface for BAC performance is often overestimated (Ö. Aktaş and Çeçen 2007b). The importance of suspended biomass in the bulk liquid is not properly addressed since it plays a significant role in the biodegradation process of slowly biodegradable organic compounds (Xiaojian, Zhansheng, and Xiasheng 1991). Moreover, the effect of carbon surface roughness and shear stress for biofilm formation and overall BAC reactor performance and AC bioregeneration have not been investigated in previous studies.

In this doctoral thesis the statements listed above were investigated and discussed. The pharmaceutical metoprolol was selected as the representative of slowly biodegradable organic compounds, whereas acetate was used as model compound for easy biodegradable organics. First separate adsorption-desorption and biodegradation experiments were performed; the results were subsequently used to design and run lab-scale BAC reactors, where shear stress and carbon surface roughness was varied. In addition to this, the phylogenetic composition of microbial biomass on the surface of AC and in suspension was assessed, and used to evaluate the adaptation of the biomass towards the conditions being applied.

Aim of the Doctoral Thesis

To investigate adsorption, desorption and biodegradation of slowly biodegradable organics in biological activated carbon systems, including how these processes are affected by each other, the presence of easily-degradable organics, the physical characteristics of the activated carbon, and the design and operation of the biological activated carbon system.

Objectives

1. To investigate if it is possible for microbial biomass to overcome the adsorption–desorption hysteresis in biological activated carbon systems and bioregenerate activated carbon, loaded with a slowly biodegradable organic, and if this is promoted by easy biodegradable organics.
2. To investigate how the design and operation of biological activated carbon systems affect biofilm formation and activated carbon bioregeneration, when biological activated carbon is loaded with acetate and metoprolol.
3. To investigate how the physical characteristics of different types of activated carbons affect adsorption–desorption hysteresis and the performance of biological activated carbon systems.

Scientific novelty

1. The effect of acetate (0–1000 mg/L) on adsorption and biodegradation of metoprolol (0–256 mg/L), and vice versa, was investigated, and the ability of microbial biomass to overcome the adsorption-desorption hysteresis was explained and proven.
2. The effect of activated carbon surface roughness ($R_a=1.6$ and $R_a=13$ μm) and different shear stress ($G=8.8$ s^{-1} and $G=25$ s^{-1}) on biofilm formation, metoprolol removal, and carbon bioregeneration was determined for biological activated carbon reactors loaded with metoprolol (10 mg/L) and acetate (100 mg/L) synthetic water mixture.
3. The relationships between activated carbon characteristics (granular size, porosity), metoprolol adsorption-desorption capacities, kinetics and adsorption-desorption hysteresis indexes were investigated, and explanations were given how these characteristics affect the bioregeneration of metoprolol loaded adsorbents and the selection of activated carbon for the biological activated carbon reactor.

Structure

This doctoral thesis consists of the following chapters: acknowledgements, an introduction, literature review, materials and methods, results and discussion, conclusions, general discussion and recommendations, acknowledgements, a reference list, a publication list and appendices. The thesis comprises 114 pages, 41 figure, 13 tables and 18 appendices.

Publications

Two articles, based on the doctoral research presented in this thesis, have been published in international journals registered in the Web of Science database. In addition, experimental results were presented at 6 conferences.

Practical Significance

This work was performed in cooperation with *Wetsus, European Centre of Excellence for Sustainable Water Technology* and partners from the company *Puurwaterfabriek* (Nieuw-Amsterdam, The Netherlands) which uses BAC filters to produce ultrapure water from WWTP effluent. This doctoral research covers the investigation and explanation of adsorption, desorption and biodegradation processes in a BAC system and how these processes affect each other. In addition, the research investigates how the presence of easily biodegradable organic matter, typically present in the influent, affects the removal of a more slowly degradable micro-pollutant. Moreover, the effect of AC characteristics on adsorption–desorption hysteresis and overall AC bioregeneration was investigated. Furthermore, lab–scale BAC reactor experiments were performed to investigate the effect of specific technological factors such as AC surface roughness and shear stress on biofilm formation, bioregeneration and overall BAC performance. The obtained results and observations will help to better understand the underlying processes in full-scale BAC systems and to predict and control full-scale BAC systems more effectively.

Author's Contribution

The results presented and discussed in this doctoral thesis are originally collected and analysed by the author. The published articles were prepared by the author under professional guidance of supervisors from *Wetsus* and Kaunas University of Technology. The author accepts full responsibility for the reliability of the experimental data.

1. Literature Review

1.1. Biological Activated Carbon (BAC)

The use of charcoal for water filtration was already applied as early as in 450 BC by Hindu (Inglezakis and Pouloupoulos 2006). The use of coal for water filtration was also reported in a Sanskrit text from around 200 AD (Ö. Aktaş and Çeçen 2007b). However, the use of charcoal as an absorbent in industry only began in the 18th century, when it was mainly used for sugar refining. The refining process was still relatively inefficient given the limited porosity of charcoal. A breakthrough was the first industrial use of activated charcoal powder at the beginning of the 20th century. In 1901, Swedish chemist Ostreijko patented two carbon activation methods, one of them chemical, by using metal chlorides, and the other one, thermal, by using steam (Sontheimer, Crittenden, and Summers 1988).

As it can be seen from the facts outlined above, AC was already used for water purification more than 100 years ago. However, the advantages of using microbial biomass for increasing the lifetime of AC in the reactor was first described only in 1967 (Matovic 2013). The process itself was named as BAC. Nowadays, BAC technology is being applied for drinking water purification and wastewater treatment (Bonné, Hofman, and van der Hoek 2002; Van Der Maas, Majoor, and Schippers 2009). However, the application is still undeservedly poor because of lack of information on how to control the technology itself.

The attractiveness of BAC technology for AC filtration and activated sludge installations was mentioned in many researches. The self-maintained bioregeneration (Rattier et al. 2012) and ability to cope with shock loads (Cha, Choi, and Ha 1998) are the advantages of BAC over more conventional technologies. Moreover, AC serves as a carrier material for the biomass (Lai, Zhou, and Yang 2013) and can reduce the toxicity of a substrate for the microorganisms (Ehrhardt and Rehm 1985). The working principle of BAC, its application for water and wastewater treatment, and the factors affecting bioregeneration and performance are summarised in the following paragraphs.

1.2. Underlying Principles

The most frequently used theories characterise BAC technology as a combination of adsorption, desorption and biodegradation. Because of the synergy established between these three parallelly running processes, the lifetime of an AC load in a reactor can be prolonged from several years to decades (Rattier et al. 2012). The process of spontaneous carbon regeneration influenced by microbial biofilm or the active suspended biomass which is present in the system is the so-called *bioregeneration*. First of all, from the bulk phase, the molecules of dissolved organic compounds pass through the boundary layer and diffuse to the biofilm. Part of the organics is biodegraded directly in the biofilm, while the remainder diffuses to the pores of AC (Figure 1.1). When the equilibrium concentration of the organic compounds in the bulk liquid or the concentration at the interphase between the carbon surface and the biofilm decreases, this promotes the desorption process from the AC pores. Therefore, the adsorbate diffuses back to the bulk liquid and is then

being biodegraded either in the biofilm or in the biomass suspension (Matovic 2013; Rattier et al. 2012; Shen, Lu, and Liu 2012). The performance of the BAC system is strongly related to the diffusion processes in/out of the pores and the biofilm (John C. Crittenden et al. 2012). Another, less investigated bioregeneration hypothesis comprises the enzymatic theory supporting the statement that enzymes secreted during the microbial activity might diffuse into the pores of AC and enhance the degradation of the adsorbed molecules (Rattier et al. 2012).

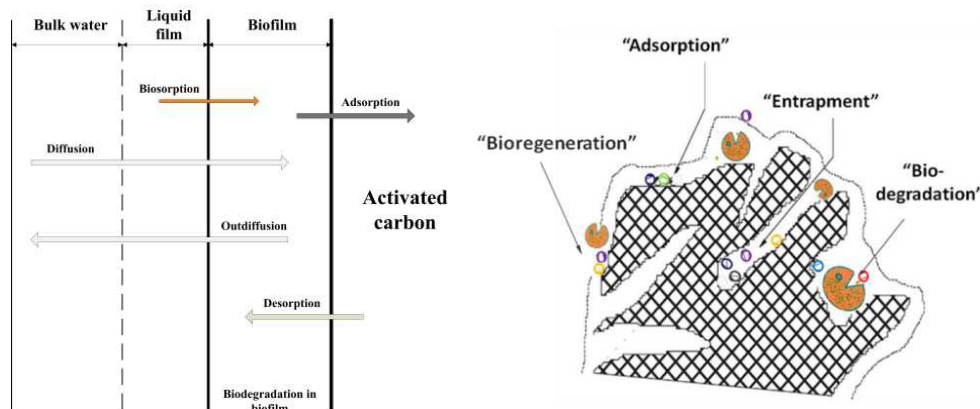


Figure 1.1. BAC working principle including the change in the substrate concentration from the bulk liquid to the AC surface (Rattier et al. 2012)

The performance and bioregeneration of BAC is strictly dependent on various technological and physical factors. The most important ones are the characteristics of AC resulting in adsorption-desorption hysteresis which has to be evaluated properly when designing a BAC reactor (Wu, Tseng, and Juang 2005). This typically includes the investigation of carbon adsorption/desorption equilibrium capacities and adsorption/desorption kinetics (Ying 2015). Moreover, the biodegradation kinetics and the pathway have also to be monitored so that to predict the biological removal of the target compounds and to ensure BAC reactor bioregeneration (Oh et al. 2012). The factors which tend to influence the adsorption and biodegradation are described in detail in the following chapters.

1.3. Adsorption

The importance of the adsorption processes is, however, not only limited to the physico-chemistry. Adsorption is very important in various physical, chemical and vital biological processes occurring in nature. In industry, adsorption is often being employed for purification purposes or used to remove the residuals whenever other technologies fail (John C. Crittenden et al. 2012; Worch 2012).

The excellent ability of granular and powdered AC to retain pollutants is widely used in drinking water purification and wastewater treatment processes. Here, adsorption is involved between two phases – the liquid phase and the solid phase (the AC surface). Before being adsorbed, solute molecules have to pass a hypothetical interfacial layer between the bulk liquid and the carbon surface. Later, internal diffusion controls the adsorption process. In general, ‘adsorption’ means a

process when molecules accumulate in the interfacial layer, while ‘desorption’ means the reverse action (Worch 2012).

1.3.1. Adsorbent Types Used for Water Treatment

Powdered AC

The preparation of PAC is slightly different from the GAC manufacturing process. PAC is usually made from wood by heating it in oxygen free environment, and, finally, by crushing or grounding the obtained carbon particles till they pass through the 0.297 mm sieve (Sontheimer, Crittenden, and Summers 1988). The average particle size of the produced PAC varies from 15 to 25 μm . PAC can be used in wastewater treatment or in pre-treatment of potable water. Unfortunately, GAC is more favourable for technological processes since the regeneration or separation of PAC is rather complicated. However, PAC can be added to activated sludge or contacted with wastewater in a separate tank.

Granular AC

Granular AC (GAC) is most commonly made from coal and coconut shells followed by thermal activation. GAC can also be prepared as pellets from pulverised powder by using binders. The granular size of GAC manufactured for industrial applications varies from 0.2 to 5 mm. In comparison with PAC, the intraparticle diffusion inside a GAC particle might become unfavourable because of the bigger AC particles. Generally, GAC is used in AC filter beds to purify drinking water, groundwater or wastewater, and to remove toxic compounds. AC granules are also more favourable in BAC bioreactors because they can also serve as a carrier for microorganisms to attach. Therefore, the combination of adsorption, desorption and biodegradation processes might be more beneficial over AC filter beds or activated sludge reactors (Inglezakis and Pouloupoulos 2006; Sontheimer, Crittenden, and Summers 1988; Suzuki 1990; Thomas and Crittenden 1998).

1.3.2. Physisorption and Chemisorption

According to the scholarly literature and practice, there are several forces inducing adsorption of molecules on the AC surface. The first driving force can be related with the hydrophobicity of a solute. Therefore, less soluble and more hydrophobic compounds adsorb better than hydrophilic and more soluble in water organic molecules. Another adsorption driving force is the electrical attraction between the AC surface and the solute, the so-called *van der Waals interaction*. This is a result of the high affinity of the solute to the adsorbent (Crittenden et al. 2012; Suzuki 1990).

The adsorption where intermolecular attractions between energy favourable sites occur is called *physisorption*. However, the exchange of the electrons does not take place during this type of interaction, and the adsorbate is attached to the surface of the adsorbent only by weak van der Waals forces. In addition, the adsorbate multilayers can be formed during adsorption, and the adsorbed molecules can travel freely through the interface. Therefore, this process is reversible, and the adsorbed

molecules can be released back to the bulk liquid phase (Thomas and Crittenden 1998; Worch 2012).

A completely different origin and its mechanism can be attributed to *chemisorption*. This typically involves an exchange of electrons between the solute molecules and the specific sites on the adsorbent's surface. As a consequence, a strong chemical bond is formed. Chemisorption is a very strong type of interaction, thus the adsorbate molecules are not free to move over the interface, and hence desorption is not possible. Chemical adsorption is dominant at high temperatures because, at high temperatures, chemical reactions are faster. In general, a single molecular layer can be adsorbed on the surface since chemical bonds can be formed only with specific active centers (Worch 2012). The comparison of physical and chemical adsorptions can be found in Table 1.1 below.

Table 1.1. Main differences between chemisorption and physisorption (Worch 2012)

	Physisorption	Chemisorption
Surface coverage	Mono, multilayer	Monolayer
Kinetics of adsorption	Very fast	Often slow
Desorption	Easy, induced by reduced pressure or increased temperature	Difficult; high temperature is required to break chemical bonds
Structure of desorbed compounds	Unchanged	Adsorbate structure might be different
Specificity for adsorption sites	Nonspecific	Requires specific sites on the surface
Temperature dependency	Adsorption decreases with the increased temperature	Adsorption increases with the increased temperature
Adsorption enthalpy, kJ/mol	5–40	40–800

Usually it is very difficult to distinguish between physisorption and chemisorption because these two types of adsorption run together (Worch 2012). Physisorption is more favourable for bioregeneration to occur. A possible explanation for this is the adsorption reversibility which occurs because of the concentration gradient. This remains possible in BAC installations because the active microbial biomass in the suspension can reduce equilibrium concentrations of target organic compounds in the liquid phase and thus enhance desorption (Korotta-Gamage and Sathasivan 2017; Ying 2015).

1.3.3. Transport Mechanisms

During the adsorption process, in all the cases, the equilibrium will be established between the adsorbed molecules and the molecules left in the bulk liquid. The rate needed to reach the equilibrium conditions is often described as *adsorption kinetics*. The time needed to reach the adsorption equilibrium is related with mass transport limitations and depends on the adsorbate and the adsorbent (John C. Crittenden et al. 2012; Thomas and Crittenden 1998). The transport of

molecules in a liquid-solid system is caused by external and internal transport, as shown in Figure 1.2 below.

When the liquid-solid system (liquid-carbon) is generated, the transport of solute molecules typically starts from the bulk liquid to the boundary layer of the water surrounding AC particles. This type of transport is called *advection* or *bulk solute transport*. The second stage, when solute molecules diffuse through the liquid film (the hydrodynamic boundary layer) surrounding carbon particles to the surface is called *external diffusion* (Worch 2008). In general, the driving force of molecular diffusion through this layer is the concentration gradient. Intraparticle diffusion or internal diffusion is the last stage when solute molecules from the carbon surface migrate to the pores of the particle. Intraparticle diffusion is strictly dependent on the carbon pore size and structure (Liu et al. 2015; Wu, Tseng, and Juang 2005).

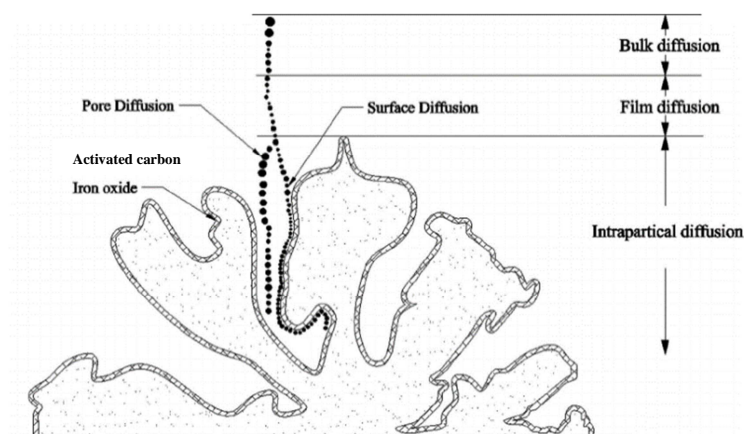


Figure 1.2. External and internal mass transport in a liquid-solid (AC) system (Yan et al. 2013)

Internal diffusion can cover two different mechanisms involving the solute molecules inside the carbon particle. Diffusion can occur in the pores which are filled with fluid, or the solute molecules can ‘travel’ through the internal surface of the adsorbent. Surface diffusion will occur only if the surface attractive forces are not sufficiently strong to interact and reduce the mobility of molecules (John C. Crittenden et al. 2012). In addition, the diffusion in the macropores is often related to the pore diffusion mechanism whereas surface diffusion is more relevant in the micropores since they are narrower, and molecules travel there mainly through the surface (Worch 2008). In order to design a fully functioning AC reactor, it is relevant to investigate adsorption kinetics. Usually, the diffusion of solute molecules to the pores of AC is identified as the rate limiting step (Ahmad, Ahmad Puad, and Bello 2014; Rahim and Garba 2016). On the other hand, physisorption is described as a relatively rapid process when an adsorption bond forms faster in comparison with diffusion. However, in the case of chemisorption, more time is required to form a chemical bond; therefore, this type of adsorption can increase the time which is necessary to remove the dissolved organic compounds from the liquid and to become the rate limiting step (Bhatnagar, Goyal, et al. 2013).

1.3.4. Single and Multi-Solute Adsorption

In general, almost all the adsorption models are based on a single solute adsorption theory which covers the idea that a solution is diluted and no interactions take place between the molecules of the dissolved compound and the solvent. The most frequently used adsorption models are *Freundlich* and *Langmuir* models (Marković et al. 2014). These two models are described in detail in Subchapter 2.1.2 in the *materials and methods* section since they were used to fit the experimental data in this doctoral thesis. However, if a multi-solute system has to be investigated, the description becomes more complicated. There is no standard model that is able to describe and predict the adsorption of multiple compounds in the liquid-solid system. The results of the adsorption experiment depend on a high number of factors, e.g., the physico-chemical characteristics of the solutes and the solvent, the concentration, and the type of AC. Typically, a bisolute system can be characterised by using a simplified version of the *Ideal Adsorbed Solution Theory*, the same as described elsewhere, where 4-methylphenol and nitrobenzene adsorption on AC has been predicted (H. Zhang and Wang 2017). However, this falls into difficulties when more compounds are dissolved in the liquid, and the water-substrate matrix becomes more complex (Al-Ghouti et al. 2016).

The application of AC for the purification of industrial water and wastewater treatment processes is one of the most widely used processes (Bhatnagar, Hogland, et al. 2013). Thus it is very important to investigate multi-solute systems, especially in BAC installations, because adsorption there is combined together with biodegradation. This becomes crucial if the bioregeneration of the BAC reactor has to be evaluated. It is known that the affinity of organic compounds for AC plays a significant role, and more affine compounds will be irreversibly adsorbed. Therefore, less absorbable compounds will be bioavailable for suspended or microbial biomass attached to the surface of AC (Jung et al. 2013; Sotelo et al. 2014).

1.4. Biodegradation of Organic Matter

As it can be seen from the scholarly literature review regarding the application of the BAC technology for potable water or wastewater treatment, adsorption and desorption processes play a significant role there. However, the biodegradation of a complex organic matter needs special attention, too, because effective bioregeneration of AC is strictly related with the active microbial biomass in the reactor. As a rule, the concentration gradient from the loaded AC particle to the bulk liquid can be created if the concentration of target organic compounds can be significantly reduced in a liquid or at the carbon-biofilm interphase (Marchal et al. 2013; Shen, Lu, and Liu 2012). This can be achieved when the active biomass is retained in a system that is capable of biodegrading this type of organics.

Organic Matter and Micropollutants

Almost in all the cases, wastewater contains a complex organic matter (carbohydrates, proteins and lipids) which is usually measured as TOC, COD or BOD. Usually, organic matter consists of biodegradable and non-biodegradable

fractions (Mutamim et al. 2012). It is very important to characterise an influent that is fed to the BAC reactor since biological systems cannot cope with soluble non-biodegradable organics; therefore, they leave the system with no substantial changes in the concentration. Otherwise, the AC load in the BAC reactor can become saturated if no bioregeneration occurs because of the significant amount of soluble non-biodegradable organics present in the reactor-feeding liquid (Craveiro de Sa and Malina 1992).

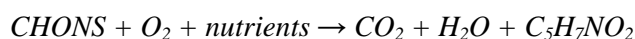
Another fraction of organic matter in wastewater usually contains easily and slowly biodegradable organics. Easily biodegradable organics typically are volatile fatty acids, alcohols, amino acids, short chain carbohydrates and other last stage biodegradation products of more complex organics that can be directly used by microorganisms. However, there are some organic compounds that first of all have to be hydrolysed outside the cell before they can be consumed by the microbial biomass (Matovic 2013; Rittmann and McCarty 2001).

The estimation of organic matter in wastewater by using TOC, COD or BOD analysis might fall into difficulties because the identification and quantification of the micropollutants present in the system is rather complicated. The concentration of micropollutants in wastewater typically varies from ng/L to µg/L; therefore, special methods have to be applied for analysis (Margot et al. 2015). Special interest in micropollutants, especially pharmaceuticals, in drinking water and wastewater is being paid to nowadays, since the presence of these compounds might cause a negative impact on human health. Moreover, the identification and removal is complicated since pharmaceuticals are poorly biodegradable because of their specific physicochemical properties (Boehler et al. 2012; Rattier et al. 2012).

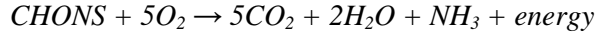
The removal of pharmaceuticals in biological systems can be hindered because special communities of 'biodegrades' need to develop. Usually, this type of microorganisms is overgrown by other communities that are responsible for the removal of easily biodegradable organic compounds; therefore, the acclimatisation of specific biodegrades can be significantly longer (Bertrand et al. 2015). Typically, easily biodegradable organic compounds are removed first in activated sludge reactors, followed by the biodegradation of more slowly biodegradable organic matter. Because of the significantly longer retention times needed to biodegrade slowly biodegradable organics and due to the low hydraulic retention times applied in WWTP, approximately 50% of pharmaceuticals can still be found in the effluent. Moreover, the mineralisation of pharmaceuticals in WWTP is often incomplete, and the formed metabolites can easily get into the surface water (Deblonde and Cossu-Leguille 2011; Vieno, Tuhkanen, and Kronberg 2007).

Removal of Organics as a Primary Carbon Source

Typically, the organic substrates which are easy to biodegrade can be converted to the energy and microbial biomass. Oxygen is required if the biodegradation process goes under aerobic conditions, the same as shown below (Bertrand et al. 2015; Rittmann and McCarty 2001):



Heterotrophs are involved in this process, and the conversion of the organic matter results in net production of bacterial cells ($C_5H_7NO_2$), carbon dioxide and water. This is valid when the amount of the organic matter is sufficient for the microbial biomass to fully function. When the concentration of organics is significantly low in the system, the starvation period starts. During this stage, endogenous respiration is dominant – microorganisms metabolise their own protoplasm (Bertrand et al. 2015; Rittmann and McCarty 2001):



Endogenous respiration often occurs in biological systems treating influents polluted with micropollutants. Since the concentrations of micropollutants can be as low as the ng/L scale, it is important to have an additional source of organic carbon in order to stimulate bacterial growth and activity (Bertrand et al. 2015).

Biodegradation can occur under anoxic conditions when the denitrification process is important for the conversion of organic matter which serves as an electron donor for the reduction of nitrates to nitrogen gas. Under anaerobic conditions, no oxygen is required; the organic matter can then be converted to carbon dioxide and methane (Bertrand et al. 2015; Rittmann and McCarty 2001).

Removal of Organics as a Secondary Carbon Source

The organic matter in water and wastewater treatment typically consists of easily biodegradable compounds and micropollutants that are less biodegradable and are present at the ng/L to $\mu\text{g/L}$ level. Even if the concentration of micropollutants is significantly low in wastewater, they can still be removed when a significantly high amount of an *easily biodegradable organic matter* (EBOM) is present which can stimulate the microbial growth (Fischer and Majewsky 2014). In this case, the EBOM serves as a primary substrate, whereas the micropollutants become a secondary source of organic matter (Bertrand et al. 2015).

The minimum concentration S_{min} which is required for the microorganisms to replicate and maintain themselves can be calculated by employing the following formula (Rittmann and McCarty 2001):

$$S_{min} = K_s \frac{b}{Y \cdot k_{max} - b} \quad (1.1)$$

where:

K_s is the half velocity constant;

b represents the decay rate;

Y denotes the yield;

k_{max} stands for the maximum specific substrate removal rate.

No net growth can occur when the substrate concentration in a biological system is kept at minimum. Under these conditions, the growth rate is equal to the decay rate. When the substrate concentration is below S_{min} , no biomass can be maintained in the system (Bertrand et al. 2015).

Cometabolic Removal of Organic Compounds

Cometabolic biodegradation covers a slightly different removal mechanism. The removal of particularly slowly biodegradable compounds is possible via the enzymatic pathway. However, in the system, the primary substrate must be present which can provide energy for cell growth and induce the production of enzymes (Rittmann and McCarty 2001).

The perfect example of cometabolism was shown in the research of Aktaş *et al.*, where the biodegradation of chlorinated phenols was attained by using phenol as a primary substrate. Phenol can be used to induce specific enzymes of phenol oxidisers for further mineralisation of 2-chlorophenol which is non-biodegradable aerobically (Ozgür Aktaş and Ceçen 2009). Moreover, the cometabolism is also possible between organic compounds which are not similar in structure. The positive effect of butyric acid on the biodegradation of three polycyclic aromatic hydrocarbons fluorene, phenanthrene and pyrene was reported in the research of Wei *et al.* (Wei et al. 2009). In addition, more efficient biodegradation of organophosphate pesticide malathion, when sodium succinate and sodium acetate were present in the samples, was also reported elsewhere (Xie et al. 2009). Cometabolic interactions are typically found to take place under aerobic conditions, when wastewater is being treated in biological systems.

1.5. AC Bioregeneration

During the last decades, the bioregeneration of AC has been extensively investigated and reported in numerous studies (Craveiro de Sa and Malina 1992; S. R. Ha, Vinitnantharat, and Ozaki 2000; Skouteris et al. 2015; Ying 2015). Bioregeneration relies on several different mechanisms and factors which directly influence the performance of the BAC system. The main observations are summarised in the following sections.

1.5.1. Mechanisms

Typically, two mechanisms are employed to explain the bioregeneration mechanism. This includes the bioregeneration occurrence because of the concentration gradient and enzymatic interactions.

Concentration Gradient

According to this theory, bioregeneration occurs because of the concentration gradient between the different substrate concentrations on the surface of the AC and in the bulk liquid. When the substrate concentration in the bulk phase or in the biofilm decreases significantly, this enhances the desorption process from the pores since the concentration of substrate on the surface becomes higher than in the bulk. Therefore, the adsorption capacity of AC can be restored. Unfortunately, AC cannot be completely regenerated because of chemisorption and pore blockage with substrate molecules (Ö. Aktaş and Çeçen 2007b; Oh et al. 2012; Shen, Lu, and Liu 2012).

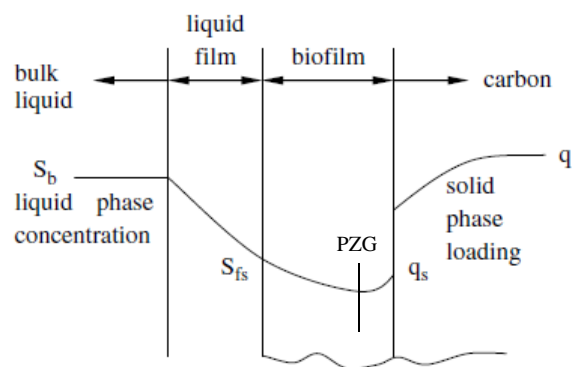


Figure 1.3. Concentration profiles over BAC particle (Shen, Lu, and Liu 2012)

The microbial biomass in suspension or the biofilm on the surface of the AC can affect the concentration gradient. Therefore, the biodegradation of the substrate in the bulk can result in the efficient desorption and bioregeneration of the adsorbent, the same as shown in Figure 1.3. Theoretically, the point of zero gradient (PZG) exists in a biofilm, at which, substrate concentration is minimal (Craveiro de Sa and Malina 1992). The PZG changes across the biofilm when the equilibrium conditions are being disturbed. When the substrate concentration in the bulk liquid increases, the PZG moves towards the AC surface; therefore, bioregeneration becomes impossible. However, if the active microbial biomass is present in the liquid phase, it can reduce the substrate concentration in the bulk. Thus bioregeneration is possible because the PZG can move closer to the liquid film.

The bioregeneration process itself depends on numerous factors, e.g., on microbial populations, adsorption-desorption hysteresis, substrate biodegradability, etc. The perfect example of bioregeneration was demonstrated in the research of Vinitnantharat *et al.*, where phenol and 2,4-dichlorophenol loaded GAC was bioregenerated during the period of 7–10 days. The removal efficiencies of 31.4% and 14.3% were achieved for both phenol and 2,4-dichlorophenol loaded carbons, respectively, close to the calculated adsorption reversibilities (Vinitnantharat *et al.* 2001). Another study also demonstrated the superior performance of BAC for phenol removal from wastewater. Up to 63% bioregeneration of phenol loaded carbon was achieved in 12 hours since the acclimated *Pseudomonas putida* (MTCC 1194) enriched biomass was used to seed the BAC reactor. Phenol removal in the parallelly running AC filter was approximately 21% lower than in the BAC reactor (Ullhyan and Ghosh 2012).

Exoenzymatic Reactions

The exoenzymatic theory covers the hypothesis that AC can be bioregenerated with extracellular enzymes produced by microorganisms. Typically, the size of bacteria varies within a range of several micrometres, much higher than the average diameter of micropores and mesopores, which is below <50 nm. However, the enzymes produced by bacteria are much smaller and can diffuse directly to the pores. Enzymes can react with the adsorbate and reduce the bonding with the surface of the AC; therefore, the desorption of the adsorbate to the bulk liquid can be

promoted (De Jonge, Breure, and Van Andel 1996; Li, Dvorak, and Li 2012; Orlandini 1999).

Some researchers contradict this hypothesis by stating that the enzyme molecules are quite big and thus cannot diffuse into the micropores. For an enzymatic reaction to occur, the diameter of a pore must be at least three times bigger than the size of the enzyme. Taking into account that the molecule of a monomeric enzyme is within the range of 31–44 angstroms, the reaction can occur only in the mesopores that are bigger than >10 nm. Therefore, low molecular weight compounds that are mainly adsorbed in the micropores with a diameter lower than <0.7 nm are inaccessible for the enzymes (Ying 2015). The regeneration efficiencies of phenol loaded ACs exceeded the desorption values in the research of Aktaş and Çeçen; considering that phenol was mainly adsorbed in the micro and mesopores, the conclusion was drawn that enzymatic reactions took place mainly in the mesopores (Ö. Aktaş and Çeçen 2006).

1.5.2. Factors Affecting Bioregeneration

The bioregeneration and performance of a BAC reactor depends on various factors. It is evident that BAC is a multicomponent system where physicochemical processes are combined together with biological processes. Therefore, the factors influencing adsorption, desorption and biodegradation processes individually also affect the overall performance of a BAC reactor (Ö. Aktaş and Çeçen 2007b; Knezev 2015; Ying 2015). In this chapter, the most crucial factors for BAC performance are discussed in detail.

AC Porosity

The porosity of AC is one of the major factors influencing the performance and bioregeneration of BAC reactors. Typically, mesoporous ACs are better alternatives for bioregeneration if compared with microporous analogues. The diffusion of molecules from carbon to the bulk liquid is better in mesopores, the same as described elsewhere (Liu et al. 2015). Therefore, micropores typically get loaded with pollutants while mesopores remain particularly clean (Dong et al. 2014). The same hypothesis was also supported by the literature review – faster and more efficient bioregeneration occurred on the outer surface of AC (N. Klimenko et al. 2003; N. A. Klimenko et al. 2002).

AC Granular Size

As described above, there are two forms of AC that are being used in water and wastewater treatment. The particle size of PAC varies between 15 to 25 µm, whereas GAC particles are bigger (0.2–5 mm). The performance of the BAC reactor also depends on whether PAC or GAC is used in the system. In this case, GAC outcompetes PAC because relatively long sludge and substrate retention times can be achieved on the surface of granular AC (Ying 2015). Unfortunately, no significant impact on bioregeneration was observed when phenol loaded thermally and chemically activated PACs and GACs were compared (Ö. Aktaş and Çeçen 2006, 2007a). The degree of hysteresis was comparable between PAC and GAC

showing that the granular size had no effect on the final adsorption reversibility and bioregeneration. However, desorption was faster from the PACs because of the relatively small granular size and the short diffusion pathway to the bulk liquid. This becomes especially important when AC has to be selected for a BAC reactor. The total retention time of organic pollutants in the reactor can be shortened if a smaller granular size fraction is chosen. Unfortunately, this might lead to technical difficulties when small AC granules are washed out during the periodical backwashing of the filters.

Substrate Desorption Kinetics

The bioavailability of adsorbed organic compounds in BAC reactors can be estimated by measuring the desorption kinetics. Usually, organic compounds showing high affinity to AC desorb less; therefore, bioregeneration can be hampered because of the decreased availability. As it was shown in the previous studies, relatively low desorption rates were directly related to slower bioregeneration (de Jonge, Breure, and van Andel 1996; Oh et al. 2012; Salvador et al. 2015).

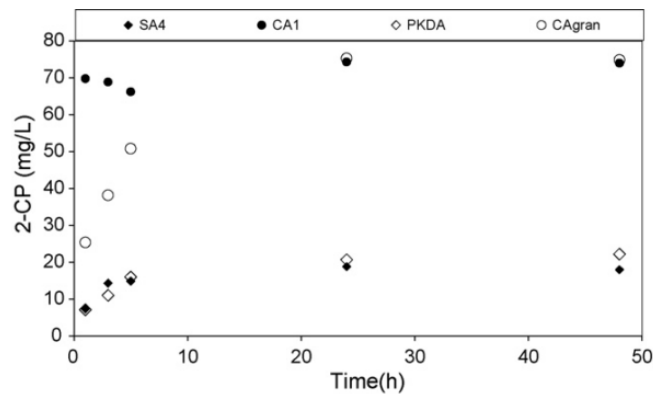


Figure 1.4. 2-Chlorophenol desorption from 4 different 2-chlorophenol loaded ACs SA4, CA1, PKDA and CAgran (Ö. Aktaş and Çeçen 2007a)

Typically, desorption consists of two phases: the fast initial phase, when the major share of desorption occurs, and the equilibrium (Figure 1.4). The distribution of the pore size of AC has a major impact on the desorption kinetics. AC with higher total pore and mesopore volumes exhibits faster diffusion in comparison with microporous carbons (Worch 2012). The species and the activity of microorganisms, the fluid dynamics and the type of AC were also identified as possible factors influencing the desorption of organic pollutants (Ying 2015).

Substrate Biodegradability

The influent to wastewater treatment plants contains various organic pollutants that are either easy or hard to biodegrade. Easily biodegradable organics are typically removed in activated sludge reactors, while a substantial part of slowly biodegradable organic compounds leaves WWTP and ends up in surface waters (Boehler et al. 2012). The ability of BAC reactors to retain slowly biodegradable

organic compounds by adsorption leads to an increased contact time between the biomass and the adsorbed compounds (Ö. Aktaş and Çeçen 2007b; Knezev 2015; Korotta-Gamage and Sathasivan 2017).

The bioregeneration of loaded carbons is highly dependent on the compounds being adsorbed. The bioregeneration process can be hampered if AC is loaded with non-biodegradable compounds. It can be enhanced if similar organics are present in a system that can increase biodegradation because of cometabolism, the same as described elsewhere (Kwon et al. 2015; Oh et al. 2016). However, biodegradation becomes a rate limiting step in the bioregeneration process. Typically, desorption is fast enough for bioregeneration to occur; unfortunately, the driving force of desorption is the concentration gradient between the bulk liquid and AC (Rahim and Garba 2016; Shen, Lu, and Liu 2012). In a BAC system, the retention time of the biomass is prominently longer in comparison with activated sludge installations. Thus, the biomass on AC particles can get acclimated to the adsorbed organic compounds and thus operate more efficiently. The less adsorbable and tended to biodegradation compounds can lead to the more efficient bioregeneration of AC. It was shown that phenol loaded AC was regenerated better than 4-chlorophenol saturated carbon. However, when carbon was saturated with a mixture of phenol and 4-chlorophenol, the overall achieved 4-chlorophenol bioregeneration was better than in a single solute system (Oh et al. 2016). The same observations were made by other authors researching the bioregeneration of toluene and trichloroethylene loaded carbon (Kwon et al. 2015). Better biodegradation of phenol versus indole also resulted in more efficient bioregeneration of phenol loaded ACs (Zhao et al. 2015). The positive effect of the acclimated biomass for bioregeneration of azo-dyes loaded adsorbents was reported elsewhere (Al-Amrani et al. 2014). However, some studies support the hypothesis that the bioregeneration of AC is only a simple combination of adsorption and biodegradation (Xiaojian, Zhansheng, and Xiasheng 1991).

Substrate Chemical Properties

The structure and origin of the substrate might also be a factor influencing AC bioregeneration. As it was shown in a previous study, the bioregeneration of carbons loaded with organic compounds having different alkyl- substitutes, was also somewhat different. ACs saturated with phenol were bioregenerated more efficiently in comparison with p-methylphenol, p-ethylphenol and p-isopropylphenol. Bioregeneration decreased significantly with the increase of the alkyl chain length (Lee and Lim 2005). Another research was conducted with o-, m- and p-cresol loaded granular AC. It was shown that the bioregeneration efficiency of o-cresol-loaded GAC was the lowest due to more irreversibility of the adsorbed o-cresol than m- and p-cresol (Kew et al. 2016).

Substrate and Carbon Contact Time

The increased substrate retention time in BAC reactors is often named as an advantage over activated sludge reactors and AC filters. The adsorbed compounds in BAC are retained for longer before being desorbed and biodegraded (Ö. Aktaş and

Çeçen 2007b; Dong et al. 2014). The longer biomass retention times in the reactor can lead to the acclimatisation of microbial communities to the substrate which might even be poorly biodegradable. The increased empty bed contact time (EBCT) and sludge age were also reported elsewhere as important factors resulting in more efficient bioregeneration (Ying 2015).

Biomass Concentration

The biofilm on the surface of AC and the biomass in suspension play a significant role in carbon bioregeneration and the overall performance of the BAC system. The advantage of having a higher biomass concentration on AC granules was shown in a research by Naidu *et al.*, where DOC removal was monitored in BAC filters used for desalination of seawater. It was found that more than 60% of DOC was removed when the BAC filter age increased since more biomass was developed on the AC surface (Naidu et al. 2013). Another study examined the effect of the increased mixed liquor volatile suspended solids (MLVSS) in suspension for bioregeneration. It was shown that the bioregeneration of AC increased up to 60% when the growth of MLVSS from 126 to 963 mg/L was recorded (Goeddertz, Matsumoto, and Scott Weber 1988).

Microorganism Cultures

The performance of the BAC reactor can be improved when specific microbial communities are present in the system. From the microbiological point of view, it is known that slowly biodegradable organic compounds can be eliminated by special biodegraders. It was shown that the acclimatisation of the activated sludge from a wastewater treatment plant to biodegrade xenobiotics yielded positive results. The bioregeneration of ACs loaded with 2-chlorophenol and 2-nitrophenol, was more efficient in comparison with the BAC reactors in which non-acclimated biomass was used (S.-R. Ha, Vinitnantharat, and Ozaki 2000). Phenol loaded carbons were also effectively regenerated (57.5% regeneration) in another study, where mixed bacterial cultures isolated from hydrocarbon polluted sediments, were used for bioregeneration experiments (Sodha, Panchani, and Nath K 2013). *Pseudomona* strains were also used to bioregenerate ACs loaded with biologically stable *surface-active substances* (SAS). It was shown that special acclimated biomass was able to regenerate microporous AC up from 25% to 95%, while mesoporous AC was regenerated up to 85% (N. Klimenko et al. 2003). In another study, *Pseudomonas* were also used to enhance phenol biodegradation and loaded AC bioregeneration. When using *Pseudomona putida* (MTCC 1194), 63% bioregeneration efficiency of the saturated filter bed was achieved in less than 12 hours (Ullhyan and Ghosh 2012).

Presence of Other Compounds and Biodegradation Products

The presence of multiple substrates for BAC bioregeneration was addressed in several studies. This becomes crucial when BAC reactors are applied to purify industrial wastewater. Typically, these streams contain easily biodegradable and non-biodegradable organic compounds. Therefore, the bioregeneration of AC in a

multi-solute system might be fairly different in comparison with a single solute system (Ying 2015). The same was observed in a research dealing with bioregeneration for GAC columns loaded with biodegradable toluene, benzene and non-biodegradable organic compound perchloroethylene. It was shown that bioregeneration was more efficient when carbon was loaded with toluene and benzene, while the sorption capacity decreased significantly when dealing with tetrachloride. In the course of investigating the multi-solute system, it was found that the regenerated pores of AC (toluene, benzene) were simply occupied by perchloroethylene (Putz, Losh, and Speitel 2005). Another study conducted the experiments in the bi-solute system with one biodegradable and another non-biodegradable organic compound. The lifetime of AC was controlled by the biodegradable organic compound and was extended by 1.2–7 times. However, this was valid only when the adsorbability was similar for both compounds (Erlanson et al. 1997).

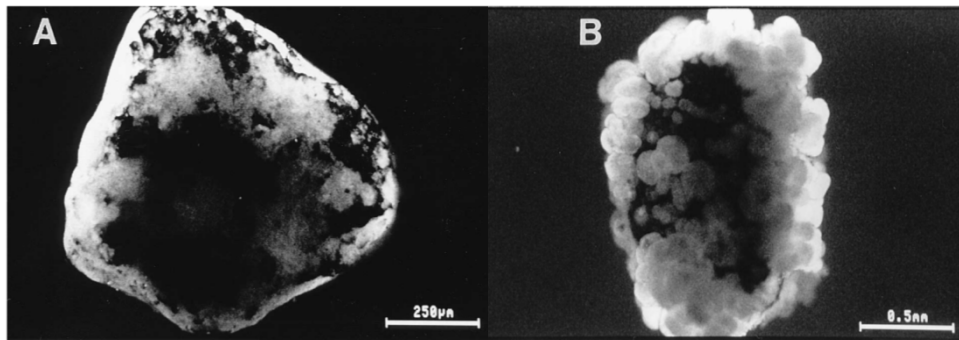


Figure 1.5. The change in the biofilm thickness from 15 to 300 μm in the reactor from day 16 (A) to day 77 (B) (Massol-Dey et al. 1995)

The fouling of AC is another factor deserving proper attention. Typically, the outer surface of GAC in the BAC reactor gets wasted over time. This happens because of the adsorption of metabolites, cells and microorganisms produced *extracellular polymeric substances* (EPS). This reduces the lifetime and bioregeneration of the AC. However, bioregeneration can still prolong the lifetime of the adsorbent regardless the fact that it will not recover fully to 100% (Ö. Aktaş and Çeçen 2007b; Ying 2015) Generally, in BAC reactors, GAC particles are covered with a yellowish slime matrix whose thickness may vary from several micrometres to hundreds of micrometres, the same as shown in Figure 1.5 (Marquez and Costa 1996; Massol-Dey et al. 1995). The biofilm layer typically increases with the increased concentration of the suspended biomass. This might hamper the adsorption and desorption processes because of pore blockage with microbial produced polymers; therefore, the bioregeneration of AC also decreases (Ö. Aktaş and Çeçen 2007b; Marquez and Costa 1996).

1.6. Operation Phases of BAC Reactor

The start-up and operation of the BAC reactor can be divided into three stages that are described in the sections below. The operation of BAC might become

specific – it depends on the organic compounds present in the influent and on the process peculiarities.

Reactor Start-Up

During the reactor start-up, organic pollutants in the reactor are removed by adsorption. The period when the adsorption process is dominant can last from several weeks to months, depending on the wastewater composition, substrate affinity to carbon, AC type, etc. The effluent from the BAC reactor typically contains organics that are not adsorbable. The formation of the biofilm on the surface of GAC is negligible during the reactor start-up (Reungoat et al. 2012; Simpson 2008).

Middle and Final Stages of Operation

After the start-up of the BAC reactor, the adsorption capacity of the AC load gradually decreases since there is almost no biofilm which is capable to regenerate GAC. Therefore, at some point, the concentration of adsorbable organic compounds in the effluent becomes higher. Because of the higher bioavailability, the microbial biomass also starts to develop faster, and the formation of the biofilm increases. Biodegradation and adsorption become the two dominant processes. However, this stage does not last forever – the AC gets partly saturated, and the acclimated biomass in the suspension as well as the formed biofilm on the surface of the AC are now able to maintain themselves and to biodegrade organic pollutants (Reungoat et al. 2012; Simpson 2008). It seems that the AC load is already saturated and not useful anymore. This is not true in case of shock loads which can be successfully adsorbed as described elsewhere (Cha, Choi, and Ha 1998). Because of the concentration gradient formed from the bulk phase to AC particles, pollutants can be adsorbed until the new equilibrium conditions have been created. If the microbial biomass is sufficiently capable to biodegrade the increased concentration in the bulk, then the adsorbed fraction can be desorbed back to the bulk liquid and mineralised. This process is called *bioregeneration*; it occurs in BAC systems because of adsorption-desorption hysteresis. Moreover, AC as a carrier material can become very favourable for the microorganisms and promote biodegradation (Knezev 2015; Ying 2015). This once again shows that the AC load perfectly serves as a buffer material which can minimise the negative impact of the increased substrate concentrations on the microbial biomass.

1.7. Application of BAC

The application of BAC for drinking water production and wastewater treatment has been reported in numerous researches. Typically, BAC reactors serve as polishing filters which are employed to remove nutrients from water streams before the final effluent reuse.

Drinking Water Production

The preparation of drinking water consists of numerous stages using various methods to prepare water for the final use. In the Western Europe, surface water is

frequently used to prepare drinking water. The influent undergoes coagulation and sedimentation steps as well as rapid sand filtration. Afterwards, ozonation is usually applied to convert poorly biodegradable organic matter into easily biodegradable organic compounds which are later removed in BAC filters. The effluent from BAC filters undergoes slow sand filtration, and, after additional disinfection, it is supplied to the customers.

In Amsterdam (the Netherlands), BAC filtration was also applied for surface water purification in Leiduin plant. The treatment is comprised of rapid sand filtration, ozonation, hardness removal, BAC filtration and slow sand filtration. For each 18 months, the reactivation of carbon beds is set in the maintenance instruction; however, this was not needed because of the active microbial biomass which colonised GAC filters (Bonné, Hofman, and van der Hoek 2002). In parallel to full scale reactors, several pilot reactors were running under the same conditions. The monitoring was based on the measurements of *adsorbable organic halogens* (AOX), *dissolved organic carbon* (DOC), pesticides and micropollutants. During the run of 4 years, no reactivation was applied. Moreover, together with the water from the Rhine River, different types of pesticides were spiked and monitored. The effluent quality from the BAC filters corresponded well with the regulations of Dutch Ministry of Drinking Water regulations: DOC was lower than 2 mg/L, and the total amount of pesticides did not exceed the limit of 5 µg/L (Bonné, Hofman, and van der Hoek 2002).

The plant in Sant Joan Despí (Barcelona, Spain) employs 20 GAC filters which are used to prepare drinking water from the Llobregat River. GAC filters receive water after ozonation which is used for disinfection purposes and also for breaking down larger organic molecules. When the operation of the filters started, adsorption was the dominant process achieving 65% removal of TOC. After partial carbon saturation, biodegradation became dominant, and the TOC removal decreased to 40%. At the start and at the end of the experiment, all the natural organic matter fractions (the low and high molecular weight organics) were removed effectively in BAC filters. It was also shown that the total volume of the micropores decreased by 24% thus supporting the hypothesis that bioregeneration occurred (Gibert et al. 2013).

The application of BAC for ammonia removal under different temperatures was also studied by Andersson *et al.* It was shown that BAC was able to remove more than 90% of ammonia at temperatures above 10°C. However, when the temperature dropped down below 4°C, this inhibited the biomass, and the ammonia removal efficiency decreased to 30% (Andersson et al. 2001). Another nitrification study was carried out in Laval (Quebec, Canada), where Rose Plant uses water from the Mille Îles River to produce drinking water. It was shown that, at mild temperatures (12°C), the removal of ammonia was greater than 93%, but it decreased to 7% when the filters were exposed to 3°C temperature (Laurent et al. 2003). This once again shows that BAC filters work as a single unit where adsorption and biodegradation are the dominant processes.

Wastewater treatment by using BAC is slightly different from drinking water production because of the significantly higher load of nutrients. Therefore, the development of the biofilm is relatively fast. Moreover, for the faster biofilm formation and development, filters are sometimes specially seeded with specific sludge capable of removing the target organic compounds. During the last decade, numerous scientific papers showed the BAC potential to remove slowly biodegradable micropollutants from the secondary WWTP effluent which can later be used for reclamation purposes. In the research of Reungoat *et al.*, the efficiency of the BAC technology to remove 54 micropollutants was investigated in a full scale reclamation plant (South Caboolture, Queensland, Australia), treating secondary effluent from domestic WWTP (Reungoat *et al.* 2010). The technological line in this plant consists of 6 stages: denitrification, pre-ozonation, coagulation/flocculation/dissolved air flotation and filtration (DAFF), main ozonation, AC filtration and final ozonation for disinfection. The first 3 stages showed poor removal of the total of 54 quantified micropollutants. However, after ozonation and biological filtration, the overall reduction of all the micropollutants was higher than 90%, often bringing down the concentration below 0.01 µg/L. Unfortunately, only 20–30% of DOC was removed in BAC filters thus showing a lower affinity of AC for the total organic matter in comparison with micropollutants (Reungoat *et al.* 2010). The same scientists examined another 2 full scale reclamation plants together with a plant in South Caboolture (Queensland, Australia) in 2012. It was shown that ozonation alone was able to remove as little as 10% of DOC thus supporting the hypothesis that organic matter was not mineralised but rather converted into intermediates. The BAC reactors alone were able to remove 20–50% of DOC, and most of trace organic pollutants up to 99%. However, the combination of ozone and BAC filters was more effective since DOC removal was greater than 50%, and more than 90% of trace organic chemicals were completely removed (Reungoat *et al.* 2012).

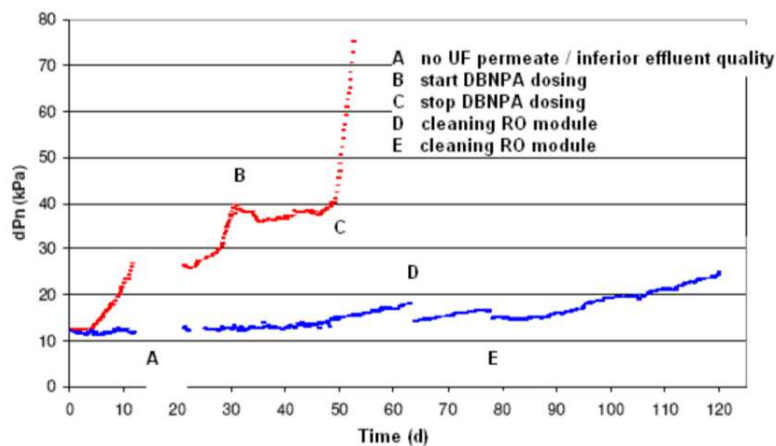


Figure 1.6. Normalised pressure drop (dPn) over the RO module with (upper line) and without (bottom line) BAC (Van Der Maas, Majoor, and Schippers 2009)

The *Puurwaterfabriek* plant (Nieuw Amsterdam, the Netherlands) deserves special attention since it uses the effluent from the local WWTP to produce ultrapure water for oil extraction. The use of BAC filters in this plant helps to remove nutrients from the WWTP effluent and to reduce the biofouling of reverse osmosis (RO) membranes (Van Der Maas, Majoor, and Schippers 2009).

It was shown that, without BAC, the pressured drop in RO membranes was observed as early as after 3 days (Figure 1.6). The situation was stabilised after one month only with the use of a biocide. However, when the biocide dosing was stopped, the pressure drop increased. When BAC was used before RO membranes, no significant pressure drop was observed for 120 days thus showing a high potential of BAC to remove nutrients from the WWTP effluent. Together with the inhibited biofouling in the RO membranes, 67% of COD and 89% of Kjeldal nitrogen was also removed in the BAC filter.

The application of powdered AC (PAC) was studied in a full scale petrochemical refinery plant which generates wastewater from the production of organic acids, solvents and aromatics (Meidl 1997). First of all, the preliminary study was carried out where the selection between the activated sludge reactor and PAC was of interest. The pilot-scale results showed that the removal of COD was greater in PAC reactors; therefore, they were applied at full scale. Because of PAC, the reactor volumes decreased by 25% comparing with the activated sludge reactors. Moreover, the operating costs decreased by 10%, the same as dewatered sludge volumes (0.5 vs. 1.4 tons per day). The COD and BOD₅ in the effluent were 135 mg/L and 30 mg/L, respectively, which was less than the discharge limits, while the registered COD values from the activated sludge reactor were above the level of 285 mg/L (the discharge limit is set at 250 mg/L) (Meidl 1997).

1.8. Summary of the Literature Review

During the last 50 years, the use of BAC for drinking water preparation and wastewater treatment has become more favoured and intensive. Typically, BAC reactors are applied as filtering media where AC particles are covered with biofilm. Therefore, the adsorption, desorption and biodegradation processes occur simultaneously, leading to the prolonged lifetime of the AC load because of the so-called self bioregeneration.

The performance of the BAC reactor and bioregeneration depends on the AC characteristics, on the biomass and the substrate. Therefore, highly porous ACs are favourable for bioregeneration. It is of major importance to have the right AC grade in the BAC reactor since very fast uptake and release of organic matter is needed for qualitative bioregeneration to take place. The granular size of GAC has to be optimal – the adsorption and desorption equilibrium when using bigger granules is slower to reach than with the use of smaller granules or powdered AC. The reversibility of adsorption is another phenomenon describing whether AC can be bioregenerated or not.

The bioregeneration of loaded carbons occurs if active acclimated biomass is present in the BAC reactor. The biofilm on the surface of AC granules and the biomass in suspension are needed for bioregeneration. However, the thick biofilm

might become unfavourable since it can clog the AC pores and disturb the transport of the substrate. Moreover, the GAC cannot be bioregenerated fully since the adsorption of the polymers, dead cells and metabolites produced by the microorganism will deteriorate the surface and decrease the ability of AC to adsorb.

BAC seems to be favourable for the removal of slowly biodegradable organic micropollutants from wastewater streams. Significantly high retention times of organic matter can be achieved in BAC reactors; thus the biomass can adapt to the new substrates and successfully biodegrade them. However, slowly biodegradable micropollutants are hardly biodegradable at low concentrations and cannot be used as a carbon source for microorganisms; therefore, the cometabolic biodegradation might become favourable. In some cases, easily biodegradable organics can stimulate the biodegradation of slowly biodegradable substrates.

The potential of the BAC technology to remove slowly biodegradable organic pollutants was widely discussed. Unfortunately, there is lack of information about the BAC application to remove slowly biodegradable pharmaceuticals from wastewater. Scarce work has been done so far to investigate the adsorption-desorption hysteresis specifically for BAC systems in which slowly biodegradable pharmaceuticals are removed since these types of experiments are more common in the water-soil research when investigating the mobility of pollutants. The effect of the AC surface roughness and the shear stress in a reactor on the BAC performance, biofilm formation and carbon bioregeneration when BAC is used to remove slowly biodegradable pharmaceuticals has not been comprehensively evaluated. Therefore, the above described problems inspired to devise specific experiments and to investigate the BAC to be applied for the treatment of synthetic wastewater polluted with slowly biodegradable pharmaceuticals. The materials and methods used in this doctoral thesis and the obtained results are described in detail in the following chapters.

2. Materials and Methods

This chapter describes all the materials and methods used in this research. The chapter is divided into four sections: Section 2.1 describes the general materials and methods used throughout the doctoral thesis; Section 2.2 describes the materials and methods pertaining to the results presented in Section 3.1 dealing with the interdependence between metoprolol biodegradation and adsorption-desorption hysteresis in the presence of acetate; Section 2.3 describes the materials and methods thus complementing to the results presented in Section 3.2 “Effect of Shear Stress and Carbon Surface Roughness on Bioregeneration and Performance of Suspended versus Attached Biomass in Metoprolol-Loaded Biological Activated Carbon Systems”, and Section 2.4 describes the materials and methods employed to obtain the results presented in Section 3.3 “Correlation between Activated Carbon Characteristics and Adsorption-Desorption Hysteresis and the Implications for the Performance of BAC Systems”. The general structure of the thesis is shown in Figure 2.1 below.

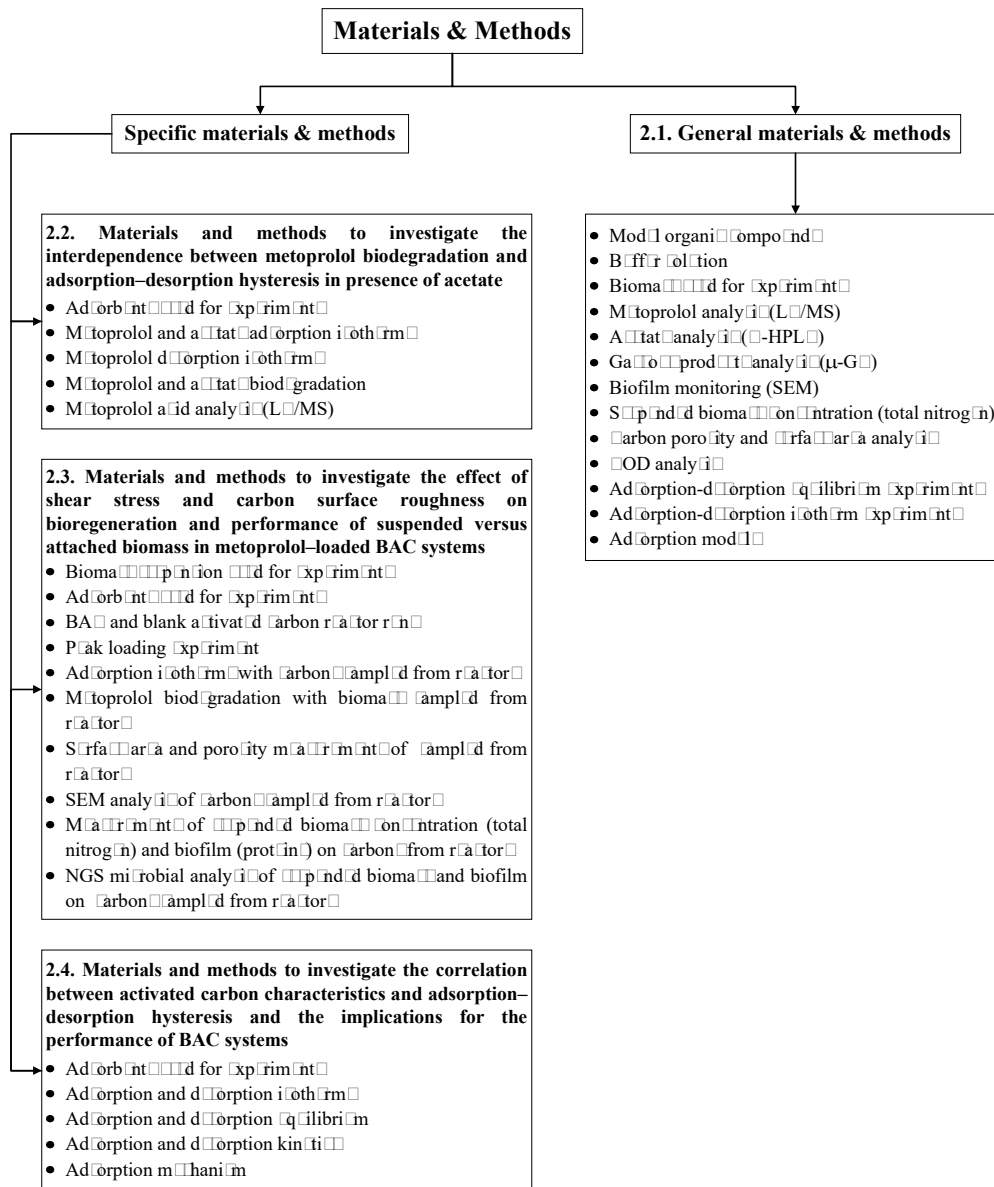


Figure 2.1. General and specific materials and methods used in this doctoral thesis

2.1. General Materials and Methods

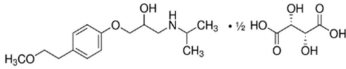
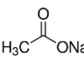
2.1.1. Chemicals and Biomass Suspension

Metoprolol and Acetate

Two model compounds were used for the experiments: a slowly biodegradable pharmaceutical compound and an easily biodegradable organic compound. *Metoprolol* was selected as a slowly biodegradable organic compound, and *acetate* was chosen as an easily-degradable compound. Metoprolol is one of the most dominant micro-pollutants in the effluent of domestic WWTPs (Waterzuivering 2012). Metoprolol was also the most abundant micro-pollutant measured in the WWTP effluent at Nieuw Amsterdam, the Netherlands. This effluent is used later on to feed industrial BAC reactors in the *Ultra-pure* water factory (Nieuw Amsterdam, the Netherlands). The low biodegradability of metoprolol was another criterion for its selection since around 50% of metoprolol is released into the surface waters (Vieno, Tuhkanen, and Kronberg 2007; Deblonde and Cossu-Leguille 2011).

Apart from the slowly biodegradable organic compounds, easily biodegradable organics are usually present in WWTP effluent as a BOD (Waterzuivering 2012); therefore, acetate was selected as the model compound. In addition to this, organic acids are usually formed as metabolites in a more complex biodegradation pathway of slowly biodegradable organics.

Table 2.1. Properties of model organic compounds used for the experiments

	Metoprolol tartrate	Sodium acetate
Structure		
IUPAC name	bis(1-[4-(2-methoxyethyl)phenoxy]-3-[(propan-2-yl)amino]propan-2-ol	Sodium Ethanoate
CAS number	56392-17-7	127-09-3
Molecular formula	(C ₁₅ H ₂₅ NO ₃) ₂ · C ₄ H ₆ O ₆	C ₂ H ₃ NaO ₂
Molar mass, g/mol	685.81	82.03
Solubility in water, g/L	50	100
LD ₅₀ (mouse), g/kg	1.5	6.9

Metoprolol tartrate (Sigma-Aldrich, USA) and sodium acetate salts (Sigma-Aldrich, USA) were used to prepare metoprolol and acetate working solutions. The properties of metoprolol tartrate and sodium acetate can be found in Table 2.1.

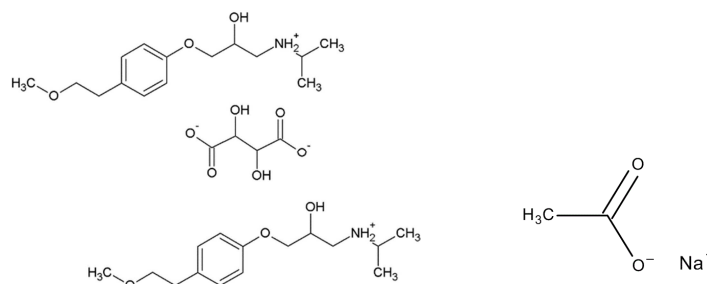


Figure 2.2. Chemical structure of metoprolol tartrate (left) and sodium acetate (right)

When dissolved in water, metoprolol tartrate dissociates into metoprolol cation and tartrate anion, the same as shown in Figure 2.2 above. Sodium acetate dissociates into sodium cation and acetate anion (Figure 2.2).

Buffer Solution Used for Biomass Washing and Adsorption-Desorption Experiments

The adsorption-desorption experiments and biomass washing were carried out in PBS containing 800 mg/L NaCl, 20 mg/L KCl, 144 mg/L Na₂HPO₄ and 24 mg/L KH₂PO₄. The pH was checked at the beginning, during each experiment, and at the end of each experiment; in all the experiments where PBS was used, pH remained between 6.7 and 7.4.

Buffer Solution Used for Biodegradation and Reactor Experiments

The experiments were performed with PBS (the composition as described above) supplemented with nutrients: 170 mg/L NH₄Cl, 8 mg/L CaCl₂·2H₂O, 9 mg/L MgSO₄·7H₂O and 1 ml/L of trace element solution. The trace element solution contained 2000 mg/L FeCl₃·4H₂O, 2000 mg/L CoCl₂·6H₂O, 500 mg/L MnCl₂·4H₂O, 30 mg/L CuCl₂·2H₂O, 50 mg/L ZnCl₂, 50 mg/L H₃BO₃, 90 mg/L (NH₄)₆Mo₇O₂₄·4H₂O, 100 mg/L Na₂SeO₃·5H₂O and 50 mg/L NiCl₂·6H₂O.

Biomass Used for Biodegradation and Reactor Experiments

The biomass-carbon suspension for our experiments was obtained from the industrial BAC filter at *Puurwaterfabriek* (Nieuw Amsterdam, the Netherlands). *Puurwaterfabriek* produces ultrapure water for oil extraction from WWTP effluent. *Puurwaterfabriek* runs the following treatment steps: sieving, ultrafiltration, primary BAC filter, polishing BAC filter, reverse osmosis and electro deionisation. The main function of the BAC filters is to remove biofouling precursors for reverse osmosis membrane filtration. In 2010, when *Puurwaterfabriek* operation started, both BAC filters were filled with Norit GAC 830 Plus GAC. So far, necessity to replace the AC has not arisen (Van Der Maas, Majoor, and Schippers 2009).

The full-scale BAC filter was sampled during the periodic back-washing. Subsequently, the bulk of the biomass was detached from the AC particles by severe agitation and filtration with a 215 µm sieve. Finally, the suspension was centrifuged at 7000 rpm for 15 min, and the supernatant was discharged. The biomass was washed twice and suspended into PBS supplemented with nutrients.

2.1.2. Analytical Tools and Methods

Metoprolol Analysis in Liquid Phase by Using Liquid Chromatography-Mass Spectrometry (LC-MS)

An Agilent 1200 HPLC chromatograph equipped with a Phenomenex Kinetex Phenyl-Hexyl column (100 mm * 2.1 mm * 2.6 µm) and an Agilent 6410 triple quadrupole MS/MS system was used for metoprolol analysis. Milli-Q water with 0.1% formic and 0.2 mM oxalic acid and acetonitrile with 0.1% formic acid were used as eluents (flow rate 0.3 mL/min). For metoprolol quantification, m/z transition 268→191 was used (Jensen et al. 2008). The total runtime for the method was set to 30 min. The calibration curves were made on the grounds of metoprolol tartrate

analytical standards obtained from Sigma Aldrich. The final concentrations of the calibration curve were set to 200, 400, 600, 800, 1000 $\mu\text{g/L}$.

Acetate Analysis in Liquid Phase by Using Ultra High Performance Liquid Chromatography (U-HPLC)

An Ultimate 3000 HPLC chromatograph equipped with a Phenomenex Rezex Organic Acid H+ column (300 x 7.8 mm) and a Dionex ultimate 3000RS UV detector (wavelength 210 nm) were used for the analysis of acetate in water samples. 2.5 mM sulphuric acid was used as an eluent at a constant flow rate of 0.5 mL/min. The column was kept at 80°C; the injection volume was 50 μL . The total runtime for the method was set to 30 min (Khiewwijit et al. 2015). The calibration curve was devised by using the acetic acid analytical standard (Fluka) and obtaining the final acetate concentrations of 5, 25, 50, 75 and 100 mg/L.

Analysis of Microorganism-Produced Gaseous Products

The headspace composition (O_2 , N_2 and CO_2) of the batch bottles was measured by using a micro gas chromatograph ($\mu\text{-GC}$, Varian CP 4900, USA). The instrument was equipped with a thermal conductivity detector and two parallel columns: a Mol Sieve 5A PLOT 10 m x 0.53 mm operated at 80°C with argon as the carrier gas and a PoraPlot U-10m column operated at 65°C with helium as the carrier gas (Khiewwijit et al. 2015).

Biofilm Analysis Using Scanning Electron Microscopy (SEM)

A SEM was used to assess the morphology and thickness of the biofilm on the AC granules. The acceleration voltage of 6 volt and magnification factors between 100 and 10000 were applied when analysing the samples. BAC granules were prepared by fixing the biofilm with glutaraldehyde for 24 hours at 4°C. After fixation, the samples were dried with ethanol-water mixtures, in which, the ethanol concentration was gradually increased from 30% to 100%. Prior to analysis, the samples had been stored in a desiccator.

Suspended Biomass Measurements as Total Suspended Nitrogen

The total nitrogen in a particular fraction was used as a measure for the biomass concentration in suspension. The total nitrogen was quantified by using Hach Lange cuvette tests LCK238 (Hach Lange, Dusseldorf, Germany). The biomass samples were centrifuged, washed with nitrogen-free PBS, and then centrifuged again in order to remove the dissolved nitrogen compounds.

AC Surface and Pore Volume Measurements

A surface area and porosity analyser (Tristar 3000, Micromeritics) was used to obtain the specific surface area (BET), the micro-pore as well as the total pore volume of granular ACs; the analysis was based on the adsorption and desorption of N_2 gas. Before conducting the analyses, all the AC samples were dried and flushed with N_2 gas at 150°C for 24 h (VacPrep 061 LB, Micromeritics) (Racyte et al. 2014).

COD Analysis in Liquid Phase

The dissolved COD was measured by using Hach Lange cuvette tests LCK 114 and LCK 414. Before conducting the analysis, the suspended samples were filtered by employing 0.45 µm membrane filters (Milipore, Millex GV).

Adsorption-Desorption Equilibrium Experiments

Metoprolol adsorption equilibrium experiments were performed in batch by using glass serum bottles and PBS. The main purpose of these experiments was to investigate the time needed to reach the adsorption equilibrium between the adsorbed metoprolol and metoprolol in the liquid phase. In general, 3–4 weeks were enough to reach equilibrium.

Desorption equilibrium experiments were conducted by using the same saturated carbon from adsorption equilibrium tests. The liquid was filtered, and AC was placed into a fresh PBS medium without metoprolol. The desorbed amounts of metoprolol were monitored over time until the equilibrium had been reached. Equilibrium was actually reached in less than 3 weeks. All the tests were performed in triplicates (Ö. Aktaş and Çeçen 2006).

Adsorption-Desorption Isotherms

The adsorption capacity of ACs for metoprolol was measured in glass serum bottles where equal amounts of ACs were equilibrated with different initial metoprolol concentrations. The same composition of PBS was used as in adsorption-desorption experiments. After 4 weeks, the samples were taken for metoprolol analysis in the liquid phase.

Desorption isotherms were obtained by using saturated AC from adsorption isotherms experiments. AC was filtered and placed into fresh PBS without metoprolol. After 4 weeks, the remaining metoprolol was measured in the liquid phase. All the tests were performed in triplicates (Ö. Aktaş and Çeçen 2006).

Adsorption Models

The adsorption and desorption experimental data was fitted with the *Freundlich* and *Langmuir* adsorption models whose non-linear and linear equations are described in Table 2.2 below. In addition, constants required for accurate comparison of ACs were obtained from the plots by picking certain slope and intercept values. The investigations were performed the same way as described in other academic sources (Sonthaimer, Crittenden, and Summers 1988).

Table 2.2. *Langmuir* and *Freundlich* adsorption models

Name	Non-linear form	Linear form	Plot	Slope	Intercept
Langmuir	$q_e = \frac{Q_m \cdot K_L \cdot c_e}{1 + K_L \cdot Q_m}$	$\frac{c_e}{q_e} = \frac{1}{K_L \cdot Q_m} + \frac{c_e}{Q_m}$	$\frac{c_e}{q_e}$ vs. c_e	$\frac{1}{Q_m}$	$\frac{1}{K_L \cdot Q_m}$
Freundlich	$q_e = K_F \cdot c_e^{\frac{1}{n}}$	$\log q_e = \log K_F + \frac{1}{n} \log c_e$	$\log q_e$ vs. $\log c_e$	$\frac{1}{n}$	$\log K_F$

Where:

q_e is the amount of the adsorbate adsorbed per gram of the adsorbent after reaching equilibrium (mg/g);

c_e denotes the substrate concentration in the liquid after reaching equilibrium (mg/L);

K_F is *Freundlich constant*, the adsorption capacity of the adsorbent (mg/g (L/mg)^{1/n});

n is *Freundlich constant* indicating the adsorption favourability;

Q_m represents the maximum adsorption capacity required to form the monolayer on the surface of the adsorbent (mg/g);

K_L is *Langmuir constant* related to the affinity of the binding sites (L/mg).

The amount of the adsorbed substrate at the equilibrium state (q_e) was calculated by using the following equation:

$$q_e = \frac{(C_0 - C_e) \cdot V}{M} \quad (2.1)$$

where:

C_0 represents the initial solute concentration in the liquid phase (mg/L);

C_e denotes the solute concentration in the liquid phase after reaching equilibrium (mg/L);

V is the volume of the solution (L);

M stands for the dry mass of the adsorbent (g).

The *Langmuir* adsorption model explains the monolayer adsorption process where no interactions takes place, when the adsorbent surface is fully loaded with the adsorbate molecules. The relevant parameter describing whether *Langmuir* adsorption process is favourable or not is *dimensionless separation factor* R_L :

$$R_L = \frac{1}{1 + K_L \cdot C_0} \quad (2.2)$$

where:

K_L stands for *Langmuir constant* (L/mg);

C_0 is the highest initial concentration (mg/L);

R_L values between 0 and 1 indicate that the adsorption process is favourable.

The *Freundlich* adsorption model takes into account heterogeneous adsorption; therefore, the adsorbate can interact with other solute molecules and form a multilayer surface. The favourability of the adsorption process is described by using *Freundlich constant* n ; values greater than >1 denote favourable adsorption.

2.2. Materials and Methods to Investigate the Interdependence between Metoprolol Biodegradation and Adsorption-Desorption Hysteresis in Presence of Acetate

Composition of Buffer and Medium Solution

The adsorption-desorption experiments and biomass washing were carried out in the PBS medium. The same medium, only supplemented with nutrients, was used for the biodegradation experiments. The exact composition is described in Subchapter 2.1.1.

Norit Granular AC Used for Adsorption and Desorption Experiments

In order to be able to extrapolate the results of this doctoral thesis to the full-scale BAC filter, we obtained the same virgin GAC that was used in 2010 to fill the *Puurwaterfabriek* BAC filter (Norit GAC 830 Plus). This adsorbent is made from coal and activated thermally, following the neutralisation with acid; the specifications are listed in Appendix 2.

Metoprolol and Acetate Adsorption Isotherm Experiments

The single solute (metoprolol or acetate only) and bisolute (metoprolol plus acetate) adsorption experiments were performed in 120 mL glass serum bottles closed with butyl rubber stoppers. The bottles were filled with 50 mL PBS and 0.020 g (0.40 g/L) AC. The exact AC content was measured down to ± 0.001 g accuracy. Subsequently, the bottles were spiked with metoprolol and/or acetate. All the metoprolol-acetate combinations of the following concentrations were applied in triplicate: 0.0, 3.79, 16.1, 61.6 and 255 mg/L metoprolol, and 0.0, 4.32, 15.8, 65.2, 262 and 1042 mg/L acetate. Subsequently, the samples were taken and filtered for metoprolol and acetate analyses, respectively, with LC/MS and UHPLC, the same as described in Subchapter 2.1.2. The bottles were placed for 504 h in a shaker (140 rpm) at 20°C to reach equilibrium between the sorbate, the solute and the sorbent (Figure 2.3). Equilibrium was achieved within 380 h.

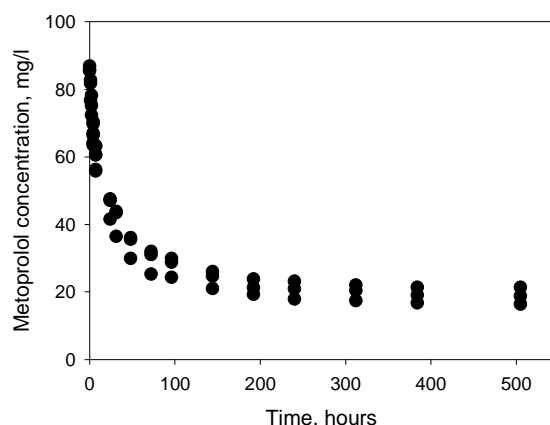


Figure 2.3. Metoprolol adsorption over time with 0.4 g/L Norit GAC; the initial metoprolol concentration was 90 mg/L

Metoprolol Desorption Isotherm Experiments

Desorption experiments were performed with the loaded AC from the single solute adsorption experiments with metoprolol and bisolute adsorption experiments with metoprolol and 65.2 or 1042 mg/L acetate. The AC was separated from the liquid by centrifuging the carbon/liquid suspension; thereafter, AC was submerged into 50 mL fresh PBS without metoprolol. The AC concentrations were the same as for the adsorption experiments (0.40 g/L). The bottles were placed for 420 h in a shaker at 20°C. Subsequently, the samples were taken and filtered for metoprolol analysis. 150 h was enough to reach the desorption equilibrium (Figure 2.4).

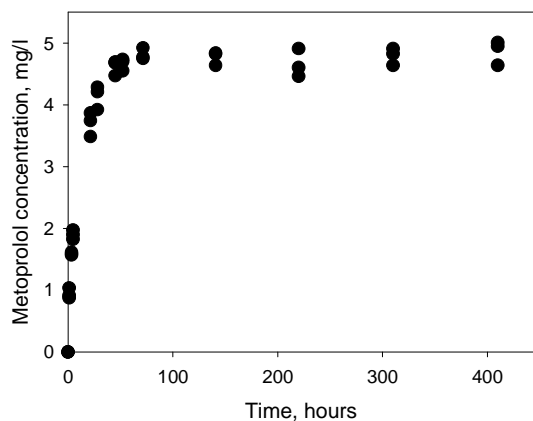


Figure 2.4. Metoprolol desorption over time from 0.4g/L loaded Norit GAC

Metoprolol and Acetate Biodegradation Experiments

Bisolute biodegradation tests were performed in order to assess the effect of easily degradable organic matter, e.g., acetate on the biodegradation of metoprolol and vice versa. The biodegradation experiments were carried out in 240 mL glass serum bottles with 70 mL of non-acclimated biomass suspension sampled from an industrial BAC bioreactor (see Subchapter 2.1.1.). Afterwards, the suspension was spiked with metoprolol and acetate and closed with butyl rubber stoppers. The headspace contained excess amounts of oxygen. The bottles were incubated in a shaker (140 rpm) in the dark at 20°C. Samples were taken three or four times a week and used for metoprolol and acetate analysis. The experiments were terminated when the organic matter had been depleted. All the biodegradation experiments were performed in triplicates.

Metoprolol Acid Analysis in Liquid Phase

Metoprolol acid, the main intermediate in the metoprolol biodegradation pathway, which shows the successful conversion of metoprolol, was quantified in the liquid samples by using LC-MS, the same as described in Subchapter 2.1.2. Pure metoprolol acid (Sigma Aldrich, USA) was dissolved in methanol and stored at –20°C prior to the analysis. The total runtime for the method was set to 30 min. The calibration curves were made with pure metoprolol acid analytical standard obtained

from Sigma Aldrich. The final concentrations of the calibration curves were set to 100, 200, 300, 400 and 500 µg/L.

2.3. Materials and Methods to Investigate the Effect of Shear Stress and Carbon Surface Roughness on Bioregeneration and Performance of Suspended versus Attached Biomass in Metoprolol-Loaded Biological Activated Carbon Systems

Buffer and Medium Solution Used for Biomass Washing and BAC Reactor Experiments

The PBS medium was used for biomass washing and adsorption experiments with virgin and wasted carbons from reactors. The composition of the explored material can be found in Subchapter 2.1.1. PBS supplemented with nutrients was used for biodegradation experiments with biomass suspension from reactors. The pH was checked at the start, during and at the end of each experiment; during all the experiments, pH remained between 6.7 and 7.4.

For the reactor experiments, the PBS with nutrients was supplemented with 10 mg/L metoprolol and 137 mg/L sodium acetate (equivalent to 100 mg/L acetate). Acetate was added as a model compound for the easily degradable organics that micro-pollutants such as metoprolol typically accompany. It was shown that the easily degradable organics influence the biodegradation of micro-pollutants (Hess, Silverstein, and Schmidt 1993). The applied ratio of 1:10 (metoprolol–acetate) was based on the ratio encountered in the secondary effluent of the wastewater treatment plants of the Netherlands. This effluent typically contains <4mg BOD/L (the BOD is an indicator of the amount of the explored easily biodegradable organic matter) (Waterzuivering 2012) whereas the sum of the slowly biodegradable organic compounds, including pharmaceuticals, varies in the range of tens to hundreds µg/L (Margot et al. 2015). The circa 100-fold higher concentrations used in this doctoral thesis were chosen to enable the monitoring of the fate of metoprolol as this research aims to understand the interaction between biomass and AC rather than to optimise full-scale BAC systems.

In order to prevent aerobic growth, PBS with nutrients, metoprolol, and acetate were fed to the reactors from a vessel which was maintained anaerobic by continuous sparging with N₂ gas. The acetate and metoprolol concentrations in the dosing vessel were monitored throughout the experiment and remained constant.

Biomass Suspension Used to Seed BAC Reactors

The biomass suspension used to inoculate lab-scale reactors was obtained from an industrial BAC bioreactor (see Subchapter 2.1.1.). The preparation of biomass for the reactor experiments is described in Subchapter 2.1.1. After the preparation, the biomass was washed twice with PBS and suspended in 3 L of PBS supplemented with nutrients but without organic substrates. This biomass suspension was used to fill the three BAC reactors (1 L per reactor). This procedure resulted in the initial biomass concentration of 12 mg_{total-N}/L in all the three BAC reactors.

ACs Used to Fill BAC Reactors

Experiments were performed with two types of AC (Table 2.3): spherical AC granules from Mast Carbon International (Basingstoke, UK) and AC granules from Norit (GAC 830 Plus). The Norit AC granules were also used in the full-scale BAC filter from which the biomass was obtained.

Table 2.3. Physical characteristics of the virgin Mast and Norit ACs

AC	Specific surface area (m ² /g)	Pore surface area, m ² /g		Pore volume, cm ³ /g		
		Micropores	Mesopores	Micropores	Mesopores	Rate meso/micro
Mast	1295	1177	73	0.47	0.60	1.3
Norit	986	863	45	0.36	0.14	0.4

The Mast AC granules were produced by using polymeric resin as a precursor followed by thermal activation. The Norit granules were produced from coal followed by thermal activation and neutralisation with acid. The size of the granules used in the blank reactor and BAC reactors varied from 0.5 to 0.6 mm. The Mast granules had a higher pore volume, a larger surface area, and a smoother spherical surface compared to the Norit granules that had many cracks and cavities (Figure 2.5).

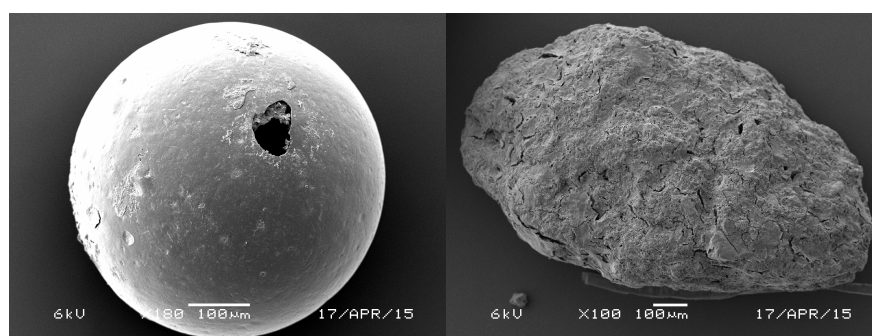


Figure 2.5. Scanning electron microscopy images of virgin Mast (left) and Norit (right) AC granules

The selected carbon granules were washed with MilliQ ultrapure water to remove fine dust and impurities from the surface and afterwards stored in a desiccator. The surface roughness of the ACs was measured with a Sensofar PLμ2300 optical profilometer featuring the measuring accuracy of 0.1 nm.

BAC and Blank AC Reactor Runs

The experiments were performed in sequential batch reactors with an operational volume of 1 L so that to investigate the effect of shear stress and AC surface roughness on biofilm formation, BAC performance and AC bioregeneration (Figure 2.6). Every 12 h, the mixing in the reactors was stopped for periodical discharge and feeding. First, the particles were allowed to settle for 15 min, then 50% of the volume was drained for 6 min, after which, the drained volume was replaced by the fresh influent from the dosing tank, which also took 6 min. Precisely

calibrated Masterflex L/S peristaltic pumps were used to dose the influent and drain the effluent from the reactors. Electronic timers were used to time the four sequential steps. The overall hydraulic retention time was 24 h.

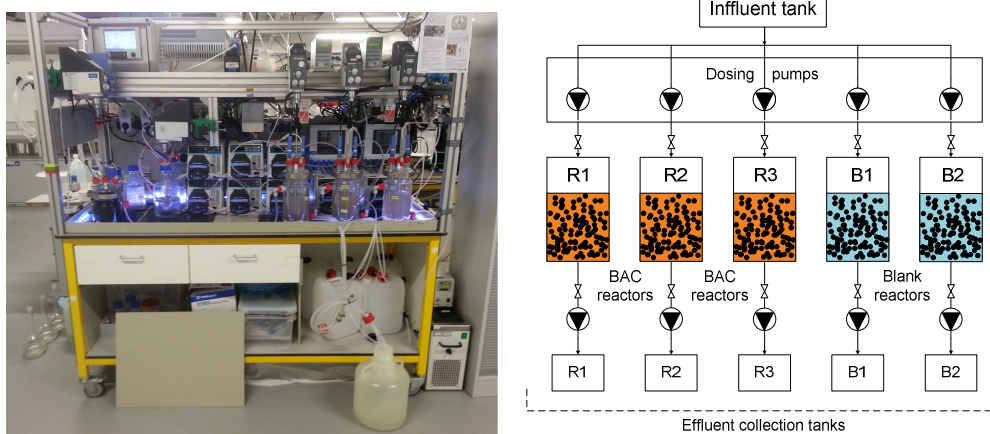


Figure 2.6. Set-up and scheme of metoprolol loaded BAC reactors

Five reactors were operated in parallel. Next to the three BAC reactors containing biomass suspension (R1, R2, and R3), there were two abiotic blank reactors which were filled with 1 L PBS (B1 and B2). To each reactor, 1.2 g AC was added. Smooth (surface roughness $R_a=1.6 \mu\text{m}$) Mast AC granules were added to B1 and R1, and rough (surface roughness $R_a=13 \mu\text{m}$) Norit AC granules were added to B2, R2, and R3 (Figure 2.6). R3 was operated at a higher shear stress (mixing at 200 rpm; gradient velocity $G=25 \text{ s}^{-1}$; impeller tip speed $v=1.03 \text{ m/s}$); the two remaining BAC reactors and the two blanks were operated at a lower shear stress (mixing at 100 rpm; gradient velocity $G=8.8 \text{ s}^{-1}$; impeller tip speed $v=0.52 \text{ m/s}$). The detailed information on how the impeller tip speeds and velocity gradients were calculated is presented in Appendix 1.

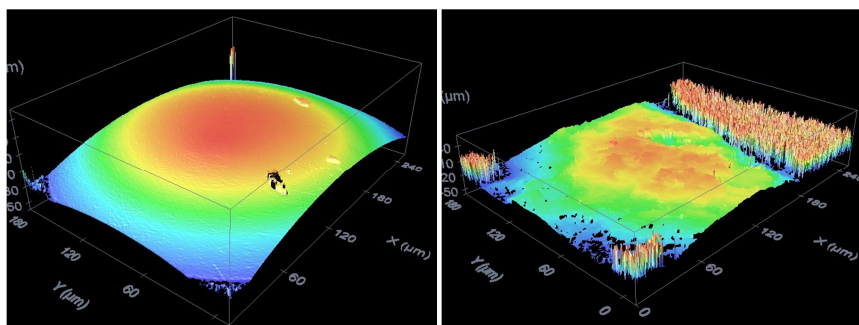


Figure 2.7. Optical profilometry images for the assessment of the surface roughness of virgin Mast AC (Left) and virgin Norit GAC 830 Plus AC (Right) granules

A blank reactor operated at a high shear stress was not included. The shear stress is expected to affect the biomass but not the adsorption. As the applied metoprolol loading rate ($0.35 \text{ mg g}^{-1} \text{ h}^{-1}$) was low compared to the adsorption rate

obtained with virgin Norit AC granules ($4.5 \text{ mg g}^{-1} \text{ h}^{-1}$), it can be safely assumed that the equilibrium between the liquid and AC is reached even when mixing at 100 rpm. In order to facilitate the assessment of the influence of the biomass, the BAC reactor at a high shear stress and with rough AC granules (R3) can thus be compared to the blank reactor at a low shear stress and with rough AC granules (B2).

All the reactors were controlled at 20°C and pH ranging between 6.8 and 7.2. R1, R2, and R3 were controlled at a dissolved oxygen concentration of 4 mg/L by air sparging; the dosing was controlled by using dissolved oxygen sensors and air mass flow controllers. The blank reactors containing AC granules but not containing biomass were sparged with N_2 so that to prevent aerobic growth. No microbial growth was observed in the blank reactors throughout the experiment. Reactor liquor samples were taken and used for biomass analyses and, after filtering through a $0.45 \mu\text{m}$ membrane filter (Millipore), were also used for acetate and metoprolol quantification. At the end of the 2664 h sequential batch reactor runs, samples of AC or BAC granules and the biomass suspension were taken for further analyses. After conducting the presently described reactor experiments, the reactors were used for the peak load experiment.

Metoprolol Peak Loading Experiment with Blank AC and BAC Reactors

In order to assess the remaining adsorption capacity at the end of the reactor experiments, all the reactors were spiked with 93 mg/L metoprolol while being operated in the batch mode at 20°C , pH ranging between 6.8 and 7.2, and the dissolved oxygen concentration of 4 mg/L. The same mixing regimes were applied as during the sequential batch reactor runs. A high sampling frequency was used to monitor the depletion of metoprolol from the liquid phase over the course of 100 hours.

Adsorption Isotherm Experiments with AC and BAC Granules Sampled from the Blank and BAC Reactors

As the second indicator for the remaining adsorption capacity of AC at the end of the sequential batch reactor experiments, adsorption isotherms were obtained with the AC granules sampled from the five reactors at the end of the reactor experiments. The samples were rinsed twice with PBS to remove any unbound biomass and dried at 105°C for 24 h to inactivate the biofilm. Then the samples were used for the triplication of single-solute metoprolol adsorption experiments in 50 mL glass serum bottles with 40 mL PBS and $0.015 \pm 0.001 \text{ g}$ of dried AC (equivalent to 0.375 g/L). Subsequently, the bottles were spiked with 10, 50, 100, 200, and 300 mg/L metoprolol. Afterwards, the bottles were placed in a shaker (150 rpm) at 20°C . After 720 h, the experiment was halted. Samples were taken, filtered through a $0.45 \mu\text{m}$ membrane filter (Millipore) and used for metoprolol analysis. The relationship between the remaining metoprolol concentration and the net uptake per amount of AC was fitted to the *Langmuir* adsorption model as described in Subchapter 2.1.2.

Metoprolol Biodegradation Experiments with Separated Biomass Suspension from BAC Reactors

In order to assess the metoprolol biodegradation rate of the suspended biomass at the end of the reactor runs, biomass was separated from the AC granules by intensive agitation and subsequent sieving with a 215 μm metal sieve. After removing the granular fraction, the biomass was suspended in PBS with nutrients in the reactor vessels. The reactors were spiked with metoprolol (yielding a concentration of 92–95 mg/L) and operated in a batch at 20°C with pH ranging between 6.8 and 7.2 and in the dissolved oxygen concentration of 4 mg/L. Samples were taken periodically until metoprolol had been completely removed.

Surface Area and Porosity Measurements of Wasted Carbons Sampled from Blank and BAC Reactors

The surface area and porosity of Mast and Norit carbon granules were measured as described in Subchapter 2.1.2. Moreover, BAC granules were dried at 120°C before analysis in order to prevent thermal decomposition of the biofilm attached to the surface.

Scanning Electron Microscopy Analysis of Carbon Particles Sampled from BAC Reactors

Scanning electron microscopy (SEM) was used to assess the morphology of the biofilm on the AC granules. Detailed information about the preparation of carbon particles can be found in Subchapter 2.1.2. 8 BAC granules from each BAC reactor were randomly chosen for analysis; the biofilm coverage was investigated for at least 10 random locations on each granule.

Measurements of Suspended Biomass Concentration and Biomass on the Surface of AC Granules Sampled from BAC Reactors

The measurements of the total nitrogen in the particular fraction (biomass suspension) are extensively described in Subchapter 2.1.2. The biofilm amount on the AC granules was measured as the total protein count by using a Pierce™ bicinchoninic acid protein assay kit (Thermo Scientific, USA) as described elsewhere (Stoquart et al. 2014). 400 mg (wet weight) of BAC granules from each reactor (R2 and R3) was used for the analysis. The BAC particles from R1 BAC reactor were not analysed because the protein extraction was not successful due to excessively low biofilm amount.

Microbial Analysis of Suspended Biomass and Biofilm on AC Granules Sampled from BAC Reactors

In order to investigate whether metoprolol was biodegraded in the suspension or in the biofilm and to identify the potentially degrading microbial populations, *Next generation sequencing* (NGS) was performed with suspended biomass from R1, R2, and R3 and with the biomass attached to the AC granules in R2 and R3 BAC reactors. The samples were collected at the end of the runs. Prior to the analysis, the BAC particles (300 mg wet weight per reactor) were washed twice with

PBS and ultra-sonicated four times for 15 s so that to detach the biofilm from the AC surface. The BAC particles from R1 BAC reactor were not analysed since the biofilm amount was insufficient for successful deoxyribonucleic acid (DNA) extraction. DNA extraction was performed by using a PowerBiofilm® DNA Isolation kit (MO BIO Laboratories, USA). The purification and concentration of isolated DNA was performed with a DNA Clean & Concentrator™-5 kit (Zymo Research, USA).

Afterwards, 16S rRNA genes were amplified by using PCR primers 341f and 805r, together with indexes as described elsewhere (Hugerth et al. 2014; Lindh, Figueroa, and Sjöstedt 2015). Illumina MiSeq pair-end sequencing technologies were performed in the *Science for Life Laboratory* (www.scilifelab.se, Stockholm). The obtained 16S rRNA reads were analysed with the UPARSE pipeline before annotation by using the SINA/SILVA database with the final data processing in Explicet 2.10.5 (Edgar 2013; Quast et al. 2013; Robertson et al. 2013). The computations were performed by employing the resources provided by the *Swedish National Infrastructure for Computing* (SNIC) via *Uppsala Multidisciplinary Center for Advanced Computational Science* (UPPMAX) in the framework of Project b2013127.

2.4. Materials and Methods to Investigate the Correlation between Activated Carbon Characteristics and Adsorption-Desorption Hysteresis and the Implications for the Performance of BAC Systems

Composition of Buffer and Medium Solution

The adsorption and desorption experiments were performed in the PBS medium; the exact composition can be found in Subchapter 2.1.1. pH was checked at the start, during experiments, and at the end of each experiment; it remained stable throughout the investigation (between 6.7 and 7.4).

Carbons Used for Metoprolol Adsorption and Desorption Experiments

The selection of granular ACs for the adsorption and desorption experiments was based on the porous structure, the activation type and the precursors that were used to prepare the adsorbents. In total, 20 ACs were selected for the experiments. There were 2 types of Mast carbons in total: granules with the specially formed spherical shape shell, and the standard granules without a shell. The selected Norit AC granules were commercially available adsorbents.

Table 2.4. List of Mast carbon granules used for experiments

Carbon code	Oil treatment to obtain smooth spherical surface	Granular size, mm	Activation	Material
S0.25+	Yes	0.25–0.5	Reduced	Polymer 1
S0.25++	Yes	0.25–0.5	Mediocre	Polymer 1
S0.25+++	Yes	0.25–0.5	Elevated	Polymer 1
S0.5+	Yes	0.5–0.6	Reduced	Polymer 1
S0.5++	Yes	0.5–0.6	Mediocre	Polymer 1
S0.5+++	Yes	0.5–0.6	Elevated	Polymer 1
S1+	Yes	1.0–1.4	Reduced	Polymer 1
S1++	Yes	1.0–1.4	Mediocre	Polymer 1
S1+++	Yes	1.0–1.4	Elevated	Polymer 1
0.25C–1	No	0.25–0.5	No activation	Polymer 2
0.25C	No	0.25–0.5	No activation	Polymer 1
0.25A–1	No	0.25–0.5	Mediocre	Polymer 2
0.25A	No	0.25–0.5	Mediocre	Polymer 1

The nine types of AC listed at the top of Table 2.4 were prepared at *MAST Carbon International* (Basingstoke, UK) from polymeric precursors by heating in oxygen free environment (see Table 2.4). Afterwards, the samples were boiled in oil so that to form a spherical smooth surface over the carbon particle which gives superior high mechanical strength and resistance to attrition. In addition, carbons differed in terms of the degree of activation and the granular size. The number of ‘+’ of the carbon code reflects the degree of activation which increases in a row from + to +++. This typically results in the increased BET area and the pore volume of ACs (see Appendix 4). The number of AC coding is directly related to the granular size and increases in a row from 0.25 mm to 1.4 mm with the respective carbon. The four final carbons 0.25C–1, 0.25C, 0.25A–1 and 0.25A were made without a shell and differed from the nine initial carbons. The 0.25C–1 carbon was made from a different cross-linked polymer from the nine initial carbons and was only carbonized (i.e. no activation was applied). In order to prepare 0.25C carbon, Polymer 1 was used; however, no activation was applied. 0.25A–1 and 0.25A were identical to the two previously described ACs; they were only activated thermally.

Table 2.5. List of Norit AC granules used for metoprolol adsorption and desorption experiments

No	Carbon code	Granular size, mm	Activation	Material
14	N1	0.32–0.5	Thermal	Coconuts
15	N1+		Thermal, acid washed	Coconuts
16	N2	0.32–0.5	Thermal	Coal
17	N2+		Thermal, acid washed	Coal
18	N3	0.32–0.5	Chemical	Wood
19	N4		Thermal	Peat
20	N5		Thermal	Lignite coal

Another set consists of 7 widely used commercial ACs produced by *Cabot Norit* (the Netherlands) (Table 2.5). ACs were selected according to the different precursors that were used to produce carbons and regarding the activation type which resulted in a different porous structure and in the active groups located on the AC surface. In addition to the ‘hard’ precursors (coal, coconut shells), ACs made from soft materials were also selected for comparison since they have a significantly higher amount of mesopores (see Appendix 5).

Metoprolol Adsorption Isotherm Experiments

Metoprolol adsorption isotherm experiments were performed in 120 ml glass serum bottles closed with butyl rubber stoppers. The bottles were filled with 50 ml PBS and 0.020 g (0.40 g/L) AC. The exact AC content was measured down to ± 0.001 g accuracy. Subsequently, the bottles were spiked with 0.87, 8.74, 43.3, 85.6, 172 and 252 mg/L metoprolol and placed for 21 days in a shaker (150 rpm) at 20°C. Afterwards, the samples were filtered by using a 0.45 μm membrane filter (Milipore, Millex GV) and analysed with LC/MS

Metoprolol Desorption Isotherm Experiments

Metoprolol desorption isotherm experiments were performed with metoprolol-loaded ACs from the adsorption isotherm tests. The ACs were separated from the liquid by centrifuging the carbon/liquid suspension; thereafter, ACs were submersed into 50 ml fresh metoprolol-free PBS. The AC concentrations were the same as for the adsorption isotherm experiments (0.40 g/l). Then the bottles were placed for 21 days in a shaker at 20°C. Subsequently, the samples were taken and filtered for metoprolol analysis by using LC/MS.

Metoprolol Adsorption Equilibrium Experiments

All the conditions for metoprolol adsorption equilibrium (AC concentration 0.40 g/L in PBS) tests were the same as in the adsorption isotherm experiments; however, the initial metoprolol concentration was constant in all the batch bottles, measuring 93 mg/L. 21 days were sufficient to reach the equilibrium. The samples were taken periodically during the period for metoprolol analysis with LC-MS.

Metoprolol Desorption Equilibrium Experiments

The metoprolol loaded ACs from the adsorption equilibrium experiments were used for desorption equilibrium tests. The ACs was centrifuged and submersed into a metoprolol-free PBS solution. The samples were incubated in a shaker at 20°C, and the metoprolol concentration was measured with LC/MS periodically during 21 days.

Metoprolol Adsorption Kinetic Models

The pseudo 1st and pseudo 2nd order kinetic models were used to describe the metoprolol adsorption on different ACs (Doke and Khan 2012; Wu, Tseng, and Juang 2005). The linear and non-linear forms of model equations can be found in Table 2.6.

Table 2.6. Pseudo first and pseudo second order kinetic models

Name	Non-linear form	Linear form	Plot	Constants
1 st order	$q_t = q_e(1 - \exp^{-k_1 \cdot t})$	$\log(q_e - q_t) = \log(q_e) - \frac{k_1 \cdot t}{2.303}$	$\log(q_e - q_t)$ vs. t	$k_1 = 2.303 \cdot S$
2 nd order	$q_t = \frac{k_2 \cdot q_e^2 \cdot t}{1 + k_2 \cdot q_e \cdot t}$	$\frac{t}{q_t} = \frac{1}{k_2 \cdot q_e^2} + \frac{1}{q_e} \cdot t$	$\frac{t}{q_t}$ vs. t	$q_e = \frac{1}{S}; k_2 = \frac{S^2}{L}$

S – slope; L – intercept

where:

q_e is the amount of adsorbate adsorbed per gram of the adsorbent after reaching equilibrium (mg/g);

q_t represents the amount of adsorbate adsorbed per gram of the adsorbent (mg/g) during time t (h);

k_1 denotes the pseudo 1st order rate constant (1/h);

k_2 represents the pseudo 2nd order rate constant (g/mg·h).

The data fitting to one of these models can define which adsorption process is leading. The pseudo 1st order model indicates that the reaction is linked to physisorption, while pseudo 2nd order kinetics covers up chemisorption process.

Metoprolol Adsorption Mechanism

In order to find out the adsorption mechanism and to identify the possible rate controlling steps, the results of the kinetic experiments were fitted to Weber's intraparticle diffusion model (Doke and Khan 2012; Wu, Tseng, and Juang 2005):

$$q_t = k_{id} \cdot t^{1/2} + L \quad (2.3)$$

where:

L is the intercept;

k_{id} is the intraparticle diffusion constant (mg/g·h^{1/2}) which can be calculated from the slope of linear plot q_t versus $t^{1/2}$.

If the regression of q_t versus $t^{1/2}$ passes through the origin, then intraparticle diffusion can be identified as a rate limiting step. Moreover, the larger is the intercept, the greater is the contribution of the surface adsorption for the rate limiting step.

3. Results and Discussion

The application of BAC (BAC) systems to clean wastewater and to produce potable water has been widely discussed. However, the role of the different processes in BAC systems contributing to the removal of slowly biodegradable pharmaceuticals, like a β -blocker metoprolol, is not completely understood.

The significance of adsorption-desorption hysteresis for the removal of metoprolol in BAC systems is described more in details in the Paragraph 3.1. Moreover, the effect of easy biodegradable organic matter, in the form of acetate, for metoprolol biodegradation is addressed.

The results from the lab-scale BAC pilot reactor runs are presented in the Paragraph 3.2. The effect of AC surface roughness and applied shear stress on biofilm formation and AC bioregeneration was investigated, using two different types of carbons. Furthermore, the possible microorganisms involved in metoprolol degradation were identified using the Next Generation Sequencing.

Paragraph 3.3 presents the results on how AC characteristics influence metoprolol removal in BAC systems. These characteristics include the porosity and type of materials, from which the AC was produced. To assess the effect of those characteristics, adsorption-desorption hysteresis indexes were quantified for 20 different carbons. The results were subsequently used for the recommendations on adsorbent selection for BAC systems.



3.1. Interdependence Between Metoprolol Biodegradation and Adsorption-Desorption Hysteresis in Presence of Acetate

1001

AWOL

1002

1003

TDMD

904

1004

3.1.1. Metoprolol and Acetate Bisolute Adsorption Isotherm Experiments

Bisolute adsorption experiments were carried out in order to assess the possible competition between metoprolol and acetate for the adsorption sites on the AC surface. Metoprolol adsorption on AC was best described by the *Freundlich* model reaching $R^2=0.96$ versus $R^2=0.53$ for the *Langmuir* model. The values for *Freundlich* constants K_f and n for metoprolol and acetate adsorption to AC are presented in Table 3.1. The isotherms were obtained from triplicates at 4 different concentrations (N=12).

K_f for metoprolol adsorption was on average 125 times higher than for acetate adsorption. The difference in sorption is largely explained by electrostatic effects. Metoprolol is protonated at neutral pH (pKa=9.6) while acetate is present in the dissociated form at neutral pH (pKa=4.76). As acetate, Norit GAC is negatively charged at neutral pH resulting in strong repelling forces between the acetate ion and the carbon surface.

Table 3.1. *Freundlich* constants for metoprolol adsorption on virgin Norit GAC in presence of different concentrations of acetate and for acetate adsorption on virgin Norit GAC in presence of different concentrations of metoprolol (N=the size of the sample set)

Metoprolol adsorption in presence of acetate					Acetate adsorption in presence of metoprolol				
Acetate concentration (mg/L)	K_f (mg/g)(L/mg) ^(1/n)	1/n	R^2	N	Metoprolol concentration (mg/L)	K_f (mg/g)(L/mg) ^(1/n)	1/n	R^2	N
0.00	62.0	0.31	0.98	12	0.00	0.2	0.59	0.82	12
4.32	61.6	0.25	0.94	12	0.92	0.2	0.63	0.80	12
15.8	58.9	0.29	0.97	12	3.79	0.4	0.48	0.91	12
65.2	56.0	0.29	0.94	12	16.1	0.5	0.48	0.76	12
262	63.7	0.30	0.95	12	61.6	0.2	0.57	0.66	12
1042	61.3	0.30	0.96	12	255	0.8	0.63	0.95	12

The molecular structure of the adsorbate also influences the distribution between the water phase and the AC surface, e.g., the hydrophobic phenol ring makes metoprolol less soluble in water (Log K_{ow} metoprolol=1.88) compared to the highly soluble acetate (Log K_{ow} Acetate=-0.17).

The correlation between *Freundlich* adsorption constants K_f for metoprolol adsorption to Norit GAC and the dissolved acetate concentrations was insignificant; the Spearman correlation coefficient was $R_S=-0.14$ ($p>0.05$). Metoprolol adsorption in the presence of acetate can be described by an acetate-independent *Freundlich* model ($R^2=95$, N=72) as shown in Figure 3.1. There was no significant competitive effect due to the presence of acetate as a second sorbate on metoprolol adsorption.

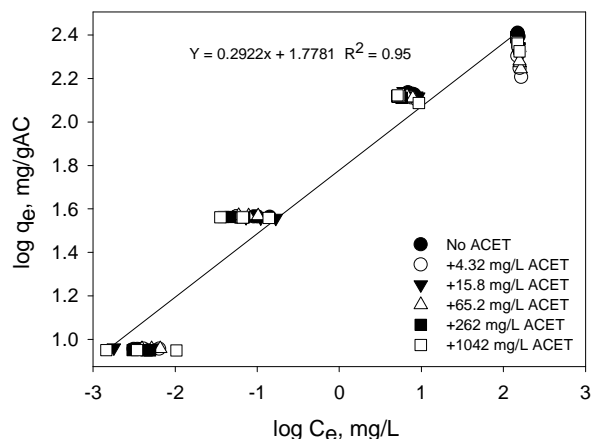


Figure 3.1. Metoprolol adsorption to virgin Norit GAC (q_e) as a function of metoprolol concentration (C_e) after reaching equilibrium for different acetate concentrations. An acetate-independent *Freundlich* model describes this data with R^2 of 0.95. In all the experiments, the AC concentration was 0.40 g/L

Metoprolol adsorption to Norit GAC is described by the following function:

$$q_e = 60.0 \cdot C_e^{0.29} \quad (3.1)$$

The high affinity of Norit GAC for a slowly biodegradable pharmaceutical such as metoprolol and its low affinity for a non-toxic easily-degradable organic material, such as acetate, is an advantage for wastewater treatment applications since the limited sorption capacity will be utilised for the immobilisation of the more harmful compound.

Another advantage of the poor adsorption of easy biodegradable organics, such as acetate, is that it will be available as growth substrates in BAC systems which might indirectly stimulate the biodegradation of slowly biodegradable organics as well.

3.1.2. Metoprolol Desorption Isotherm Experiments

The metoprolol-loaded AC from the adsorption experiments was used for the subsequent desorption experiments in metoprolol-free PBS. From q_e obtained from the adsorption experiments and the equilibrium concentrations obtained after desorption, isotherms were built. Like during the adsorption, the desorption isotherms fitted well ($R^2=0.97$) with the *Freundlich* model (Table 3.2).

Table 3.2. *Freundlich* constants for metoprolol desorption from pre-loaded Norit GAC (N=the size of the sample set)

Sample set from the adsorption experiment	K_f (mg/g)(L/mg) ^(1/n)	1/n	R^2	N
Metoprolol without acetate	98.2	0.34	0.98	12
Metoprolol + 65.2 mg/L acetate	86.1	0.30	0.96	12
Metoprolol + 1042 mg/L acetate	93.3	0.31	0.98	12

Metoprolol desorption from the loaded Norit GAC is described by the following equation:

$$q_e = 92.5 \cdot C_e^{0.31} \quad (3.2)$$

Only a part of the adsorbed metoprolol was desorbed back into the PBS medium; the K_f values obtained from the desorption experiments were therefore higher than those obtained from the adsorption experiments.

The desorption/adsorption ratio was not lower for the less loaded AC; therefore, this data does not support the hypothesis that up to a certain q (the load of AC), sorption is irreversible (Yonge et al. 1985). However, there is a clear barrier associated with the reversibility of adsorption; that is the activation energy of desorption. The relatively high activation energy for metoprolol desorption from Norit GAC might be related with its microporous nature. Mesoporous adsorbents might be more favourable for desorption (N. Klimenko et al. 2003).

3.1.3. Metoprolol Adsorption-Desorption Hysteresis in the Relation between Adsorption Capacity q_e and Equilibrium Concentration C_e

Figure 3.2 presents the linearised isotherm obtained from adsorption and the linearised isotherm obtained from desorption experiments. For a certain q_e , the concentration at the site where desorption takes place will be lower than the concentration where adsorption takes place. In other words, hysteresis is observed in the relation between q_e and C_e . Desorption could only take place if the metoprolol concentration in the bulk liquid is reduced due to the wash-out or microbial degradation. However, these processes would also have prevented AC from getting loaded in the first place. AC regeneration will therefore only take place after major changes in the loading or operation of the BAC system. This is in agreement with the findings of de Jonge *et al.* that desorption is a limiting factor for the BAC system due to the slow and inefficient desorption of hydrophobic slowly biodegradable organics (De Jonge, Breure, and Van Andel 1996).

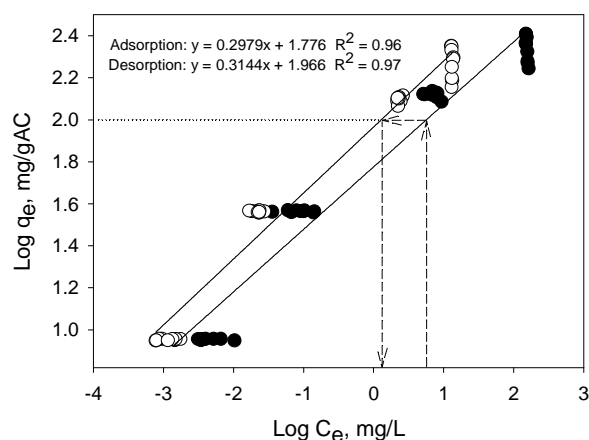


Figure 3.2. *Freundlich* adsorption isotherms of metoprolol obtained after adsorption (●) and desorption (○) on/from Norit GAC

Based on the obtained isotherms, the concentration where desorption takes place ($C_e=1.3$ mg/L; $\log C_e=0.11$ mg/L) would be 4.4 times lower than the concentration where adsorption takes place ($C_e=5.7$ mg/L; $\log C_e=0.75$ mg/L) for a given q_e (100 mgMET/gAC). The accuracy of the hysteresis prediction depends on the precision of the models. Given the R^2 values of ≥ 0.96 , we cannot determine the precise value but we can still predict the order of magnitude.

3.1.4. Metoprolol and Acetate Bisolute Biodegradation Experiments

Single solute and bisolute biodegradation experiments were performed with metoprolol and acetate to investigate the effect of an easily biodegradable organic matter, such as acetate, on the biodegradation rate of a slowly biodegradable organic material, such as metoprolol, and vice versa. The substrate concentration was plotted against time for each incubation; the biodegradation rate for the specific incubation was subsequently obtained from the maximal slope over at least 5 data points divided by the averaged initial biomass concentration. Table 3.3 presents acetate biodegradation rates expressed in mg of acetate converted per h per g of *volatile suspended solids* (VSS) for various initial metoprolol and acetate concentrations.

Table 3.3. Effect of the initial metoprolol and acetate concentration on the acetate biodegradation rate ($\text{mg}_{\text{acetate}}/(\text{h}\cdot\text{g}_{\text{VSS}})$) (standard deviation). The biomass concentration was 0.15 $\text{g}_{\text{VSS}}/\text{L}$

Initial acetate conc., mg/L	Initial metoprolol concentration, mg/L					
	0.00	0.92	3.79	16.1	61.6	255
4.32	19.3 (0.4)	16.9 (0.5)	16.7 (0.1)	16.5 (0.1)	15.1 (0.1)	13.7 (0.3)
15.8	21.8 (1.5)	20.9 (2.8)	18.8 (0.9)	24.9 (0.6)	22.9 (0.1)	18.9 (0.7)
65.2	23.1 (1.4)	30.9 (3.9)	27.7 (0.8)	24.9 (2.6)	28.7 (0.5)	25.1 (1.1)
262	283 (3.6)	256 (7.5)	242 (12)	255 (15)	232 (1.7)	239 (2.1)
1042	67.9 (3.3)	68.2 (4.9)	67.3 (1.9)	69.3 (1.3)	62.5 (6.0)	76.3 (3.1)

From the data obtained during the acetate biodegradation experiments, it is evident that metoprolol was not inhibitory for acetate biodegradation up to the concentration of 255 mg/L. The maximum acetate biodegradation rate ($283 \text{ mg}_{\text{acetate}}/(\text{h}\cdot\text{g}_{\text{VSS}})$) was achieved at acetate concentration of 262 mg/L. The increasing rate with the increasing substrate concentration follows the Michaelis-Menten kinetics; however, at a concentration of 1042 mg/L, a clear inhibitory effect of acetate was observed. A possible explanation is that acetate at neutral pH exists in ionised and protonated forms. The protonated form can be easily transformed through the membrane to the cell and dissociate; consequently, the internal pH of the cell will decrease. Microorganisms need energy to maintain the correct internal pH; therefore, this can explain that a lower biodegradation rate was observed at 1042 mg/L (Luli and Strohl 1990). Headspace and COD analysis showed that acetate was completely mineralised to carbon dioxide and water (Appendix 3). However, the calculated O_2 consumption exceeded the consumed COD; most likely, this was due to the oxidation of suspended organics which are not included in the COD measurements. It is possible that growth of microorganisms was involved in acetate and metoprolol degradation, but it resulted in the net decrease in VSS contents.

Table 3.4. Effect of the initial metoprolol and acetate concentration on the metoprolol biodegradation rate ($\mu\text{g}_{\text{metoprolol}}/(\text{h}\cdot\text{g}_{\text{VSS}})$) (standard deviation). The biomass concentration was $0.15 \text{ g}_{\text{VSS}}/\text{L}$ in all incubations

Initial acetate conc., mg/L	Initial metoprolol concentration, mg/L						
	0.009	0.09	0.45	0.92	3.79	65.2	255
0	0.12 (0.03)	2.0 (0.1)	8.5 (1.9)	24.3 (0.2)	107 (6)	1069 (136)	473 (76)
262	n.d.	n.d.	n.d.	65 (13)	87 (20)	878 (22)	2028 (101)
1024	n.d.	n.d.	n.d.	795 (39)	4922 (258)	3078 (108)	2093 (552)

Table 3.4 presents the metoprolol biodegradation rates expressed as μg of metoprolol degraded per 1 h per g of VSS for different initial metoprolol and acetate concentrations. No clear inhibitory effect of acetate on metoprolol biodegradation was observed. The presence of acetate enhanced metoprolol biodegradation up to 46 times. The highest positive effect of acetate on metoprolol biodegradation was observed when the acetate concentration in the liquid increased to 1042 mg/L . However, the removal over time shows that metoprolol and acetate were not consumed simultaneously (Figure 3.3). Apparently, metoprolol removal was not a result of co-metabolism with acetate as the primary substrate. Acetate consumption likely resulted in the growth or activation of microorganisms which were subsequently able to biodegrade metoprolol below $<0.08 \mu\text{g/L}$. This was observed in incubations where metoprolol was present from the start as well as in incubations where metoprolol was added only after acetate depletion (Figure 3.3) although in the latter case the lag phase for metoprolol removal was longer.

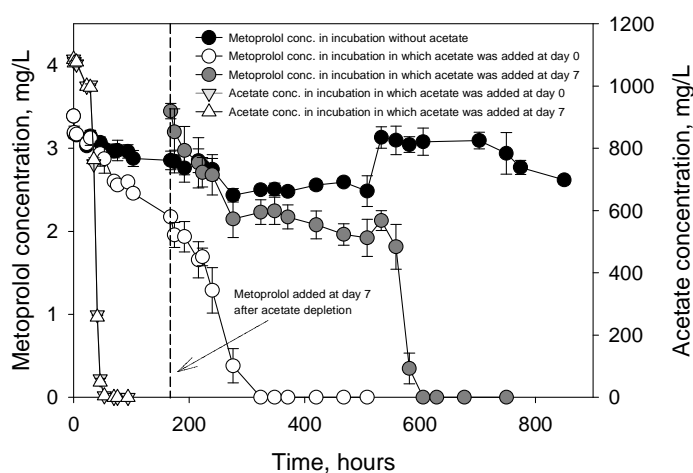


Figure 3.3. Metoprolol and acetate removal over time in 3 incubations: incubation spiked with 3.40 mg/L metoprolol and no acetate, incubation simultaneously spiked with both 3.40 mg/L metoprolol and 1042 mg/L acetate and incubation spiked with 1042 mg/L acetate at day 0 and spiked with 3.40 mg/L metoprolol at day 7 (after the acetate was depleted). The biomass concentration was $0.15 \text{ g}_{\text{VSS}}/\text{L}$ in all incubations

Unlike acetate, which was completely mineralised, the metoprolol biodegradation pathway is not completely clear. The COD and headspace measurements indicated that metoprolol was not completely mineralised but rather converted to intermediates (Appendix 3). Metoprolol acid was identified in all the samples from the incubations where metoprolol was degraded. Metoprolol acid is a major metabolite in the metoprolol biodegradation process as described elsewhere (Fang, Semple, and Song 2004; Harman, Reid, and Thomas 2011; Rubirola et al. 2014).

3.1.5. Full-Scale BAC Filter at Nieuw Amsterdam

The influent of the full-scale BAC at Nieuw Amsterdam contains approximately 1.3 µg/L metoprolol (data not shown); at this concentration, AC can take up to 8.7 mg metoprolol per gram GAC. The filters contain 170.1 tons of GAC and have a nominal flow of 10560 m³/d; it would take 300 years to saturate this AC based only on the metoprolol loading rate. Moreover, according to the isotherm calculations, 0.49 µg/L of metoprolol can be desorbed – the difference between adsorption and desorption equilibrium concentrations is 2.7 times.

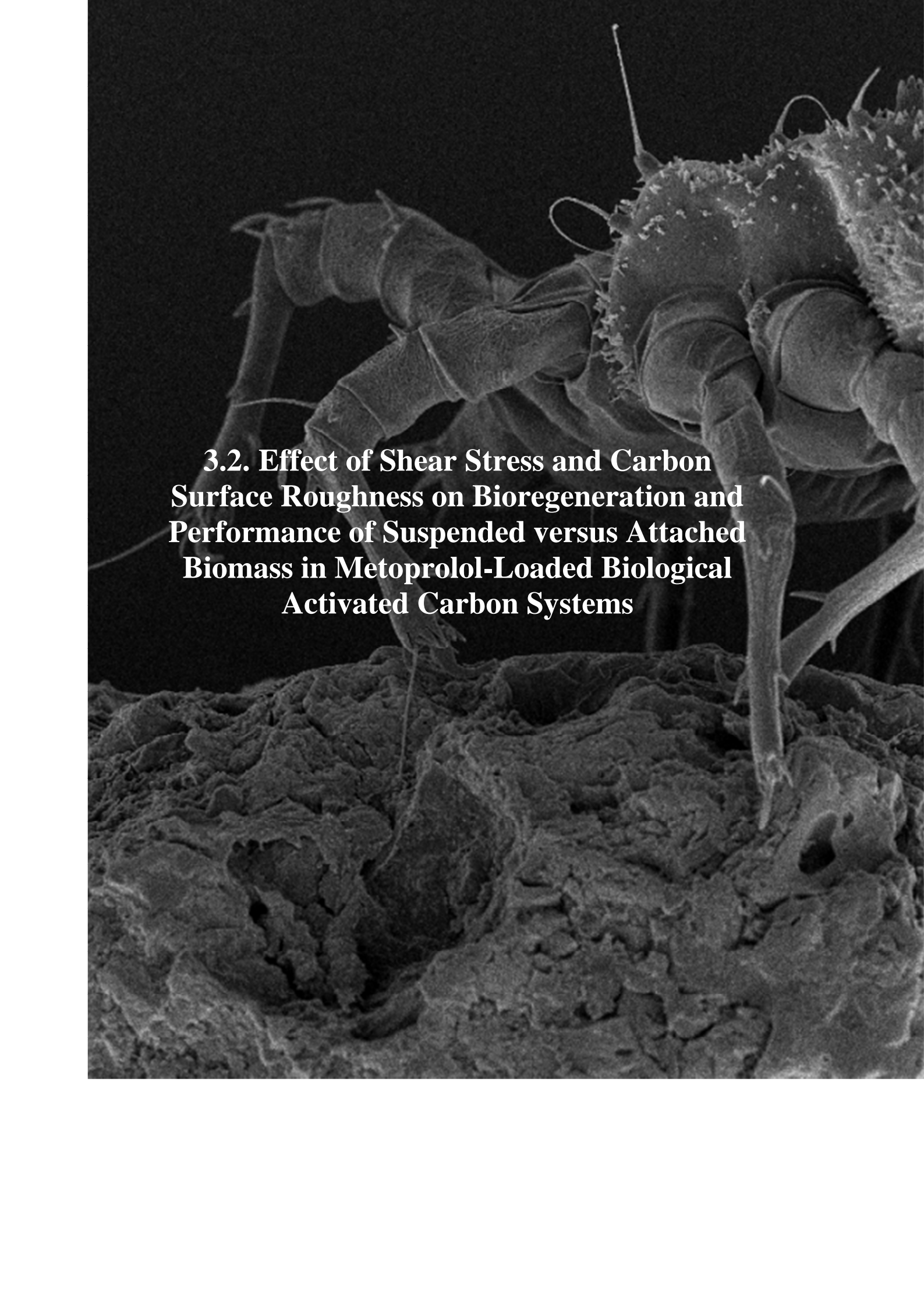
Given the observed metoprolol biodegradation rates (Table 3.4) and the threshold concentration (<0.08 µg/L), it is likely that biodegradation plays a major role in the metoprolol removal in the BAC systems similar to the one in Nieuw Amsterdam, especially when the influent also contains easily degradable organics, such as acetate. Bioregeneration (simultaneous desorption and biodegradation) might also take place. The hysteresis between adsorption and desorption does limit the regeneration; however, the threshold concentration for metoprolol biodegradation (<0.08 µg/L) is low enough to allow desorption to take place after the carbon first got loaded with 1.3 µg/L metoprolol in the influent. However, for the sorption to take place first, the loading rate needs to temporarily exceed the biodegradation rate. This would take place after a disturbance resulting in biomass loss or a drop in activity.

3.1.6. Summary of Chapter *Interdependence between Metoprolol Biodegradation and Adsorption-Desorption Hysteresis in Presence of Acetate*

The adsorption, desorption and biodegradation bisolute experiments of slowly biodegradable pharmaceutical metoprolol and easily biodegradable acetate were performed. It was established that acetate, up to a concentration of 1042 mg/L, does not influence metoprolol adsorption on Norit GAC 830 Plus. This is related with the much higher affinity of AC for metoprolol. Metoprolol adsorption on Norit GAC 830 Plus showed hysteresis between adsorption and desorption; desorption will only take place if the concentrations in the bulk liquid are reduced by a factor of 2.7 compared to the concentrations at which the carbon was loaded. However, the microorganisms present in the full-scale BAC at Nieuw-Amsterdam have a threshold concentration (<0.08 µg/L) allowing to achieve these desorption conditions after saturation to the level of 1.3 µg/L metoprolol present in the influent.

The conducted biodegradation experiments revealed that metoprolol, up to a concentration of 255 mg/L, is not inhibitory for acetate degradation by

microorganisms from the full-scale BAC at Nieuw-Amsterdam, whereas the presence of acetate enhanced metoprolol biodegradation – likely due to the growth of metoprolol degrading microorganisms on acetate. Our findings show that the presence of easily biodegradable organics in the influent enhances the biodestruction of slowly biodegradable organics in BAC systems. It is possible to apply BAC for the removal of slowly biodegradable organics. However, in order to prevent AC saturation and allow AC regeneration, active slowly biodegradable organic degrading biomass needs to be maintained in the BAC system. The consequences of this for the design and operation of BAC systems need to be explored further.

A scanning electron micrograph (SEM) showing a bacterium with a complex, multi-lobed structure and several long, thin appendages. The bacterium is positioned on a highly textured, porous surface that resembles activated carbon. The background is dark, highlighting the intricate details of the microorganism and the surface it is attached to.

3.2. Effect of Shear Stress and Carbon Surface Roughness on Bioregeneration and Performance of Suspended versus Attached Biomass in Metoprolol-Loaded Biological Activated Carbon Systems

3.2.1. Metoprolol Removal in Blank and BAC Reactors over Time

Figure 3.4 shows the cumulative metoprolol load and wash-out for three different BAC reactors and their respective abiotic blanks. In addition to 10 mg/L metoprolol, the influent contained 100 mg/L acetate that was completely degraded in all three BAC reactors within 3 h of dosing (Figure 3.5). In the blank reactors, acetate was not removed, which can be explained by the low affinity of acetate for adsorption onto AC and the absence of microbial activity.

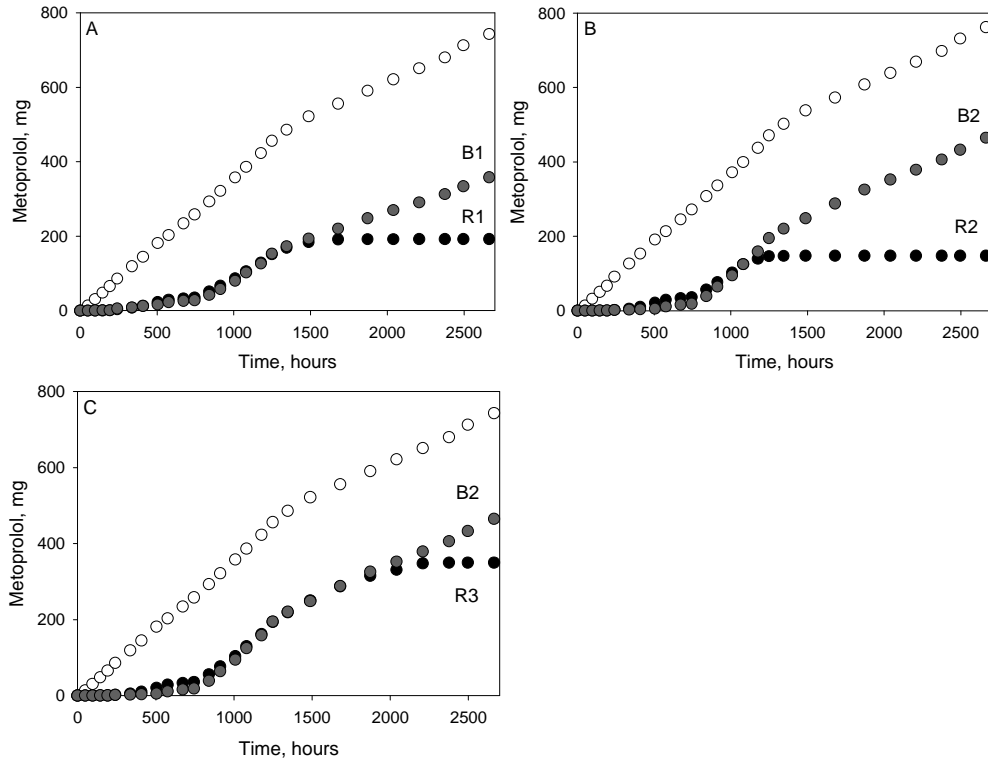


Figure 3.4. The cumulative metoprolol load (\circ), the cumulative metoprolol wash-out from the BAC reactors (\bullet), and the cumulative metoprolol wash-out from the abiotic blank reactors (\bullet). R1 and B1 were operated at a shear stress of $G=8.8 \text{ s}^{-1}$ and with smooth ($R_a=1.6 \text{ }\mu\text{m}$) Mast AC granules (A), R2 and B2 were operated at a shear stress of $G=8.8 \text{ s}^{-1}$ and with rough ($R_a=13 \text{ }\mu\text{m}$) Norit AC granules (B), whereas R3 was operated at a shear stress of $G=25 \text{ s}^{-1}$ (not applicable for the blank) and with rough ($R_a=13 \text{ }\mu\text{m}$) Norit AC granules (C)

Unlike acetate, metoprolol was initially completely removed in the blank reactors due to its high affinity to the AC granules. The affinity coupled with the absence of biomass and oxygen suggested that this removal of the non-volatile metoprolol could be attributed to adsorption. After a cumulative load of 150 mg per gram AC, metoprolol started to wash out from the blank reactors at an increasing rate until the washout rate was equal to the loading rate. The concentration in the effluent surpassed 1 mg/L after the net removal of 150 mg metoprolol per gram of AC. This is in agreement with the relation between the equilibrium concentration

and the uptake capacity obtained for metoprolol sorption onto the virgin Norit AC granules that was also used in B2, R2, and R3.

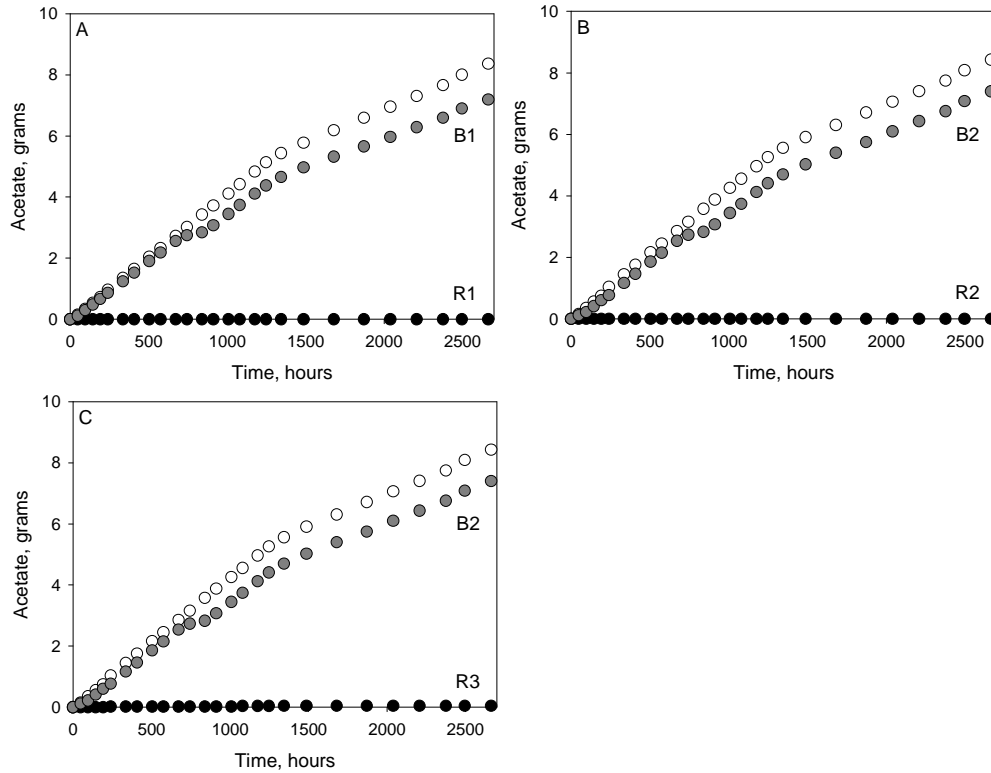


Figure 3.5. The cumulative acetate load (\circ), the cumulative acetate washout from the blank reactor (\bullet), and the cumulative acetate wash-out from the BAC reactor (\bullet). Experiments were performed at a shear stress of $G=8.8 \text{ s}^{-1}$ and with smooth ($R_a=1.6 \text{ }\mu\text{m}$) Mast AC granules (A), at a shear stress of $G=8.8 \text{ s}^{-1}$ and with rough ($R_a=13 \text{ }\mu\text{m}$) Norit AC granules (B), and at a shear stress of $G=25 \text{ s}^{-1}$ (not applicable for the blank) and with rough ($R_a=13 \text{ }\mu\text{m}$) Norit AC granules (C)

During the first 1200 h, the metoprolol washout from the three BAC reactors was the same as the washout from the blank reactors, which indicates that metoprolol was initially adsorbed rather than biodegraded. However, in contrast to the blank reactors, the washout rate from the BAC reactors flattened out again after a period of the increased washout. During the period of the increased washout, the bioavailability of metoprolol was high, which presumably resulted in an increase of the metoprolol degradation rate until the biodegradation rate had become equal to the loading rate.

The recovery of metoprolol removal occurred in R1 between hour 1400 and hour 1600, in R2 between hour 1100 and hour 1300, and in R3 between hour 1900 and hour 2100. For each BAC reactor, this recovery coincided with an increase in the suspended biomass as measured via particulate nitrogen concentration (Figure 3.6). The particulate nitrogen concentration in both blanks was below the detection

limit (<0.5 mg/L). Therefore, these results confirm that metoprolol was biologically removed during the last phase of the experiment.

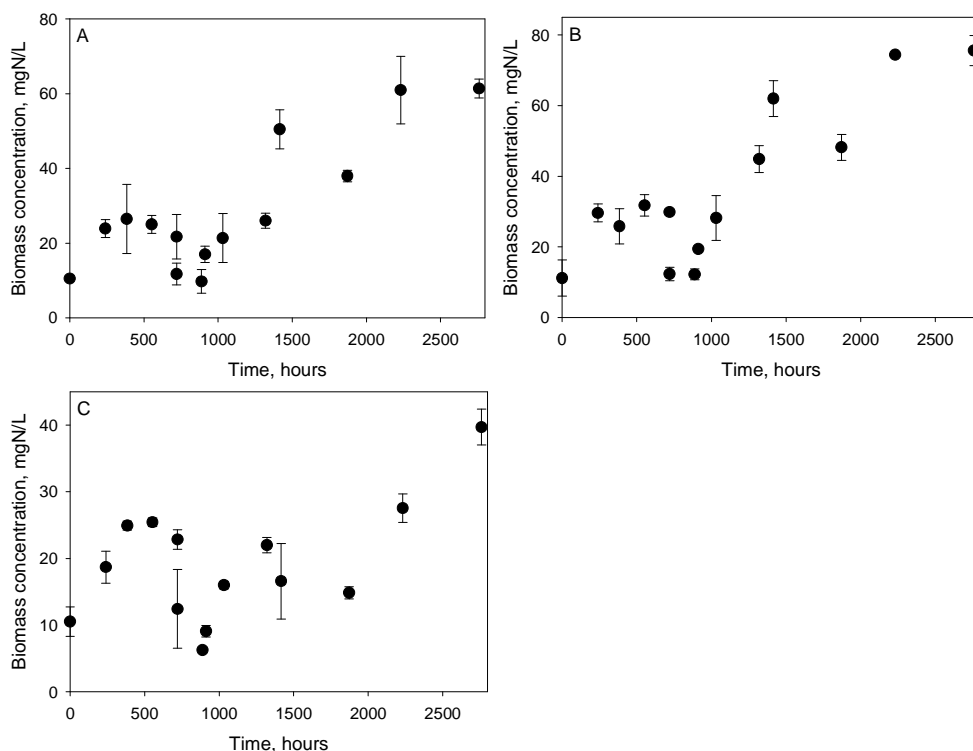


Figure 3.6. The concentration of the suspended biomass over time expressed as the total nitrogen in the BAC reactor at a shear stress of $G=8.8 \text{ s}^{-1}$ and with smooth ($R_a=1.6 \text{ }\mu\text{m}$) Mast AC granules (R1, A), BAC reactor at a shear stress of $G=8.8 \text{ s}^{-1}$ and with rough ($R_a=13 \text{ }\mu\text{m}$) Norit AC granules (R1, B), and BAC reactor at a shear stress of $G=25 \text{ s}^{-1}$ and with rough ($R_a=13 \text{ }\mu\text{m}$) Norit AC granules (R3, C). The analyses were performed in triplicate; the error bars represent standard deviations

The total metoprolol washout in the BAC reactor with rough ($R_a=13 \text{ }\mu\text{m}$) AC granules (148 mg; Figure 3.4, B) was slightly lower than in the AC reactor with the smooth ($R_a=1.6 \text{ }\mu\text{m}$) AC granules (192 mg; Figure, 3.4 A). With the rough AC granules, the total washout was lower in the BAC reactor at a shear stress of $G=8.8 \text{ s}^{-1}$ (148 mg, Figure 3.4, B) than in the BAC reactor at a shear stress of $G=25 \text{ s}^{-1}$ (350 mg; Figure 25, C).

3.2.2. Metoprolol Peak Loading Experiment with Blank and BAC Reactors

After the 2664 h long reactor runs, sequential feeding was stopped, and the reactor's operation was switched to the batch mode. The reactors were subsequently spiked with 93 mg/L metoprolol, after which, the evolution of the metoprolol concentration in the bulk liquid was monitored (Figure 3.7).

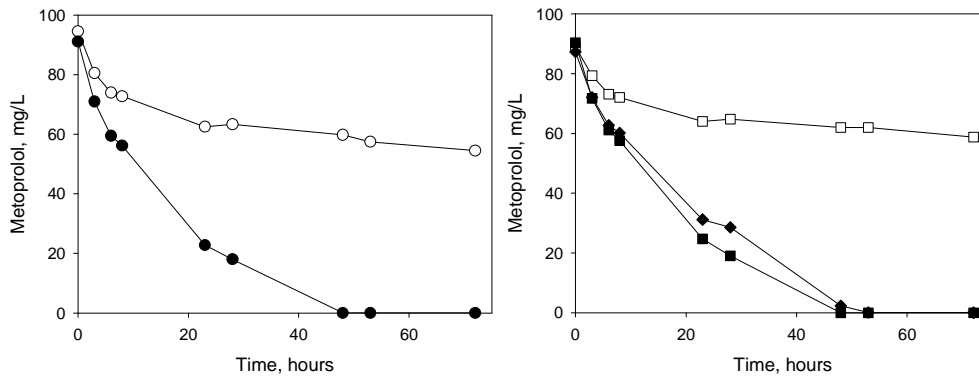


Figure 3.7. The metoprolol removal over time after spiking with 93 mg/L metoprolol in the blank reactor at a shear stress of $G=8.8 \text{ s}^{-1}$ with smooth ($R_a=1.6 \mu\text{m}$) Mast AC granules (B1, \circ), the BAC reactor at a shear stress of $G=8.8 \text{ s}^{-1}$ with smooth ($R_a=1.6 \mu\text{m}$) Mast AC granules (R1, \bullet), the blank reactor at a shear stress of $G=8.8 \text{ s}^{-1}$ with rough ($R_a=13 \mu\text{m}$) Norit AC granules (B2, \square), the BAC reactor at a shear stress of $G=8.8 \text{ s}^{-1}$ with rough ($R_a=13 \mu\text{m}$) Norit AC granules (R2, \blacksquare), and the BAC reactor at a shear stress of $G=25 \text{ s}^{-1}$ with rough ($R_a=13 \mu\text{m}$) Norit AC granules (R3, \blacklozenge). The spiking experiment was carried out immediately after the reactor experiment shown in Figure 3.4

The removal efficiency in the three BAC reactors was $>99\%$ while the removal in the blank reactors was approximately 42%. The removal in the blank reactors was poor because AC had already been saturated with 10 mg/L metoprolol in the influent during the 2664 h long reactor run. However, there was still some adsorption because of the higher initial metoprolol concentration used in this peak loading experiment.

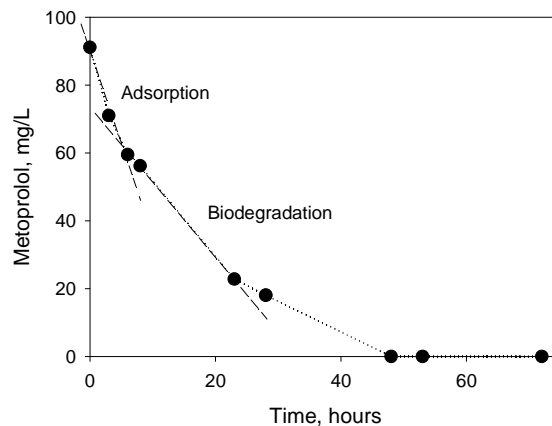


Figure 3.8. Estimation of the adsorption and biodegradation rates from the metoprolol removal over time after the peak load of 93 mg/L

Adsorption and biodegradation can both contribute to metoprolol removal; however, in a BAC reactor, immediately after the peak load, the adsorption rate considerably exceeds the rate of biodegradation (Sirotkin, Koshkina, and Ippolitov 2001). Therefore, the removal rate immediately after the peak load is an indicator for

the adsorption rate, the same as shown in Figure 3.8. This rate for the three BAC reactors was 1.5–1.8 times higher than for the blank reactors (see Appendix 18). This shows that, at the end of the reactor run, the adsorption capacity of AC in the BAC reactors was considerably higher than the adsorption capacity of AC in the blank reactors.

In contrast, between hour 1000 and hour 1200 of the operation, the washout of metoprolol was equal to the load in all the five reactors (Figure 3.4); during this time, AC was saturated with the 10 mg/L equilibrium concentration in the bulk liquid. This indicated that AC in the three BAC reactors was regenerated between the time AC became saturated (hour 1200) and the end of the reactor runs (hour 2664).

3.2.3. Surface and Porosity Measurements of AC Granules Sampled from the Blank and BAC Reactors

Table 3.5 presents the physical characteristics of virgin AC added to the reactors at the start-up and the AC sampled from the five reactors at the end of the 2664 h reactor runs. The micropore volume of AC at the end of the reactor runs was lower than the micropore volume of the virgin AC. In the blank reactors, this decrease was 97% and 95%, respectively, for B1 and B2, which can be explained by the saturation of AC with the compounds in the influent. In the BAC reactors, this decrease was lower (77%, 78%, and 81% for R1, R2, and R3, respectively). This shows that AC in the BAC reactors was at least partly regenerated between the time of AC saturation (hour 1200) and the end of the reactor runs (hour 2664).

Table 3.5. Physical characteristics of virgin AC granules from Mast and Norit and the AC granules sampled at the end of the reactor experiments, from the blank reactor at a shear stress of $G=8.8 \text{ s}^{-1}$ and with smooth ($R_a=1.6 \text{ }\mu\text{m}$) Mast AC granules (B1), the blank reactor at a shear stress of $G=8.8 \text{ s}^{-1}$ with rough ($R_a=13 \text{ }\mu\text{m}$) Norit AC granules (B2), the BAC reactor at a shear stress of $G=8.8 \text{ s}^{-1}$ and with smooth ($R_a=1.6 \text{ }\mu\text{m}$) Mast AC granules (R1), the BAC reactor at a shear stress of $G=8.8 \text{ s}^{-1}$ and with rough Norit ($R_a=13 \text{ }\mu\text{m}$) AC granules (R2), and the BAC reactor at a shear stress of $G=25 \text{ s}^{-1}$ and with rough ($R_a=13 \text{ }\mu\text{m}$) Norit AC granules (R3)

AC	Specific surface area (m^2/g)	Pore surface area, m^2/g		Pore volume, cm^3/g	
		Micropores	Mesopores	Micropores	Mesopores
Mast (virgin)	1295	1177	73	0.47	0.60
Norit (virgin)	986	863	45	0.36	0.14
B1 (Mast)	108	42	50	0.02	0.40
B2 (Norit)	86	35	29	0.02	0.10
R1 (Mast)	336	225	57	0.11	0.45
R2 (Norit)	257	160	37	0.08	0.12
R3 (Norit)	195	113	33	0.07	0.10

The volume of the mesopores did not dramatically change. This indicated that metoprolol was mainly adsorbed in the micropores, whereas the mesopores might have been required for the transportation of metoprolol between the micropores and the bulk liquid though.

3.2.4. Metoprolol Adsorption Isotherms of the AC Granules Sampled from the Blank and BAC Reactors

Adsorption experiments were performed with virgin AC granules and ACs or BAC granules sampled from the five reactors at the end of the 2664 h long reactor runs. In order to deactivate the biomass, BAC granules were dried at 105°C for 24 h. Subsequently, batch adsorption experiments were carried out at different initial metoprolol concentrations. The obtained isotherms were compared with the *Langmuir* monolayer adsorption model and the *Freundlich* adsorption model; the data fitted best with the *Langmuir* monolayer adsorption model ($R^2=0.84$ for AC from B1 and $R^2>0.96$ for the other models). The isotherm constants are presented in Table 3.6. Separation factor R_L for all the seven isotherms varied between 0 and 0.5, indicating favourable adsorption ($0 < R_L < 1$) (Fierro et al. 2008).

Table 3.6. Langmuir adsorption isotherm constants obtained with virgin AC granules from Mast and Norit and the AC granules sampled at the end of the reactor experiments, from the blank reactor at a shear stress of $G=8.8 \text{ s}^{-1}$ and with smooth ($R_a=1.6 \text{ }\mu\text{m}$) Mast AC granules (B1), the blank reactor at a shear stress of $G=8.8 \text{ s}^{-1}$ with rough ($R_a=13 \text{ }\mu\text{m}$) Norit AC granules (B2), the BAC reactor at a shear stress of $G=8.8 \text{ s}^{-1}$ and with smooth ($R_a=1.6 \text{ }\mu\text{m}$) Mast AC granules (R1), the BAC reactor at a shear stress of $G=8.8 \text{ s}^{-1}$ and with rough ($R_a=13 \text{ }\mu\text{m}$) Norit AC granules (R2), and the BAC reactor at a shear stress of $G=25 \text{ s}^{-1}$ and with rough ($R_a=13 \text{ }\mu\text{m}$) Norit AC granules (R3)

Carbon	R^2	Adsorption capacity, Q_m , mg/g	Equilibrium constant, K_L , L/mg	Separation factor R_L	Decrease in Q_m , relative to the virgin material, %
Mast (virgin)	1.00	297	0.43	0 – 0.2	n.a.
Norit (virgin)	1.00	202	0.84	0 – 0.1	n.a.
B1	0.96	37	0.18	0 – 0.3	88
B2	0.84	47	0.03	0 – 0.5	77
R1	1.00	82	0.43	0 – 0.2	72
R2	0.99	74	0.19	0 – 0.3	63
R3	0.99	55	0.33	0 – 0.2	73

n.a. = not applicable

Adsorption capacity Q_m of AC at the end of the reactor runs was lower than the adsorption capacity of the virgin AC. In the blank reactors, this decrease was 88% and 77%, respectively, for B1 and B2. In the BAC reactors, this decrease was 72%, 63%, and 73% for R1, R2, and R3, respectively. The adsorption capacity is the 3rd parameter, next to the metoprolol removal rates, immediately after the peak load (Figure 3.7) and the decrease in the micropore volumes (Table 3.5) showing that the AC granules were regenerated in the BAC reactors after first being saturated to 10 mg/L metoprolol.

In order to assess to what extent metoprolol adsorption (Table 3.6) was dependent on the physical characteristics of AC (Table 3.5), Spearman rank correlation coefficients were calculated. This correlation coefficient describes the relationship between two variables based on the ordinal level while using ranking.

By employing rank statistics, variables do not need to be assigned relationship distributions (Brown 2002). Statistically significant correlations were observed between the micropore volumes and the adsorption capacity and between the surface area and the adsorption capacity; Spearman correlation coefficients were $R_s=0.99$ and $R_s=0.96$ for $p<0.05$, respectively. When the micropore volume and the surface area were plotted against the adsorption capacity, a linear relation appeared (Figure 3.9).

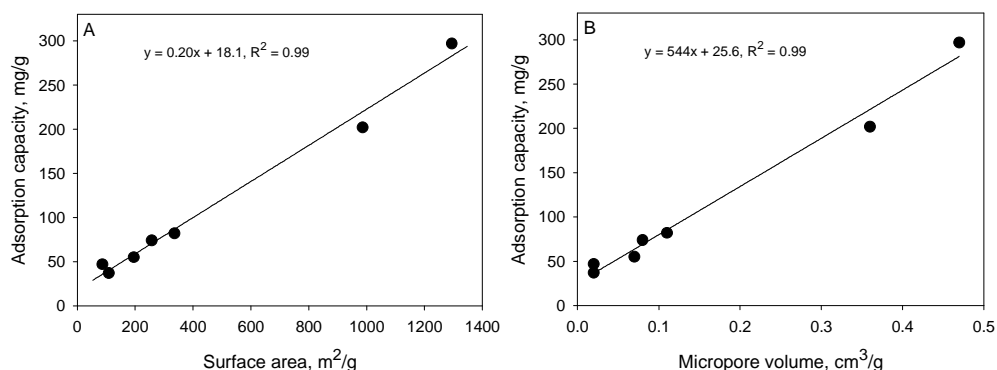


Figure 3.9. Relationship of adsorption capacity versus surface area (A) and pore volume (B) of virgin ACs and metoprolol loaded ACs from the reactors

The correlation between the mesopore volume and the adsorption capacity was poor ($R=0.56$; $p=0.15$), which supported the hypothesis that adsorption occurred mainly in the micropores while mesopores may have facilitated the transport of metoprolol between the pores and the bulk liquid (Ebie et al. 2001).

3.2.5. Morphology and Concentration of the Suspended Biomass and Biomass Attached to the AC Granules Sampled from BAC Reactors

The biofilm development on AC granules during the 2664 h reactor runs was analysed with scanning electron microscopy (Figure 3.10) and optical microscope (Figure 3.11). Small biofilm aggregates were found on the surface of the smooth ($R_a=1.6 \mu\text{m}$) Mast carbon granules from R1, although mainly on the damaged parts of the granules. In contrast, the relatively rough ($R_a=13 \mu\text{m}$) Norit AC granules from R2 were almost completely covered with microorganisms after the 2664 h reactor run. However, the densest biofilm was observed on the AC granules from R3 BAC reactor which had a thickness ranging from 50 to 400 μm .

The total protein counts were used as a measure for the biomass amount on AC granules. The total protein count on AC granules from R3 BAC reactor was 2.6 mg proteins per gram AC. The protein content on AC granules from R1 and R2 BAC reactors was $<0.5 \text{ mg/g AC}$, which is too low a value for accurate quantification.

R3 contained the same rough Norit AC granules as R2, but the mixing rate was higher (the suspension was mixed at $G=25 \text{ s}^{-1}$ instead of $G=8.8 \text{ s}^{-1}$). The high shear stress resulted in formation of dense biofilms, probably because this protected the microorganisms from wash-out (Rochex et al. 2008). This is supported by our

observation of the suspended biomass; in R1 and R2, the suspended biomass was mainly present as flocks which settled well during the 6 min before a half of the liquid was replaced, while the high shear stress in R3 hampered the flocculation, which resulted in the wash-out of suspended single cells at the beginning of the experiment.

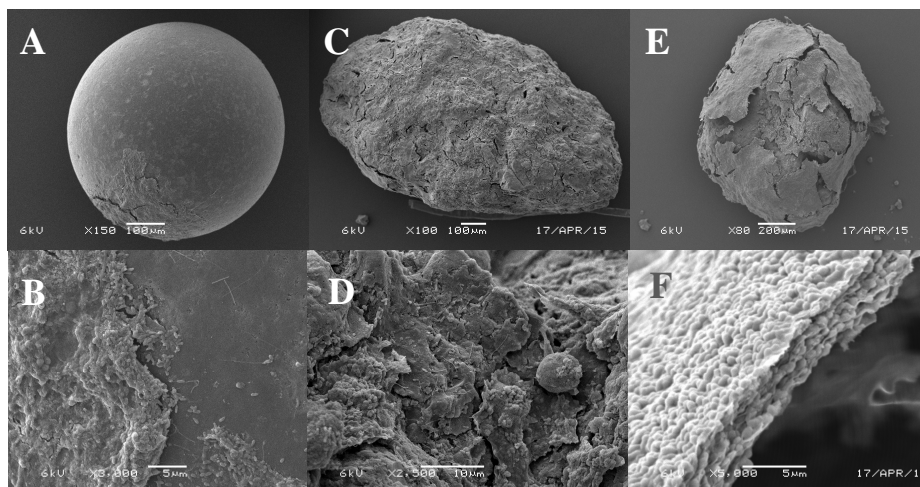


Figure 3.10. Scanning electron microscopy images of the BAC granules sampled at the end of the reactor experiments, from the BAC reactor at a shear stress of $G=8.8 \text{ s}^{-1}$ and smooth ($R_a=1.6 \text{ }\mu\text{m}$) Mast AC granules (R1, A, B), the BAC reactor at a shear stress of $G=8.8 \text{ s}^{-1}$ and rough ($R_a=13 \text{ }\mu\text{m}$) Norit AC granules (R2, C, D), and the BAC reactor at a shear stress of $G=25 \text{ s}^{-1}$ and rough ($R_a=13 \text{ }\mu\text{m}$) Norit AC granules (R3, E, F)

The high shear stress in a combination with rough AC granules in R3 BAC reactor resulted in a dense biofilm. Percival *et al.* observed a similar effect when monitoring biofilm growth on steel plates (Percival *et al.* 1999). In comparison, smooth AC granules were covered only with small biofilm aggregates.

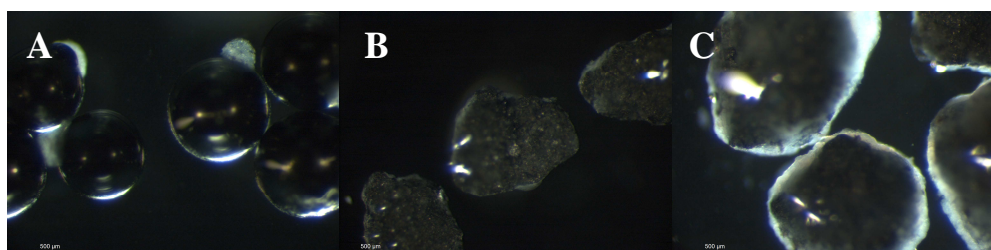


Figure 3.11. Optical microscopy images of the BAC granules sampled at the end of the reactor experiments from the BAC reactor at a shear stress of $G=8.8 \text{ s}^{-1}$ and smooth ($R_a=1.6 \text{ }\mu\text{m}$) Mast AC granules (R1, A), the BAC reactor at a shear stress of $G=8.8 \text{ s}^{-1}$ and rough ($R_a=13 \text{ }\mu\text{m}$) Norit AC granules (R2, B), and the BAC reactor at a shear stress of $G=25 \text{ s}^{-1}$ and rough ($R_a=13 \text{ }\mu\text{m}$) Norit AC granules (R3, C)

The biofilm may have a positive effect on the bioregeneration because of the short transportation distance between the pores and the biomass and because the

surface boundary layer does not have to be crossed. However, such a biofilm may also exert a negative impact due to pore blockage (Massol-Dey et al. 1995). In this study, the initial adsorption rates after the 2664 h reactor run (Figure 3.7), the remaining pore volume (Table 3.5), and the remaining adsorption capacity (Table 3.6) were lower for the AC granules from R3 compared to the AC granules from R1 or R2 BAC reactors. The net effect of the conditions which favoured the formation of a dense biofilm was therefore negative, which indicated that the negative effect of pore blockage outweighed the positive effect of biomass being in the direct proximity of the AC surface.

3.2.6. Metoprolol Biodegradation with Suspended Biomass Sampled from BAC Reactors

After the peak load experiment, AC granules were removed by filtering the reactor suspension twice through a 215 μm sieve, and the remaining biomass was used to assess the biodegradation rates. The experiments were carried out in the BAC reactors operated at the batch mode and spiked with approximately 93 mg/L metoprolol. Figure 3.12 shows the evolution of metoprolol concentrations. The suspended biomass concentration and specific rates are presented in *Appendix 18*.

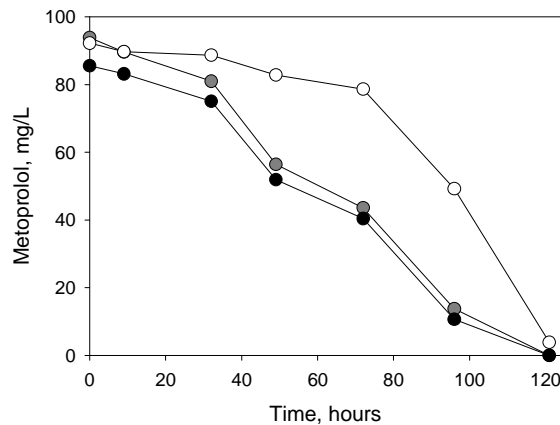


Figure 3.12. Metoprolol biodegradation by the suspended biomass from the BAC reactor at a shear stress of $G=8.8 \text{ s}^{-1}$ and with smooth ($R_a=1.6 \mu\text{m}$) Mast AC granules (R1, ●), the BAC reactor at a shear stress of $G=8.8 \text{ s}^{-1}$ and with rough ($R_a=13 \mu\text{m}$) Norit AC granules (R2, ●), and the BAC reactor at a shear stress of $G=25 \text{ s}^{-1}$ and with rough ($R_a=13 \mu\text{m}$) Norit AC granules (R3, ○)

The initial rates obtained from Figure 3.12 were about 10 times lower than those in the presence of AC (Figure 3.7), which confirms that the initial rates in Figure 3.7 were a good measure for adsorption. The delay in metoprolol removal in R3 was related to the lower suspended biomass concentration (Figure 3.6) as a result of the high shear stress. This hypothesis can be verified when the values of metoprolol removal in the BAC reactors and biomass concentrations were plotted together, as seen in Figure 3.13 below. The removal rates of metoprolol dropped down below 20% in the BAC reactors until the moment when the suspended

biomass concentration started to increase. From that moment, the metoprolol removal efficiency also increased: for R1 BAC reactor from 1200 h, R2 BAC reactor from 1000 h, and for R3 BAC reactor from 1700 h.

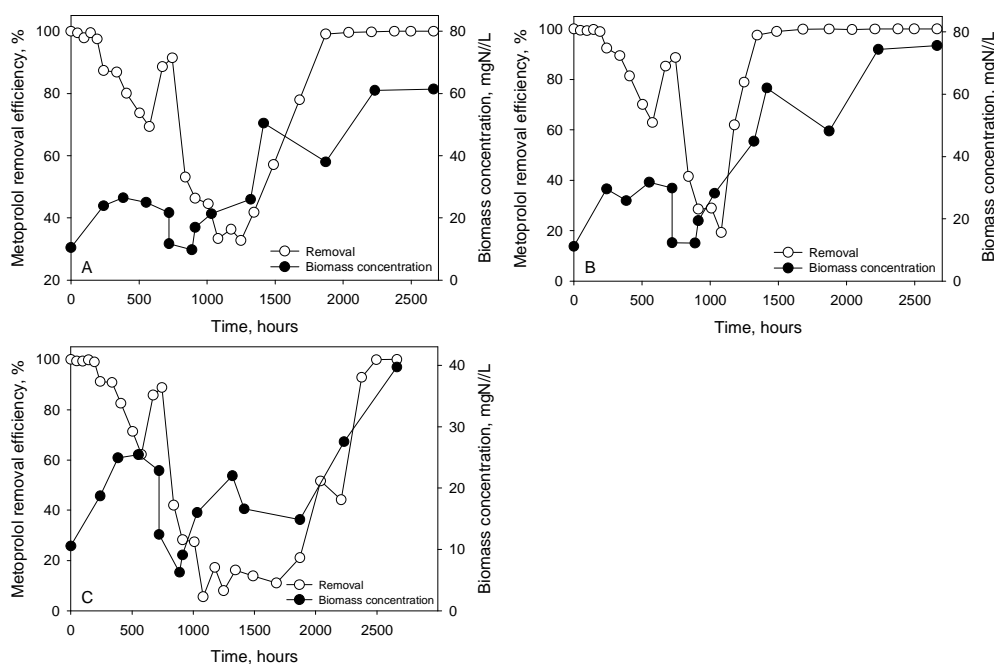


Figure 3.13. Changes in the suspended biomass concentration expressed as total nitrogen and metoprolol removal efficiency over time, in the BAC reactor at a shear stress of $G=8.8 \text{ s}^{-1}$ and with smooth ($R_a=1.6 \text{ }\mu\text{m}$) Mast AC granules (R1, A), the BAC reactor at a shear stress of $G=8.8 \text{ s}^{-1}$ and with rough ($R_a=13 \text{ }\mu\text{m}$) Norit AC granules (R1, B), and the BAC reactor at a shear stress of $G=25 \text{ s}^{-1}$ and with rough ($R_a=13 \text{ }\mu\text{m}$) Norit AC granules (R3, C)

The specific metoprolol biodegradation rates of the biomass obtained at the end of the BAC reactor experiments were approximately 5–10 times higher ($97 \text{ vs. } 8 \text{ }\mu\text{g}/(\text{mg}_{\text{total-N}}\cdot\text{h})$) than the rates of the biomass used for inoculation which were determined by Abromaitis *et al.* (Abromaitis *et al.* 2016). This can be explained by the adaptation of the biomass to the metoprolol-rich feeding water.

3.2.7. Phylogenetic Composition of the Suspended Biomass and the Biofilm on the AC Granules Sampled from Three BAC Reactors

Next generation sequencing (NGS) of partial 16S rRNA genes from the microbial community was applied on the biomass suspension used for inoculation, on the biomass suspension from the three BAC reactors after removing the AC granules, and on the biofilm growing on AC granules from R2 and R3 BAC reactors (Figure 3.14). The smooth ($R_a=1.6 \text{ }\mu\text{m}$) Mast AC granules in R1 did not contain sufficient biomass for further analysis. The samples from the reactors were taken at the end of the 2664 h long reactor runs.

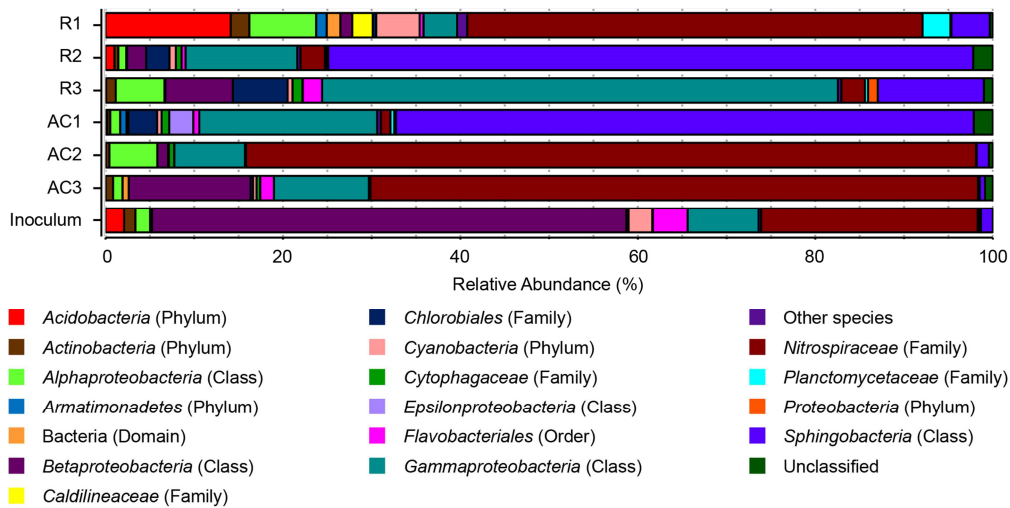


Figure 3.14. The relative abundance of specific phylogenetic groups in the biomass suspension used for inoculation, the suspension from the BAC reactor at a shear stress of $G=8.8 \text{ s}^{-1}$ and with smooth ($R^a=1.6 \text{ }\mu\text{m}$) Mast AC granules (R1), the suspension from the BAC reactor at a shear stress of $G=8.8 \text{ s}^{-1}$ and with rough ($R_a=13 \text{ }\mu\text{m}$) Norit AC granules (R2), the suspension from the BAC reactor at a shear stress of $G=25 \text{ s}^{-1}$ and with rough ($R_a=13 \text{ }\mu\text{m}$) Norit AC granules (R3), the biofilm on the AC granules from the BAC reactor at a shear stress of $G=8.8 \text{ s}^{-1}$ and with rough ($R_a=13 \text{ }\mu\text{m}$) Norit AC granules (AC2) and the biofilm on the AC granules from the BAC reactor at a shear stress of $G=25 \text{ s}^{-1}$ and with rough ($R_a=13 \text{ }\mu\text{m}$) Norit AC granules (AC3)

The suspended biomass at the end of the reactor runs was much brighter and more concentrated than the biomass used for inoculation (Figure 3.15). The 16S rRNA gene sequencing results showed prominent transformation in the relative proportions of the community members in the inoculum, BAC reactors, and the biofilm on AC. *Betaproteobacteria*, which are linked to ammonium oxidation, was dominant in the biomass suspension used for inoculation, but this phenomenon was not observed in the BAC reactor samples after 2664 h of operation. Members of the *Nitrospira* genus were also present in the inoculum; these bacteria use inorganic carbon sources, such as HCO_3^- or CO_2 , and are not linked to acetate oxidation (Daims et al. 2001). Together with *Betaproteobacteria*, they are associated with nitrification (ammonia/ammonium oxidation to nitrite and then nitrate) in wastewater treatment plants (Purkhold et al. 2000; Wang et al. 2016). In the BAC reactors fed with influent containing 170 mg/L ammonium, these lithotrophs exhibited a higher relative proportion of the total community in the AC biofilms from R2 and R3.



Figure 3.15. Photos of the biomass suspension used to inoculate three lab-scale BAC reactors (right) and the biomass suspension obtained from R2 at the end of the reactor runs (left)

Previous studies showed *Gammaproteobacteria* and *Sphingobacteria* to be potential degraders of micropollutants and xenobiotics (Bertrand et al. 2015; Grenni et al. 2013, 2014; Haiyan et al. 2007). In this study, these two phylogenetic groups were also dominant in the suspended biomass in the three BAC reactors, but not in the AC biofilms from R2 and R3. This indicated that metoprolol was predominately removed in the biomass suspension rather than in the biofilm on the AC granules. However, the relative abundance of *Gammaproteobacteria* and *Sphingobacteria* varied between the BAC reactors. *Gammaproteobacteria* were dominant in the suspended biomass from R2, while *Sphingobacteria* were dominant in the suspended biomass from R1 and R3. The cumulative metoprolol washout (Figure 3.4) and the remaining AC adsorption capacity (Table 3.6) were marginally better for R2 than for R1 and R3, which might be related with *Gammaproteobacteria* members being effective metoprolol degraders.

3.2.8. Bioregeneration of Metoprolol Loaded Carbons in BAC Reactors

Bioregeneration is often linked to BAC systems. However, for AC regeneration to occur, the concentration of the target organics at the AC surface should be low enough for desorption to take place (Ö. Aktaş and Çeçen 2007b). As shown in previous studies, this concentration is typically several orders of magnitude lower than the concentration at which the AC was loaded. The difference in adsorption and desorption equilibrium concentrations is called *hysteresis*. Microbial biomass is able to biodegrade metoprolol to $<0.08 \mu\text{g/L}$ thus overcoming adsorption-desorption hysteresis and allowing for desorption. Therefore, the bioregeneration of loaded carbon can in principle occur (Oh et al. 2012). However, in continuously-loaded BAC systems, we also have to consider possible transport limitations. Therefore, this study sought to find out whether bioregeneration actually takes place in BAC systems. Based on three lines of evidence (the initial metoprolol removal rate after the peak load, the micropore volume, and the adsorption capacity), it was shown that after saturation to 10 mg/L metoprolol, the AC granules in the BAC reactors recovered a part of their adsorption capacity. However, bioregeneration only took place after a period of net adsorption in the presence of sufficient biological degradation. In all the three BAC reactors, biodegradation

eventually became equal to the loading rate; at this stage, adsorption is no longer a factor. Xiaojian *et al.* also showed that phenol was mainly biodegraded in BAC systems rather than adsorbed (Xiaojian, Zhansheng, and Xiasheng 1991).

3.2.9. Effect of Applied Shear Stress and Carbon Surface Smoothness for Metoprolol Removal and Bioregeneration of Loaded Carbons in BAC Reactors

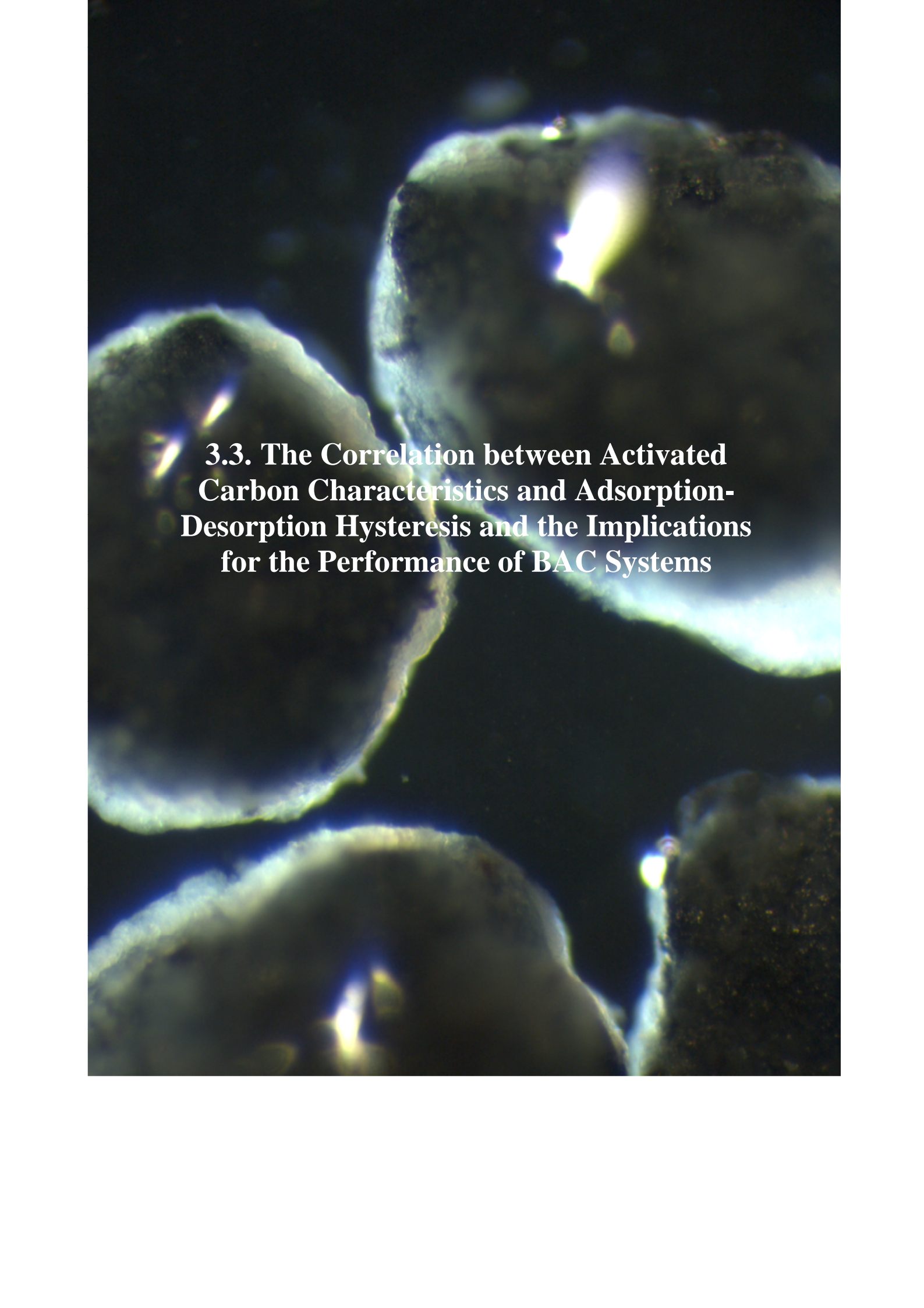
Of the three BAC reactors, the reactor with the highest amount of attached biomass (R3) showed the lowest cumulative metoprolol removal (Figure 3.4) and the lowest recovery of the adsorption capacity (Table 3.6). Apparently, a dense biofilm does not necessarily improve AC regeneration, although this was not in agreement with the data obtained by Aktas *et al.* who demonstrated that biofilm formation on the AC surface is crucial for BAC performance (Ö. Aktaş and Çeçen 2007b). In the two reactors with the higher cumulative metoprolol removal and recovery of the adsorption capacity (R1 and R2), the biofilm formation may have been poorer; however, the concentration of the suspended biomass started to increase sooner and reached higher concentrations compared to R3 (Figure 3.6). This, and the dominance of the phylogenetic group associated with pharmaceutical degradation (Figure 3.14), indicated that the suspended biomass retained in the BAC reactors was an important factor for BAC performance, and AC regeneration as well as the development of suspended biomass is hampered by the increased shear stress, such as the shear stress applied in R3.

Given the small differences between R1 and R2 in suspended biomass concentration (Figure 3.6), the development of suspended biomass was independent from the surface roughness of the AC granules. However, the cumulative metoprolol washout was 1.3 times higher in R1 than in R2 (Figure 3.4) whereas the cumulative metoprolol washout in B1 was 1.4 times lower than in B2. This can be explained by the higher adsorption capacity of the AC granules from Mast compared to the Norit AC granules (Table 3.6) rather than the difference in surface roughness. The better adsorption characteristics resulted in a lower metoprolol bioavailability and, therefore, it took longer (1488 h instead of 1176 h) before metoprolol biodegradation became dominant in R1 compared to R2.

3.2.10. Summary of Chapter *Effect of Shear Stress and Carbon Surface Roughness on Bioregeneration and Performance of Suspended versus Attached Biomass in Metoprolol-Loaded Biological Activated Carbon Systems*

Metoprolol, a pharmaceutical that is slowly biodegradable, and acetate are removed in mixed aerated sequential-batch reactors containing virgin AC granules and inoculated with biomass (12 mg total-N/L) from an industrial BAC filter. Metoprolol was initially removed by adsorption due to its low biological activity. After AC partial saturation and microbial growth, biodegradation became the dominant metoprolol removal mechanism. This shows that the presence of AC in biological treatment plants is beneficial since AC adsorbs pollutants during periods of low biological activity. The initially saturated AC was partly regenerated during the phase of increased biological activity. A biofilm covering the AC surface is not essential for bioregeneration. In fact, AC bioregeneration in such systems is driven by the suspended biomass rather than by the biomass attached to the AC granules.

Members of *Gammaproteobacteria* and *Sphingobacteria* lineages were identified as possible metoprolol biodegraders in the suspended biomass, while the attached biomass on the surface of AC was occupied by *Nitrospira* bacteria, which use an inorganic carbon source while gaining energy from nitrification. Shear stress enhances the formation of biofilms on the AC granules; however, this does not necessarily result in more efficient bioregeneration. The formation of suspended biomass flocks is hampered by elevated shear stress resulting in a net negative effect on AC regeneration. In contrast to granular AC with a surface roughness of $R_a=13\ \mu\text{m}$, granular AC with a smoother surface ($R_a=1.6\ \mu\text{m}$) was not overgrown by a biofilm within a period of 2664 h thus showing that the amount of biofilm on the AC particles in the BAC reactor can be controlled by the surface smoothness. These findings show that it might be possible to regenerate saturated AC by contacting it for a limited period with active suspended biomass. However, a more detailed investigation has to be conducted since bioregeneration is highly dependent on the physical characteristics of AC and active microbial biomass.

The image shows a microscopic view of several activated carbon particles. The particles are dark, irregularly shaped, and have a porous, granular texture. They are set against a dark background, which makes their edges and internal structures stand out. The lighting is somewhat uneven, with some areas appearing brighter than others, highlighting the rough surfaces and internal voids of the carbon. The overall appearance is that of a highly porous material with a complex, interconnected network of small cavities and channels.

3.3. The Correlation between Activated Carbon Characteristics and Adsorption-Desorption Hysteresis and the Implications for the Performance of BAC Systems

3.3.1. Physical Properties of AC Granules Used for Adsorption-Desorption Experiments

Adsorption and desorption are strongly related to the pore structure of activated carbon (Ruthven 1984). Therefore, N_2 adsorption and desorption analyses were performed to investigate the porosity of the ACs, used in this study. Figure 3.16 shows the distribution of micro- and mesopores for different AC granules from the companies Mast (Figure 3.16, A) and Norit (Figure 3.16, B). The micropore volume of Mast carbon granules increased, with increasing activation level and surface area, from 0.26 to 0.67 cm^3/g . A similar increase was observed for mesopore volumes (0.37 to 0.70 cm^3/g); the distribution between micro- and mesopores was more or less the same (50/50) for all Mast carbon granules (Figure 3.16, A).

Thermal activation resulted in a doubling of the micropore volume; the micropore volume of Mast granules without shell was 0.22 cm^3/g after carbonisation and 0.49 cm^3/g after activation. For the mesopores this effect was less profound. The BET, micropore surfaces and mesopore surfaces follow the same trends (Appendix 4 and Appendix 5).

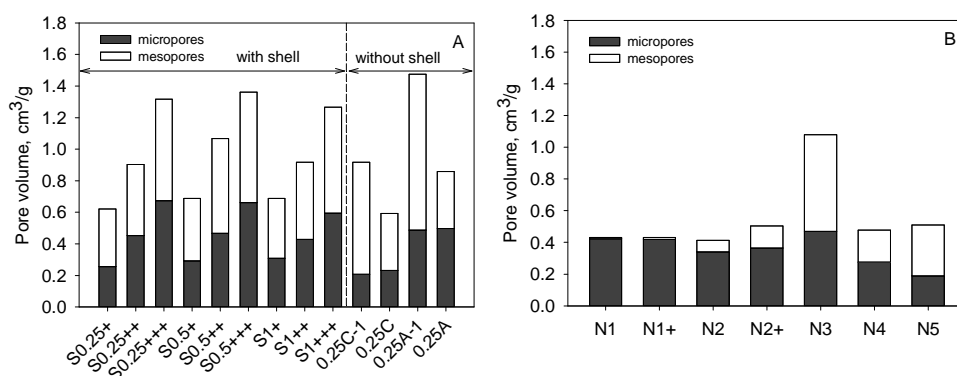


Figure 3.16. Micropore and mesopore volumes, obtained after the physical analysis of spherical Mast AC granules (A, with shell), carbonized Mast granules (A, 0.25C-1 & 0.25C), standard Mast AC granules (A, 0.25A-1 & 0.25A) and Norit AC granules (B)

The results obtained with Norit AC granules (Figure 3.16, B) showed that the material used to produce the adsorbents affected the mesopore volume. The mesopore volume of the ACs produced from coconut shells (N1 and N1+), coal (N2 and N2+), wood (N3), peat (N4) and lignite coal (N5) were respectively <0.01 cm^3/g , 0.07–0.14 cm^3/g , 0.6 cm^3/g , 0.2 cm^3/g and 0.4 cm^3/g . The mesopore volumes of Mast ACs were relatively high (similar values as for the micropores). These Mast ACs, were produced from synthetic organic polymers. These results show that relatively soft and/or less dense precursors for AC production result in a mesopore structure, while hard precursors not or hardly results in mesopores. Similar findings were observed by other authors (Mechati et al. 2015; Román et al. 2017).

3.3.2. Metoprolol Adsorption Capacity

Adsorption and desorption equilibrium experiments were performed for a range of concentrations with all twenty carbons. Both the Freundlich and Langmuir adsorption models were fitted to the experimental data of the individual experiments, see Appendix 6 and Appendix 7. To compare the two models the normalized standard deviation percentage (Δq_e) was calculated (Wu, Tseng, and Juang 2005):

$$\Delta q_e = 100 \sqrt{\frac{\sum [(q_{e,exp} - q_{e,cal}) / q_{e,exp}]^2}{(N-1)}} \quad (3.3)$$

Where:

N is the number of data points;

$q_{e,exp}$ is the measured concentration after reaching equilibrium between adsorbent and solvent;

$q_{e,cal}$ is equilibrium concentration based on the Freundlich or Langmuir model.

The calculated Δq_e values for Langmuir and Freundlich adsorption models were 4.7 and 23.7%, respectively. The better fit with the Langmuir model is also evident from the higher coefficients of determination (R^2); over 0.97 for Langmuir and between 0.81 and 0.98 for Freundlich. This indicates that the adsorption of metoprolol onto the AC approached a maximum, according to the formation of monolayer on the AC surface. Others also reported that the adsorption of metoprolol on AC followed the Langmuir adsorption model (Acero et al. 2012).

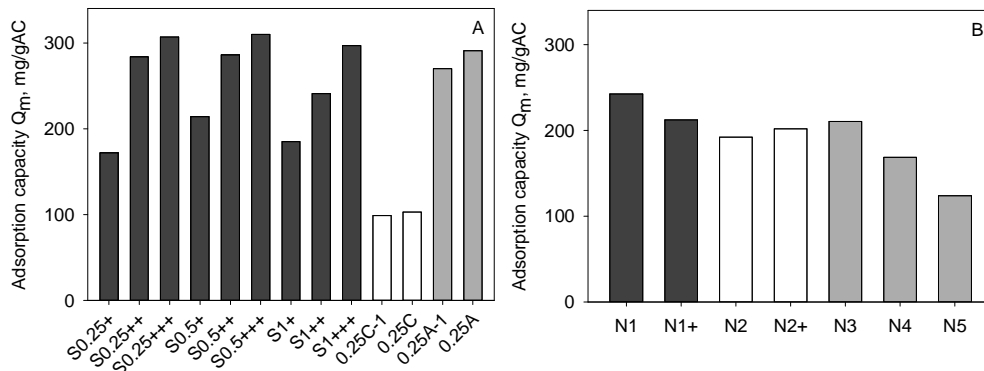


Figure 3.17. Metoprolol adsorption capacities Q_m , obtained from adsorption equilibrium experiments with spherical Mast AC granules (A, ■), carbonized Mast granules (A, □), standard Mast AC granules (A, ▒), and Norit AC granules (B)

The Q_m values, obtained from the Langmuir adsorption isotherms fitted to the experimental data, are present in Figure 3.17. The highest values were obtained with the spherical Mast AC granules with the highest level of activation (S0.25+++), (S0.5+++), (S1+++)) and standard Mast AC granules (0.25A). For the ACs from Norit, the highest Q_m values (192 to 222 mg/gAC) were obtained for ACs made from the coconut shells (N1, N1+), coal (N2, N2+) and wood (N3).

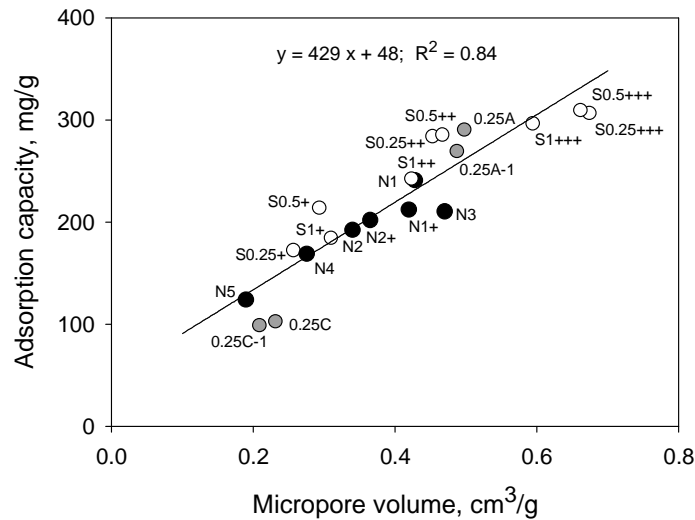


Figure 3.18. Relationship between metoprolol adsorption capacities Q_m and micropore volumes obtained from adsorption equilibrium experiments with spherical Mast AC granules, standard Mast AC granules, carbonized Mast granules and Norit AC granules

The differences in adsorption capacities can be largely explained by the differences in porosity; a linear relationship was found between the adsorption capacities and micropore volumes (Figure 3.18). The Spearman rank correlation coefficient was $R_s=0.94$, for $p<0.05$. Such relationship was also found between the adsorption capacity Q_m and both the micropore area and total surface area (Appendix 15); the Spearman rank correlation coefficients were $R_s=0.97$ and $R_s=0.91$, respectively. No statistically significant relationship was observed between the adsorption capacity and mesopore volume ($R_s=0.38$, $p<0.05$), indicating that metoprolol molecules might diffuse through the mesopores, but are at large retained in the micropores. Similar observations were made in the research of Ebie et al., indicating that the microporosity of ACs was a significant factor affecting the adsorption capacity for fenitrothion (Ebie et al. 2001).

Functional groups on the AC surface (e.g. carboxylic, carbonyl, hydroxyl, ether, quinone, lactone, anhydride, etc.) have also been shown to affect the adsorption (Wu, Tseng, and Juang 2005), in this study functional groups were not quantified, however the production method will affect the presence of such groups in the AC surface, nevertheless, no clear difference in metoprolol adsorption was observed between chemically and thermally activated carbon. Therefore, the results support the hypothesis that metoprolol adsorption mainly depends on the micropore volume, surface or area of the adsorbent.

3.3.3. Kinetics of metoprolol adsorption and desorption

Three simplified kinetic models were used to examine the adsorption kinetics: the pseudo-first order kinetic model, the pseudo-second order kinetic model and the pore diffusion model.

Pseudo-First Order Kinetic Model

The values of pseudo-first order rate constant k_1 and coefficient of determination R^2 were calculated from the plot $\log(q_e - q_t)$ versus t and can be found in Appendix 9. The calculated R^2 values were low and varied from 0.51 to 0.98. The measured q_e values did not agree with q_e based on the linear plots. This shows that metoprolol adsorption onto any of the tested ACs does not follow the first-order reaction kinetics.

Pseudo-Second Order Kinetic Model

High R^2 values (0.98 to 1.00) were obtained when the pseudo-second order kinetic model was fitted to the data. A linear relation is obtained when t/q_t is plotted against t (Appendix 10 and Appendix 11). Moreover, a good agreement between experimental and calculated q_e values is visual. The normalized standard deviation $\Delta q_e, \%$ values for the pseudo-first and pseudo-second order kinetic models were 26 and 3.0 %, respectively. Pseudo-second order kinetics corresponds to the chemisorption model as described elsewhere (Doke and Khan 2012; Tan, Ahmad, and Hameed 2009).

Figure 3.19 compares the calculated adsorption rates h (mg/g·h) for the different ACs. The highest rates were observed for the Mast spherical AC granules with the highest activation level and the smallest diameter (S0.25+++) and for one of the standard activated ACs from Mast (0.25A).

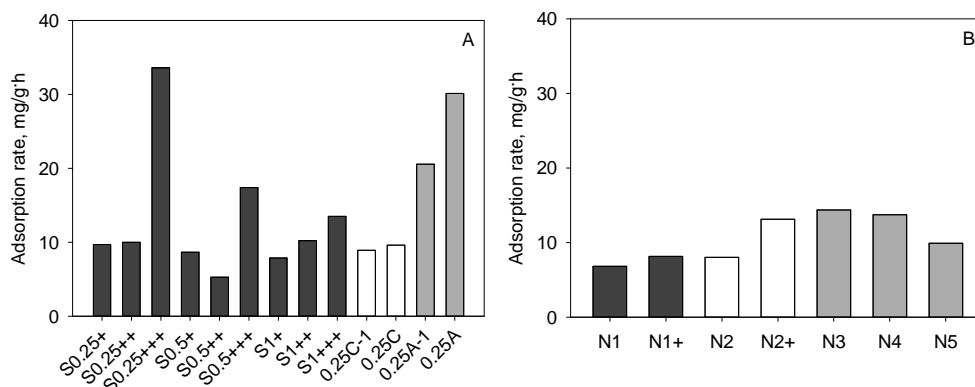


Figure 3.19. Adsorption rates h obtained from metoprolol adsorption kinetic experiments with spherical Mast AC granules (A, ■), carbonized Mast granules (A, □), standard Mast AC granules (A, ▒), and Norit AC granules (B)

Relatively low h numbers were recorded for all Norit AC granules (Figure 3.19, B). Norit AC granules made from the coconut shells or coal showed the lowest rates, the ACs made from soft materials showed somewhat higher adsorption rates, this can be related with greater amount of mesopores for Norit N3, N4 and N5.

One key parameter in BAC design and operation is the *hydraulic retention time* (HRT). Typically HRTs are pretty short (<12h). Therefore, conditions can change fast and adsorption and desorption need to follow suit for effective bioregeneration to occur in BAC reactors. In this study, the relationships between

the AC porosity and the adsorption rates were analysed statistically by calculating Spearman rank correlation coefficients R_s . Spherical Mast activated carbon granules (S0.25+ to S1+++) were excluded from the statistical analysis. The distribution of micropore and mesopore volumes in spherical shape Mast AC granules is relatively equal (50/50%); therefore, this results in uncertainties whenever R_s is calculated and the same ranks are assigned equally for mesopores and micropores. It was discovered that strong and statistically significant relationship exists between metoprolol adsorption rates versus AC mesoporic volume and mesoporic area values. The calculated R_s values at $p < 0.05$ were 0.66 and 0.70, respectively. Unfortunately, no clear relationship was observed between the micropore volume or micropore area versus the adsorption rate when spherical Mast AC granules were excluded from the calculations. When R_s was recalculated for all the 20 carbons, this expanded set of results was treated statistically and yielded a relatively clear vision about the effect of the micropore volume and the micropore area for the adsorption rates. It was found that the micropore volume ($R_s=0.52$, $p < 0.05$) and the micropore area ($R_s=0.45$, $p < 0.05$) correlated with the adsorption rate. All this indicates that micropores are important not only for the AC adsorption capacity but also for faster adsorption. However, for superior and fast metoprolol adsorption, it is more advantageous to have a mesoporic adsorbent since the intraparticle transport through mesopores is more efficient and effective, the same as described elsewhere (Ebie et al. 2001).

Another important characteristic which may affect the bioregeneration of AC in BAC reactors is its granular size. In this study, the effect of the granular size for the adsorption rates was also visible when S0.25+++ , S0.5+++ and S1+++ spherical Mast AC granules were compared. When the granular size increased from 0.25 to 1.4 mm, the adsorption rate decreased from 34 to 13.5 mg/g·h. This shows how important it is to select the right granular fraction when designing BAC reactors. Therefore, the hydraulic retention time of a BAC reactor can be reduced if the correct granular fraction is selected.

Intraparticle Diffusion Model

In order to obtain more information about the adsorption mechanism and the rate controlling steps affecting the adsorption kinetics, the experimental results were fitted to Weber's intraparticle diffusion model (Figure 3.20). Intraparticle diffusion rate constant k_{id} can be defined from linear plot q_t versus $t^{1/2}$, as described in Chapter 2.4. If the linear dependence passes through the origin, then intraparticle diffusion is a rate limiting step (Hameed, Mahmoud, and Ahmad 2008). However, in this study, multilinear regression, which consists of three regions, was observed almost for all the examined carbons except for the plots for carbonized Mast granules 0.25C-1 and 0.25C, for which, the final equilibrium stage was absent. This indicates that metoprolol adsorption was controlled not only by intraparticle diffusion. All the three regions are presented as an example in Appendix 16. The first sharp line off the plot refers to metoprolol diffusion through the boundary layer on the external carbon surface. The second, less steep, regression line is related with gradual metoprolol diffusion to the internal pores of the granules with negligible adsorption

on the external surface. Finally, the third portion shows metoprolol adsorption on the internal surface of the granules, the same as described elsewhere (Tan, Ahmad, and Hameed 2009; Wu, Tseng, and Juang 2005).

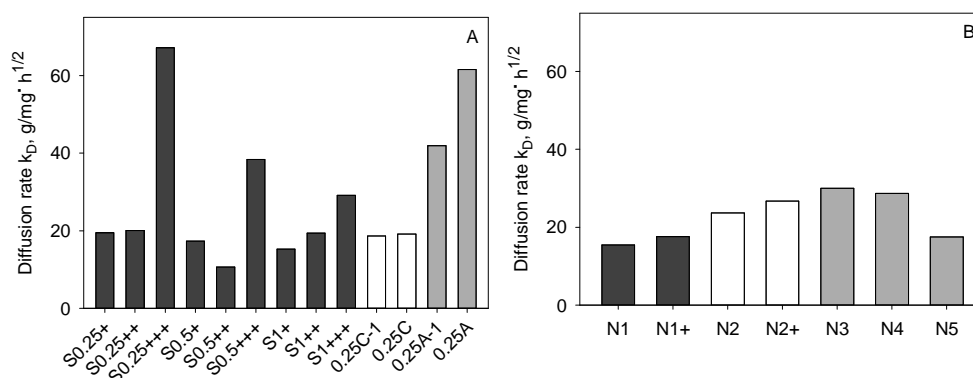


Figure 3.20. Diffusion rates obtained from metoprolol adsorption kinetic experiments with spherical Mast AC granules (A, ■), carbonized Mast granules (A, □), standard Mast AC granules (A, ▒), and Norit AC granules (B)

A strong correlation was observed between diffusion rate constant k_l and carbon surface area; Spearman rank correlation coefficient was $R_s=0.70$ at $p<0.05$. This supports the hypothesis that the higher k_l rates were obtained with carbons having a higher surface area (e.g., spherical Mast AC granules S0.25+++ , S0.5+++ and standard Mast AC granules 0.25A-1, 0.25A) resulting in enhanced metoprolol transport through the surface. The experimentally calculated metoprolol diffusion rate constants over all the three regions for Mast carbons are listed in Appendix 12.

A similar pattern was observed with Norit AC granules as highly mesoporous carbons resulted in higher metoprolol surface diffusion rates (Appendix 13). It can be seen when N1 and N1+ AC granules are compared together with N4 and N5 AC granules. The granular size of these ACs was similar; however, the amount of mesopores differed significantly resulting in higher k_l values of N4 and N5 AC granules.

The adverse effect of the granular size for metoprolol diffusion rates k_l was also visible when spherical Mast AC granules S0.25+++ , S0.5+++ and S1+++ were compared in parallel. The lowest rate was determined for 1.4 mm granular fraction (29 g/mg·h^{1/2}) whereas a 2.3 times higher rate was registered for the smallest 0.25 mm AC granules (67 g/mg·h^{1/2}). This shows that metoprolol adsorption was strictly dependent on the carbon granular size. The application of smaller granules in a BAC reactor may yield a positive effect since it results in faster adsorption. However, the use of relatively small granules might cause technical difficulties in BAC maintenance.

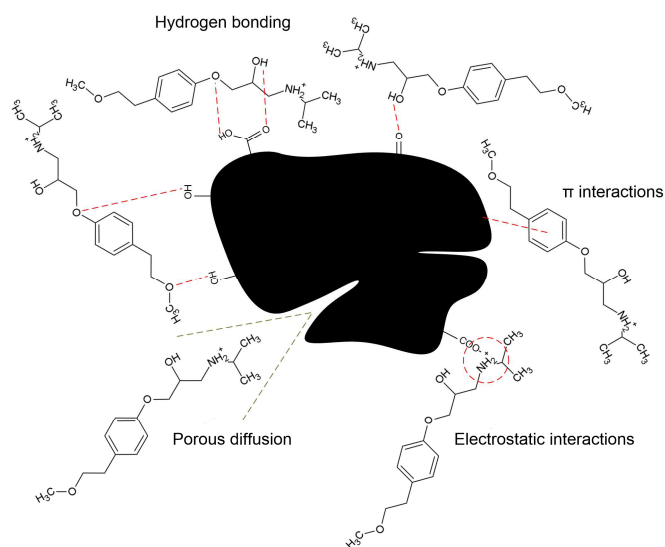


Figure 3.21. Graphical representation of possible mechanisms of metoprolol adsorption onto AC

The adsorption of metoprolol undergoes physical and chemical interactions within the AC surface. Metoprolol pK_a equals to 9.6; therefore, it exists in water in the protonated form and adsorbs pretty well on negatively charged surfaces. Metoprolol diffusion to the pores, together with hydrogen bonding to carbonyl, carboxyl and phenolic groups, might be one of the proposed metoprolol adsorption mechanisms. π - π interactions between the p-electrons in a carbonaceous adsorbent and the p-electron in the phenol aromatic ring of an adsorbate can also play a role in the adsorption process. Taking into account that metoprolol is fully dissociated at neutral pH, electrostatic interaction between the ionised carboxyl group and the amine may in principle occur.

Desorption Kinetics

As described above, relatively short HRTs are typically maintained in BAC reactors; therefore, fast adsorption and desorption of organic pollutants is required since this can directly affect the bioregeneration process. In this chapter, we calculated the metoprolol desorption rates from loaded Mast and Norit carbons. The results obtained after single cycle adsorption kinetic experiments are shown in Figure 3.22 below.

A clear difference between the desorption rates is observed for all the investigated Mast carbons. Significantly low desorption rates (0.02–0.25 mg/g·h) were registered for spherical Mast AC granules (black bars, Figure 3.22, A) in comparison with carbonized granules and standard Mast AC granules. Possibly the smooth-surfaced shell forms a barrier hampering desorption. Approximately 3.8 times lower metoprolol desorption rates were found for spherical Mast AC granules S0.25+, S0.5+ and S1+ in comparison with carbonized Mast granules 0.25C-1 and 0.25C.

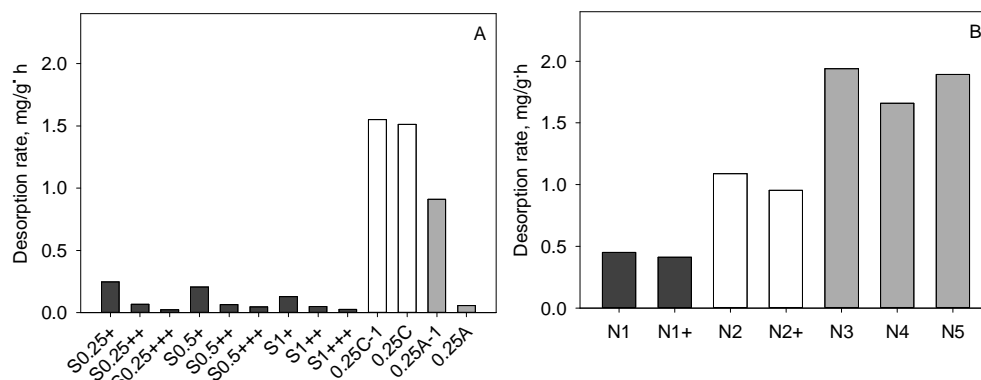


Figure 3.22. Desorption rates obtained from single cycle desorption experiments with metoprolol loaded spherical Mast AC granules (A, ■), carbonized Mast granules (A, □), standard Mast AC granules (A, ■), and Norit AC granules (B)

However, metoprolol desorption rates decreased significantly (22.4 times) with the increased surface area of spherical Mast AC granules when using S0.25+++ , S0.5+++ and S1+++ in comparison with carbonized Mast granules. This shows that the desorption process was controlled by chemisorption since more active centers were developed on the surface of highly activated spherical Mast AC granules (e.g., S0.25+++). Higher desorption rates were recorded for carbonized Mast granules because they contained a substantial amount of mesopores, macropores and a limited amount of surface active centers in the micropores causing a higher degree of adsorption irreversibility.

The granular size is another characteristic influencing metoprolol desorption rates. It was evident when spherical Mast AC granules were used for desorption experiments. The drop of metoprolol desorption rates from 0.25 to 0.02 mg/g·h was observed when the granular size of AC particles decreased from 1.4 to 0.25 mm. This once again shows that it is important to choose the right granular fraction of AC which is later used to fill BAC reactors.

Norit AC granules showed the best performance for metoprolol desorption. The highest metoprolol desorption rates (1.7–1.9 mg/g·h) were recorded for N3, N4 and N5 AC granules made from soft precursors (wood, peat and lignite). The desorption rate decreased with Norit carbons made from hard materials (N1, N1+, N2, N2+). This can be explained by their internal structure since a lower amount of mesopores in N1, N1+, N2, N2+ AC granules resulted in decreased desorption rates. This statement was investigated further by performing statistical analysis of the desorption data. It was established that the increasing micropore area resulted in decreased desorption rates ($R_s = -0.75$, $p < 0.05$) while higher desorption rates correlated well with the increased mesoporic area ($R_s = 0.62$, $p < 0.05$) of AC granules.

3.3.4. Metoprolol Adsorption-Desorption Hysteresis

The difference in the adsorption capacities when the net-desorption process occurred in comparison with net-adsorption is the so-called *hysteresis*. The reversibility of adsorption can be calculated by using the *Hysteresis Index* (HI). The

HI values close to 1 indicate a reversible adsorption process whereas low HI values show that adsorption is irreversible (J. Zhang and He 2013). HI can be calculated as a difference between the single cycle net-adsorption ($q_{e,S}$) and net-desorption ($q_{e,D}$) equilibrium capacities at a certain equilibrium concentration C_e in the liquid phase (Berhane et al. 2016; Weilin Huang; and Walter J. Weber 1997):

$$HI = \frac{q_{e,D} - q_{e,S}}{q_{e,S}} \Big|_{C_e} \quad (3.4)$$

Adsorption and desorption equilibrium capacities were calculated from non-linearised isotherms, the same as shown in Figure 3.23 below. The linearised isotherms were not used for the calculations of the equilibrium capacities since the ideal parallelism between the linearised adsorption and desorption isotherms could not be achieved for some of the investigated carbons. Therefore, the gap between linearised adsorption and desorption isotherms at lower equilibrium concentrations was narrower in comparison with the gap at higher equilibrium concentrations. This was observed for 5 carbons out of 20, and yet we ran into difficulties while using the obtained experimental data for calculations. All the adsorption and desorption isotherm model equations can be found in Appendix 14.

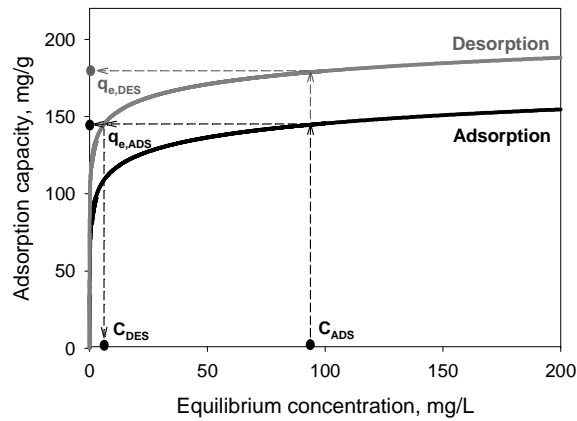


Figure 3.23. Metoprolol adsorption and desorption isotherms of spherical Mast AC granules S0.25+ calculated on the grounds of the natural logarithm model at 93 mg/L equilibrium concentration

The range of the initial metoprolol concentrations used during the adsorption kinetic experiments in this study varied from 1 to 300 mg/L. Moreover, the adsorption kinetic experiments with all the 20 carbons were performed while using initial metoprolol concentration of 93 mg/L, the same as during the adsorption and biodegradation kinetic experiments with the lab-scale BAC reactors (Chapter 3.2). Therefore, the concentration of 93 mg/L was also selected for the calculations of HI. All the calculated HI values for Mast and Norit carbons are shown in Figure 3.24.

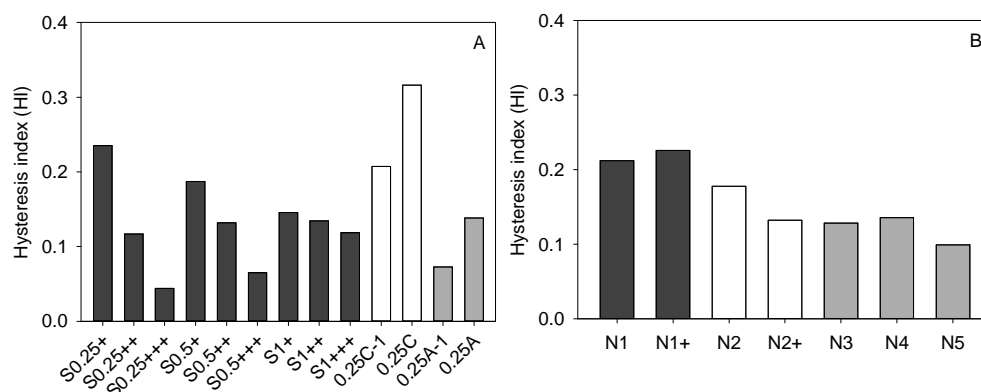


Figure 3.24. Adsorption-desorption hysteresis indexes calculated at 93 mg/L metoprolol equilibrium concentration for spherical Mast AC granules (A, ■), carbonized Mast granules (A, □), standard Mast AC granules (A, ▒), and Norit AC granules (B)

The calculated HI indexes for Mast carbons decreased with the increased surface area of the carbon (Figure 3.24, A); therefore, a relatively strong correlation between HI and BET was observed (with Spearman rank correlation coefficient equaling to $R_s = -0.65$ when $p < 0.05$). The least activated spherical Mast AC granules S0.25+ and S0.5+ (BET around $800 \text{ m}^2/\text{g}$) showed considerably higher HI values varying from 0.19 to 0.23. In comparison, spherical Mast AC granules S0.25+++ , S0.5+++ and S1+++ featuring a high surface area (BET around $1800 \text{ m}^2/\text{g}$) resulted in significantly lower HI values (0.04–0.12). Difficulties might arise if this type of AC were used in a BAC reactor because the bioregeneration of the loaded carbon could be insufficient.

However, carbonized Mast granules 0.25C-1 and 0.25C showed the highest hysteresis which varied from 0.21 to 0.32 (Figure 3.24, A). This can be explained by the mesoporosity of carbonized Mast granules. The ratio between the mesoporic and microporic volumes for 0.25C-1 and 0.25C was 3.4 and 1.6, respectively, which is almost the double value of spherical Mast AC granules S0.25+++ , S0.5+++ and S1+++ (ratio 1.1). The higher number of mesopores and the limited amount of surface active centers of the carbonized Mast granules positively influenced metoprolol desorption. Carbonized Mast 0.25C-1 and 0.25C granules might be used as an alternative adsorbent in the BAC reactor for metoprolol removal from wastewater streams. Unfortunately, the poor mechanical strength and the low sorptive capacity of charcoal might limit the application of carbonized Mast granules for wastewater treatment.

The calculated HI values for metoprolol adsorption/desorption on Norit AC granules were somewhat comparable in between (Figure 3.24, B). The highest HI values of 0.21 and 0.23 were calculated for N1 and N1+ AC granules, respectively. The lower HI values (0.10–0.13) were calculated for mesoporous Norit N3, N4 and N5 AC granules which showed relatively good metoprolol desorption rates (Figure 3.22, B). Typically, mesopores promote faster desorption; thus our data corroborates other scholarly sources (Ö. Aktaş and Çeçen 2007b). Moreover, low HI values

indicate that adsorption tends to lead to irreversibility; thus the application of this type of the adsorbents is disadvantageous.

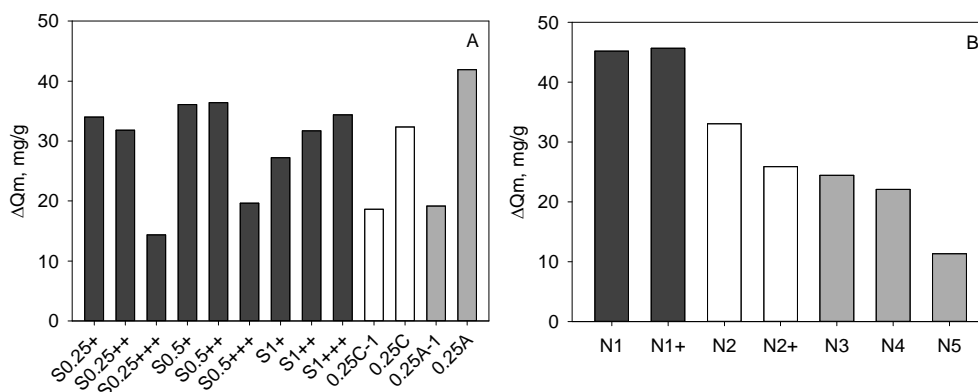


Figure 3.25. Difference (mg/g) in metoprolol sorption capacities after adsorption and desorption calculated at equilibrium concentration of 93 mg/L for spherical Mast AC granules (A, ■), carbonized Mast granules (A, □), standard Mast AC granules (A, ▒), and Norit AC granules (B)

The calculated differences in metoprolol sorption capacities ΔQ_m after adsorption and desorption showed a similar trend to that of HI calculations. The highest ΔQ_m was calculated for spherical Mast AC granules S0.25+, S0.25++, S0.5+, S0.5++ and S1+++; carbonized AC granules 0.25C-1 and standard AC granules 0.25A (Figure 3.25, A). No clear relationships were registered between ΔQ_m and carbon characteristics. However, it could be clearly seen that the difference between almost all the Mast carbons was relatively small, which showed the limiting effect of the carbon surface area and porosity. Carbons featuring the lowest and the highest surface areas and the total pore volumes desorbed similar amounts of metoprolol. This indicates that ACs having lower adsorption capacities and lower amounts of pore volumes are more efficient in desorption – thus the bioregeneration of these adsorbents tends to be more efficient.

Norit microporous AC granules N1 and N1+ showed a better performance for metoprolol desorption in comparison with mesoporous analogues N3, N4 and N5 (Figure 3.25, B). This can be related with the direct contact of micropores with the bulk phase; therefore, more metoprolol, which is stored in the micropores, can be desorbed back to the liquid.

3.3.5. Adsorbent Selection for BAC Reactor

Experimental data obtained from the metoprolol adsorption and desorption experiments was used to select the most suitable carbon for a BAC reactor. The choice was based on specially selected parameters – the measured carbon adsorption capacity Q_m and adsorption-desorption rates as well as on the calculated adsorption-desorption hysteresis indexes (HI) including the differences between adsorption-desorption capacities ΔQ_m .

The best alternative for a BAC reactor might be carbonized Mast granules 0.25C which were produced by using special polymeric resins. The use of

carbonized 0.25C granules resulted in a moderate metoprolol adsorption rate (9.6 mg/g·h) which is one of the highest desorption rates among all the investigated carbons (1.5 mg/g·h), the highest HI index (0.32) and the best overall regeneration (24%), as shown in Figure 3.26. It is essential to have active microbial biomass in BAC reactors; therefore, the bioavailability of metoprolol has to be sufficient for the proper maintenance of the microbial population. This can be achieved when carbon has a nominal adsorption capacity and adsorbs metoprolol relatively fast, whereas the desorption process is comparably rapid. Similar conclusions were drawn during lab-scale BAC reactor runs, when two different AC granules were used (Chapter 3.2). It was shown that the performance of the BAC reactor having AC granules with a lower total surface area and adsorption capacity was better than that of a BAC reactor filled with AC granules which were highly adsorptive as this also resulted in poor desorption. The consequence was the reduced metoprolol bioavailability; therefore, a reactor with highly adsorptive carbon was the latest to reach the steady state condition.

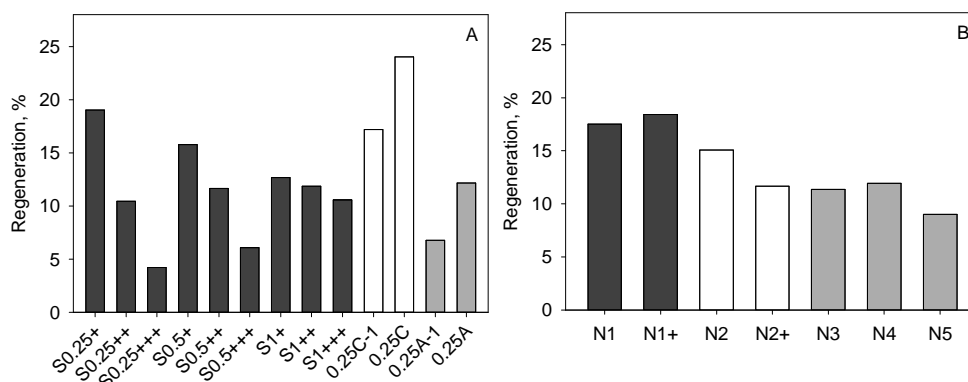


Figure 3.26. Regeneration values of metoprolol loaded spherical Mast AC granules (A, ■), carbonized Mast granules (A, □), standard Mast AC granules (A, ▨), and Norit AC granules (B) calculated at metoprolol equilibrium concentration of 93 mg/L

As it was stated before, the successful performance of BAC depends on the active microbial biomass in the reactor. The results from reactor experiments showed that metoprolol biodegradation rates together with the reactor biomass were relatively high – 32 $\mu\text{g}/\text{mg}_{\text{totalN}}\cdot\text{h}$. After the recalculation to 1 mg of dry biomass, the biodegradation rate would translate to 3.84 $\mu\text{g}/\text{mg}_{\text{biomass}}\cdot\text{h}$ or 3.84 $\text{mg}/\text{g}_{\text{biomass}}\cdot\text{h}$. The hydraulic retention time of 24 hours would be sufficient to remove 93 mg/L of metoprolol in the influent by using 0.25C granules as the adsorbent since the adsorption rate of the adsorbent is 9.6 mg/g·h. Moreover, a relatively fast desorption rate (1.51 mg/g·h) and wide adsorption-desorption hysteresis (0.32) can ensure efficient bioregeneration of carbon. Unfortunately, the use of carbonized 0.25C granules in a BAC reactor can be complicated since carbonized granules are denoted by poor mechanical strength. Thus the degradation of the particles will occur in the reactor. Norit N3 AC granules can serve as an alternative to 0.25C carbonized granules. This type of AC is denoted by good adsorption capacity ($Q_e=192$ mg/g), a

mediocre adsorption rate (8.0 mg/g·h), a good desorption rate (1.1 mg/g·h), wide hysteresis (0.18) and excellent resistance to attrition since this type of carbon is made out of coconut shell.

3.3.6. Summary of Chapter *The Correlation between Activated Carbon Characteristics and Adsorption-Desorption Hysteresis and the Implications for the Performance of BAC Systems*

The adsorption and desorption experiments with slowly biodegradable pharmaceutical metoprolol and 20 carbons which differed in porosity and precursor materials was performed in this research. The precursor material which was used to prepare the adsorbents directly influenced carbon porosity. Relatively soft materials, such as wood and peat, resulted in mesoporous carbons whereas the use of coal and coconut shells generated microporous adsorbents. The specific structure of tailored spherical AC granules S0.25+++ , S0.5+++ and S1+++ resulted in superior metoprolol adsorption. The adsorption capacity of wood based commercially available Norit AC granules N3 was relatively good as well. The kinetic adsorption and desorption tests indicated that the highest metoprolol uptake rates were achieved when spherical Mast AC granules S0.25+++ , S0.5+++ and standard AC granules 0.25A, 0.25A-1 were used. The increase in the carbon granular size negatively affected the adsorption rates because of the increased intraparticle transport. However, the desorption rates from these carbons were rather poor in comparison with carbonized Mast granules 0.25C, 0.25C-1 and all Norit AC granules. Metoprolol adsorption was controlled by diffusion through the boundary layer and diffusion to the carbon pores. The calculated hysteresis index values showed that the highest reversible adsorption is inherent with the least activated spherical Mast AC granules S0.25+ , S0.5+ (HI=0.19÷0.22), carbonized Mast granules 0.25C-1, 0.25C (HI=0.21÷0.32) and Norit AC granules N1, N1+, N2 (HI=0.18÷0.23). Norit N2 AC granules were selected as the most suitable adsorbent for BAC since the experimental results revealed that N2 carbon is characterised by good adsorption capacity, a moderate adsorption rate, a relatively high desorption rate and wide hysteresis.

4. General Discussion and Recommendations

The overall performance and bioregeneration of BAC systems treating water, polluted with slowly biodegradable pharmaceuticals, depend on many factors. Therefore, the qualitative assessment of BAC systems is needed to achieve full performance. The biodegradation and adsorption-desorption of target compounds are the main factors that have to be evaluated prior the successful operation of BAC reactors (Ö. Aktaş and Çeçen 2007b).

4.1. Interdependence between Metoprolol Biodegradation and Adsorption-Desorption Hysteresis in Presence of Acetate

Chapter 3.1 described the results of metoprolol adsorption and biodegradation experiments in absence and presence of the easy biodegradable organic compound acetate. Typically, organic carbon present in wastewater consists of easy and slowly biodegradable organic compounds. The biodegradation of slowly biodegradable organics can be enhanced through the cometabolism of using easy biodegradable organics as a carbon source.

Not acclimated microbial biomass was able to biodegrade metoprolol down to a concentration below 0.08 µg/L, the convention rate was correlated to the metoprolol concentration. The biodegradation rate of metoprolol was enhanced several times by the presence of acetate. Metoprolol was not inhibitory for active microbial biomass. However, at high concentrations, metoprolol did increase the lag phase; the time needed for the development and activation of the specific microbial community. Metoprolol biodegradation without acetate did not or hardly result in an increase in biomass concentration. This supports hypothesis that often slowly biodegradable organics are not suitable substrates for microorganisms to conserve energy for growth. Metoprolol was completely mineralised and metoprolol acid was identified as an intermediate in the metoprolol biodegradation pathway.

Given these findings, it is recommended to ensure water treated in industrial BAC systems do not only contain pollutants that are resistant to biodegradation, but also easy biodegradable compounds, as this will help to maintain healthy and active biomass. Moreover, for successful removal of slowly biodegradable pharmaceuticals, the biomass retention time in the BAC system has to be long enough to allow the active biomass to be formed. Technologically this is feasible by changing the operation and design of BAC systems in order to reduce biomass washout, i.e. by reducing the frequency at which BAC filters are backwashed or by introducing more effective biomass carriers.

4.2. Effect of Shear Stress and Carbon Surface Roughness on Bioregeneration and Performance of Suspended versus Attached Biomass in Metoprolol Loaded Biological Activated Carbon Systems

The importance of the biofilm for BAC reactor performance and bioregeneration was mentioned in numerous studies (Ö. Aktaş and Çeçen 2007b; Shen, Lu, and Liu 2012). However, the results from the experiments with BAC reactors, described in Chapter 3.2, revealed that proper maintenance of suspended biomass in the reactors might become even more beneficial. It was shown, that BAC

reactor which contained more suspended biomass outperformed BAC reactor where the biofilm formation on the surface of the AC particles was stronger. This showed that the retention of suspended biomass is crucial for BAC reactor performance and bioregeneration. More biofilm on the surface can lead to pore clogging, which reduces the intraparticle transport of the substrate, which can explain the poorer AC bioregeneration results with thick biofilms.

Three phases can be identified during the start-up of a BAC reactor. The first phase is dominated by the adsorption process; resulting in the gradual saturation of the AC. During the second phase the concentration of the pollutant in the bulk liquid increases due to a partial saturation of the AC. The microbial biomass, exposed to the higher concentrations, will become more active. During the third stage, the biodegradation process becomes dominant; there is no more net adsorption. In the case the biomass is hampered due to the wash-out or a shock load, the recovery process can be expected to follow the same three phases.

Increased shear stress has a positive effect on the biofilm formation on the AC surface. The biofilm thickness ranged from 50 to 400 μm at high shear stress, while only a very thin biofilm was observed on AC granules in the BAC reactor operated at low shear stress. When two ACs with different surface roughness were compared, it was found that biomass colonized rough surfaces much more efficiently. However, in both cases better biofilm formation did not result in better regeneration of the AC.

The phylogenetic study of the biofilm on the AC granules and the suspended biomass showed significant changes compared to the inoculum that was obtained from the full-scale BAC filter. Potential metoprolol degraders were found in suspension rather than in the biofilms. This indicates that it is beneficial to maintain suspended biomass in BAC systems. Classical BAC filters are not design for this, but it is possible to equip a BAC system with a settler to achieve this.

In this study, the best BAC performance was achieved with a suspended biomass concentration of 80 $\text{mg}_{\text{totalN}}/\text{L}$ (approximately 0.5 g/L), the hydraulic retention time was 24 hours. AC granules with a smooth surface ($R_a < 2 \mu\text{m}$) can be used in a BAC reactor to prevent fouling of the AC. Lower shear ($G=8.8 \text{ s}^{-1}$) is enough to allow for effective bioregeneration of saturated AC granules to occur. New BAC systems can be inoculated with biomass suspension from existing BAC systems. Furthermore, it might be beneficial to not use AC with the highest adsorption capacity, since this would increase the first adsorption-dominated phase after start-up, before the pollutants become bioavailable and the biological activity starts to increase.

4.3. The Correlation between Activated Carbon Characteristics and Adsorption-Desorption Hysteresis and the Implications for the Performance of BAC Systems

In the previous two paragraphs, it was discussed how the biological component is best utilised in BAC systems. Here it will be discussed how the physical properties of different types of ACs will affect the BAC process, based on the results presented in Chapter 3.3.

The precursor material used to produce AC affects the internal pore structure of the adsorbent. Soft materials, such as wood and peat, lead to the mesoporic adsorbents, while hard materials, such as coal and coconuts shells, predominately lead to the formation of the micropores. The micropore volume correlated well with the adsorption capacity, while the mesopore volume correlated with the desorption rate.

A powerful tool to estimate the bioregeneration potential of AC is the hysteresis index. This gives a good indication to which extent saturated AC can be bioregenerated. The adsorption-desorption experiments showed the highest HI values and desorption rates for carbonized adsorbent. However, because of a low resistance to attrition it is not a suitable for BAC systems. However, there were also harder AC granules tested that combined a good sorption capacity with a good regeneration potential, these were characterised by both, a high micro and meso pore volumes. The results show that 100% regeneration is not possible. This can be related to the uneven distribution of the pores, some too small and inaccessible for desorption to take place. Furthermore, some of the metoprolol may be irreversibly bounded to the surface through chemisorption.

It is recommended to use the AC with relatively high adsorption capacity ($Q_m > 200$ mg/gAC) and a high HI value (> 0.30) to allow for sufficient desorption and thus bioregeneration to occur. Smaller AC granules (0.25–0.5 mm) showed good results, but their retention in BAC reactors will be more problematic.

4.4. BAC Reactor Design for the Removal of slowly Biodegradable Pharmaceuticals from Water

The Paragraph 4.1 and 4.2 stressed the importance of biomass retention, but here the configuration of the BAC reactor is discussed in more detail. Typically BAC reactors are designed as single-pass up-flow AC filters, which developed into BAC because of biomass growth and attachment on the AC particles. Because of periodical backwashing of BAC filters, relatively low biomass retention times are obtained. This might especially be problematic for the removal of slowly biodegradable pollutants as many pharmaceuticals. Longer biomass retention times are for example achieved in sequencing batch BAC reactors (SBR–BAC). The lab-scale experiments with SBR–BAC (Paragraph 3.2) showed that suspended biomass had enough time to adapt and biodegrade the slowly biodegradable pharmaceutical metoprolol present in both, the influent and in the partial saturated AC. Such SBR–BAC would for example be suitable for the treatment of wastewater from a pharmaceutical plant. Typically, such wastewater contains drugs that are poorly biodegradable. Moreover, the wastewater flows are relatively low. The SBR operational phases are presented in a Figure 4.1 below and consist of 1) reactor filling with wastewater, 2) treatment, 3) settling after treatment, 4) effluent draining and 5) idle phase.

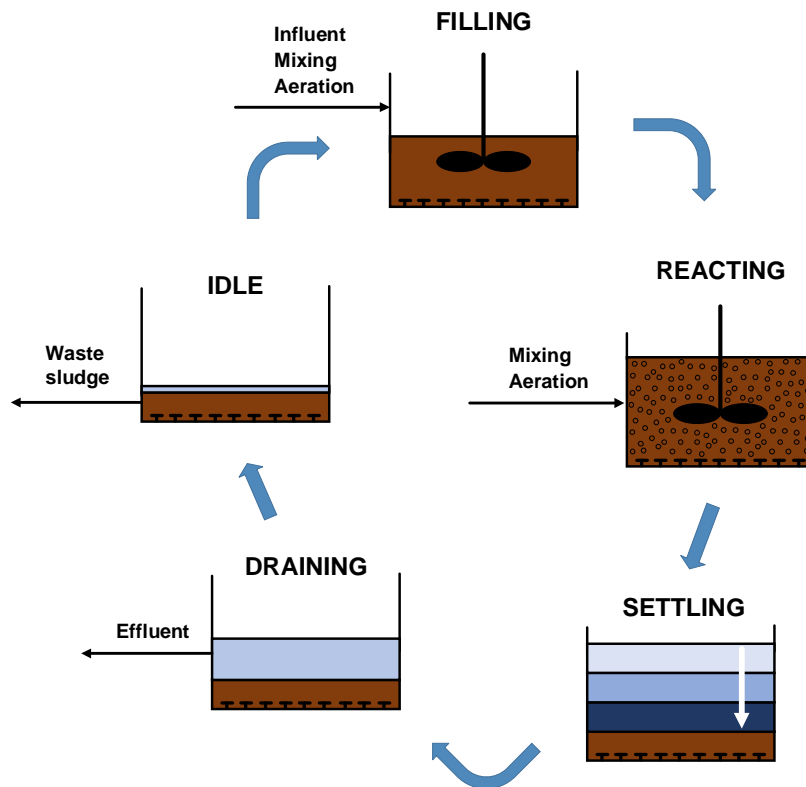


Figure 4.1. Operational stages of a sequential batch reactor (SBR)

These operational phases would also be applied in the proposed SBR-BAC reactor; however, unlike in a traditional activated sludge SBR, the retention of pharmaceuticals is guaranteed by the AC, even at start-up, peak loads or temporal biomass inhibition. The SBR-BAC needs to be aerated to support the oxidation of the pollutants; bottom-mounted aerators will also facilitate mixing of the AC-biomass suspension (Figure 4.2). The AC concentration in such system can be as high as 100 g/L, allowing for the efficient treatment of high strength wastewater.

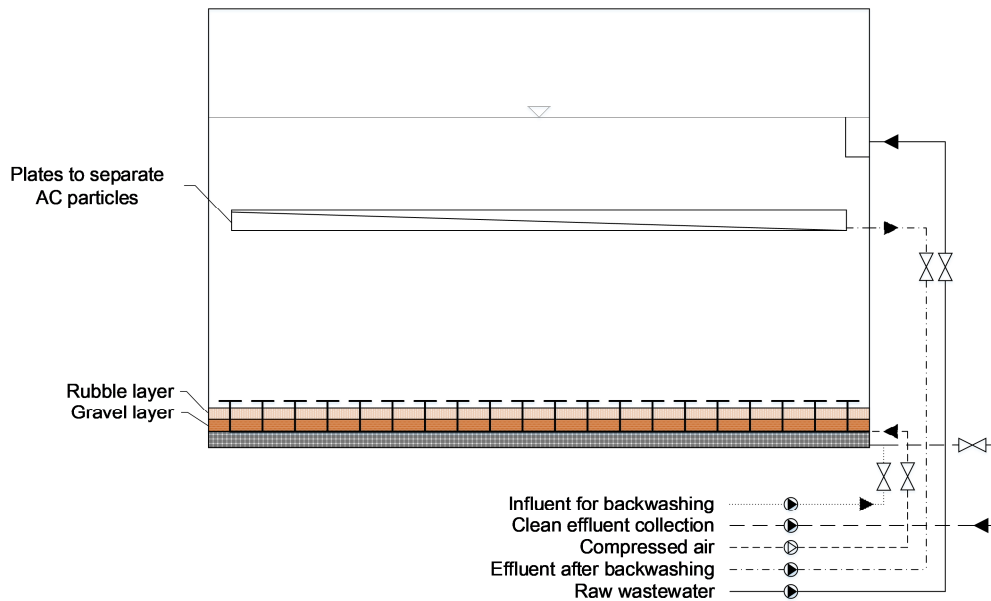


Figure 4.2. The proposed BAC-SBR design to treat wastewater polluted with slowly biodegradable pharmaceuticals

The addition of the relatively heavy gravel and sand, will allow the effluent to be recovered from the bottom, as the AC and biomass particles will not pass formed sand/gravel layer.

When needed, the periodical back-washing of the reactor is performed with clean effluent stored in the separate tanks. First, the gravel, sand, AC and biomass are loosen by flushing with a compressed air/water mixture for 10–15 minutes. After that, the liquid for back-flushing is pumped for 20 minutes over the sand/gravel/AC/biomass bed to remove the excess biomass. To keep the AC granules in the reactor during the back-washing, filter plates (0.25 mm) are constructed in the outlet chamber, which allows separating granules from the washed sludge. The recommended hydraulic retention time is at least 12 hours and the suspended biomass concentration 2–6 g/L.

5. Conclusions

The following conclusion can draw from this investigation of adsorption, desorption and biodegradation of the slowly biodegradable pharmaceutical metoprolol in BAC systems:

1. The biodegradation of slowly biodegradable pharmaceutical metoprolol is enhanced by the presence of the easy biodegradable organic compound acetate. Acetate biodegradation is not hampered by metoprolol and vice versa. Metoprolol can be biodegraded to a concentration below 0.08 µg/L. Metoprolol adsorption was not hampered by the presence of acetate. Acetate adsorption onto Norit GAC 830 Plus AC is very poor (1 mg/gAC), while compared to metoprolol adsorption (56 to 61 mg/gAC). Microbial biomass can overcome the adsorption–desorption hysteresis, by reducing the concentration in the bulk liquid below desorption equilibrium concentration. Therefore, bioregeneration of metoprolol-loaded AC is possible.
2. In BAC reactors, AC granules with a rough surface ($R_a=13\ \mu\text{m}$) give rise to good biofilm formation on the AC, while there is no or very limited biofilm formation on smooth AC granules ($R_a=1.6\ \mu\text{m}$). High shear stress in the reactor ($G=25\ \text{s}^{-1}$) results in a thicker biofilm (50–400 µm) than mediocre shear stress ($G=8.8\ \text{s}^{-1}$). However, the development of biofilms on AC granules does not result in better BAC performance or more efficient bioregeneration. A BAC reactor operated under low shear outperformed a BAC reactor operated under high shear, despite the better biofilm formation for the latter. Furthermore, bioregeneration is obtained in the BAC reactor containing smooth AC granules without biofilm. At low shear stress and with smooth AC granules there is growth of suspended biomass. AC granules can thus be regenerated by the suspended biomass; a biofilm is not needed to drive the diffusion of the pollutants out of the AC granules. Phylogenetic groups that are linked to the degradation of the pollutants as metoprolol (*Gammaproteobacteria*, *Sphingobacteria*) were found to grow in the suspension rather than in the biofilm
3. The effect of activated carbon porosity (0.41–1.48 cm³/g) and granular size (0.25–1.4 mm) for metoprolol adsorption and desorption differed with each carbon type. The carbons produced from hard materials featured a high amount of micropores (0.41–0.50 cm³/g), differently from the mesoporosity of the carbon developed from soft precursors. Microporous AC showed the best metoprolol adsorption capacities (243–310 mg/g) and adsorption kinetics (22–34 mg/g·h). Moreover, the adsorption rate was also related with the higher amount of mesopores. There was no clear relation between the hysteresis index (HI) values and carbon characteristics; however, tolerable correlation was observed between HI and mesopores (Spearman correlation coefficient $R_s=0.62$, $p<0.05$). Lower HI values ($HI<0.09$) were related with the increased carbon surface area (BET 1300–1832 m²/g) thus indicating that chemisorption

caused adsorption irreversibility, whereas carbonized granules (no activation was applied, BET <650 m²/g) showed the highest HI values (0.22–0.32).

4. Norit N3 AC granules (BET 1124 m²/g, V_{Micropores}=0.41 cm³/g, V_{mesopores}=0.27 cm³/g) were selected as the most suitable adsorbent for BAC since the experimental results showed that N3 carbon was characterised by good adsorption capacity (Q_e=192 mg/g), moderate adsorption rate (8.0 mg/g·h), fast desorption rate (1.1 mg/g·h) and significantly high hysteresis index values (0.18).

References

- ABROMAITIS, V. *et al.* (2017). Effect of Shear Stress and Carbon Surface Roughness on Bioregeneration and Performance of Suspended versus Attached Biomass in Metoprolol-Loaded Biological Activated Carbon Systems. In: *Chemical Engineering Journal*, 317, 503–511.
- ABROMAITIS, V., RACYS, V., VAN DER MAREL, P., MEULEPAS, R.J.W. (2016). Biodegradation of Persistent Organics Can Overcome Adsorption-Desorption Hysteresis in Biological Activated Carbon Systems. In: *Chemosphere*, 149, 183–189.
- ACERO, J.L., BENITEZ, F.J., REAL, F.J., TEVA, F. (2012). Coupling of Adsorption, Coagulation, and Ultrafiltration Processes for the Removal of Emerging Contaminants in a Secondary Effluent. In: *Chemical Engineering Journal*, 210, 1–8.
- AHMAD, M.A., PUAD, N.A.A., BELLO, O.S. (2014). Kinetic, Equilibrium and Thermodynamic Studies of Synthetic Dye Removal Using Pomegranate Peel Activated Carbon Prepared by Microwave-Induced KOH Activation. In: *Water Resources and Industry*, 6, 18–35.
- AKTAŞ, Ö., ÇEÇEN, F. (2007). Adsorption Reversibility and Bioregeneration of Activated Carbon in the Treatment of Phenol. In: *Water Science and Technology: a Journal of the International Association on Water Pollution Research*, 55(10), 237–244.
- AKTAŞ, Ö., ÇEÇEN, F. (2009). Cometabolic Bioregeneration of Activated Carbons Loaded with 2-Chlorophenol. In: *Bioresource Technology*, 100(20), 4604–4610.
- AKTAŞ, Ö., ÇEÇEN, F. (2006). Effect of Type of Carbon Activation on Adsorption and Its Reversibility. In: *Journal of Chemical Technology & Biotechnology*, 81(1), 94–101.
- AKTAŞ, Ö., ÇEÇEN, F. (2007a). Adsorption, Desorption and Bioregeneration in the Treatment of 2-Chlorophenol with Activated Carbon. In: *Journal of Hazardous Materials*, 141(3), 769–777.
- AKTAŞ, Ö., ÇEÇEN, F. (2007b). Bioregeneration of Activated Carbon: A Review. In: *International Biodeterioration & Biodegradation*, 59(4), 257–272.
- AL-AMRANI, W.A., LIM, P.-E., SENG, C.-E., NGAH, W.S.W. (2014). Bioregeneration of Azo Dyes-Loaded Mono-Amine Modified Silica in Batch System: Effects of Particle Size and Biomass Acclimation Condition. In: *Chemical Engineering Journal*, 251, 175–182.
- AL-GHOUTI, M.A. *et al.* (2016). Multivariate Analysis of Competitive Adsorption of Food Dyes by Activated Pine Wood. In: *Desalination and Water Treatment*, 1–12.
- ANDERSSON, A. *et al.* (2001). Impact of Temperature on Nitrification in Biological Activated Carbon (BAC) Filters Used for Drinking Water Treatment. In: *Water Research*, 35(12), 2923–2934.
- BERHANE, T.M., LEVY, J., KREKELER, M.P.S., DANIELSON, N.D. (2016). Adsorption of Bisphenol A and Ciprofloxacin by Palygorskite-Montmorillonite: Effect of Granule Size, Solution Chemistry and Temperature. In: *Applied Clay Science*, 132, 518–527.
- BERTRAND, J.-C., CAUMETTE, P., LEBARON, P., MATHERON, R. (eds.). (2015). *Environmental Microbiology: Fundamentals and Applications*. Berlin, Heidelberg: Springer.
- BHATNAGAR, A., GOYAL, M. *et al.* (2013). *Application of Adsorbents for Water Pollution Control*. Oak Park, Bentham Science Publishers.
- BHATNAGAR, A., HOGLAND, W., MARQUES, M., SILLANPÄÄ, M. (2013). An Overview of the Modification Methods of Activated Carbon for Its Water Treatment Applications. In: *Chemical Engineering Journal*, 219, 499–511.
- BOEHLER, M. *et al.* (2012). Removal of Micropollutants in Municipal Wastewater Treatment Plants by Powder-Activated Carbon. In: *Water Science & Technology*, 66(10), 2115–2121.
- BONNÉ, P.A.C., HOFMAN, J.A.M.H., VAN DER HOEK, J.P. (2002). Long Term Capacity of Biological Activated Carbon Filtration for Organics Removal. In: *Water Science and Technology: Water Supply*, 2(1), 139–146.
- BROWN, P.M.B.L.C. (2002). Environmental and Engineering Geoscience. In: *Statistics for Environmental Engineers*.
- CHA, W.S., CHOI, H.C., HA, S.R. (1998). The Buffer Effect of Biological Activated Carbon to the Shock Loadings in Sequencing Batch Reactor. In: *Environmental Engineering Research*, 3(1), 41–44.
- CRAVEIRO DE SA, F.A., MALINA, J.F. (1992). Bioregeneration of Granular-Activated Carbon. In: *Water Science and Technology*, 26(9–11), 2293–98.
- CRITTENDEN, J.C., HARZA, M.W. (2012). *MWH's Water Treatment: Principles and Design*. Hoboken, NJ, USA: John Wiley and Sons, Inc.

- CRITTENDEN, J.C. *et al.* (2012). MWH's Water Treatment. In: *MWH's Water Treatment*. Hoboken, NJ, USA: John Wiley & Sons, Inc., 1–16.
- DAIMS, H. *et al.* (2001). In Situ Characterization of Nitrospira-Like Nitrite-Oxidizing Bacteria Active in Wastewater Treatment Plants. In: *Applied and Environmental Microbiology*, 67(11), 5273–5284.
- DEBLONDE, T., COSSU-LEGUILLE, C. (2011). Emerging Pollutants in Wastewater: A Review of the Literature. In: *International Journal of Hygiene and Environmental Health*, 214(6), 442–448.
- DOKE, K.M., KHAN, E.M. (2012). Equilibrium, Kinetic and Diffusion Mechanism of Cr(VI) Adsorption onto Activated Carbon Derived from Wood Apple Shell. In: *Arabian Journal of Chemistry*, 10(1), 252–260.
- DONG, L., LIU, W., JIANG, R., WANG, Z. (2014). Physicochemical and Porosity Characteristics of Thermally Regenerated Activated Carbon Polluted with Biological Activated Carbon Process. In: *Bioresource Technology*, 171, 260–264.
- EBIE, K. *et al.* (2001). Pore Distribution Effect of Activated Carbon in Adsorbing Organic Micropollutants from Natural Water. In: *Water Research*, 35(1), 167–179.
- EDGAR, R.C. (2013). UPARSE: Highly Accurate OTU Sequences from Microbial Amplicon Reads. *Nature Methods*, 10(10), 996–998.
- EHRHARDT, H.M., REHM, H.J. (1985). Phenol Degradation by Microorganisms Adsorbed on Activated Carbon. In: *Applied Microbiology and Biotechnology*, 21–21(1–2), 32–36.
- ERLANSON, B.C., DVORAK, B.I., SPEITEL, G.E., LAWLER, D.F. (1997). Equilibrium Model for Biodegradation and Adsorption of Mixtures in GAC Columns. In: *Journal of Environmental Engineering*, 123(5), 469–478.
- FANG, J., SEMPLE, H.A., SONG, J. (2004). Determination of Metoprolol, and Its Four Metabolites in Dog Plasma. In: *Journal of Chromatography B*, 809(1), 9–14.
- FIERRO, V., TORNE-FERNANDEZ, V., MONTANE, D., CELZARD, A. (2008). Adsorption of Phenol onto Activated Carbons Having Different Textural and Surface Properties. In: *Microporous and Mesoporous Materials*, 111(1), 276–284.
- FISCHER, K., MAJEWSKY, M. (2014). Cometabolic Degradation of Organic Wastewater Micropollutants by Activated Sludge and Sludge-Inherent Microorganisms. In: *Applied Microbiology and Biotechnology*, 98(15), 6583–6597.
- GASPARD, S., NCIBI, M.C. (2014). *Biomass for Sustainable Applications: Pollution Remediation and Energy*. Cambridge, Royal Society of Chemistry.
- GIBERT, O. *et al.* (2013). Fractionation and Removal of Dissolved Organic Carbon in a Full-Scale Granular Activated Carbon Filter Used for Drinking Water Production. In: *Water Research*, 47(8), 2821–2829.
- GOEDDERTZ, J.G., MATSUMOTO, M.R., SCOTT WEBER, A. (1988). Offline Bioregeneration of Granular Activated Carbon. In: *Journal of Environmental Engineering*, 114(5), 1063–1076.
- GRENNI, P. *et al.* (2013). Degradation of Gemfibrozil and Naproxen in a River Water Ecosystem. In: *Microchemical Journal*, 107, 158–164.
- GRENNI, P. (2014). Capability of the Natural Microbial Community in a River Water Ecosystem to Degrade the Drug Naproxen. In: *Environmental Science and Pollution Research*, 21(23), 13470–13479.
- HA, S.-R., VINITNANTHARAT S., OZAKI, H. (2000). Bioregeneration by Mixed Microorganisms of Granular Activated Carbon Loaded with a Mixture of Phenols. In: *Biotechnology Letters*, 22(13), 1093–1096.
- HAIYAN, R. *et al.* (2007). Degradation Characteristics and Metabolic Pathway of 17 α -Ethinylestradiol by Sphingobacterium Sp. JCR5. In: *Chemosphere*, 66(2), 340–346.
- HAMEED, B.H., MAHMOUD, D.K., AHMAD, A.L. (2008). Equilibrium Modeling and Kinetic Studies on the Adsorption of Basic Dye by a Low-Cost Adsorbent: Coconut (Cocos Nucifera) Bunch Waste. In: *Journal of Hazardous Materials*, 158(1), 65–72.
- HARMAN, C., REID, M., THOMAS, K.V. (2011). In Situ Calibration of a Passive Sampling Device for Selected Illicit Drugs and Their Metabolites in Wastewater, And Subsequent Year-Long Assessment of Community Drug Usage. In: *Environmental Science & Technology*, 45(13), 5676–5682.
- HESS, T.F., SILVERSTEIN, J.A., SCHMIDT, S.K. (1993). Effect of Glucose on 2,4-Dinitrophenol Degradation Kinetics in Sequencing Batch Reactors. In: *Water Environment Research*, 65(1), 73–

- HUGERTH, L.W. *et al.* (2014). DegePrime, a Program for Degenerate Primer Design for Broad-Taxonomic-Range PCR in Microbial Ecology Studies. In: *Applied and Environmental Microbiology*, 80(16), 5116–5123.
- INGLEZAKIS, V.J., POULOPOULOS, S.G. (2006). *Adsorption, Ion Exchange and Catalysis: Design of Operations and Environmental Applications*. Amsterdam: Elsevier.
- JENSEN, B.P., SHARP, C.F., GARDINER, S.J., BEGG, E.J. (2008). Development and Validation of a Stereoselective Liquid Chromatography-Tandem Mass Spectrometry Assay for Quantification of S- and R-Metoprolol in Human Plasma. In: *Journal of Chromatography. B, Analytical technologies in the Biomedical and Life Sciences*, 865(1–2), 48–54.
- DE JONGE, R.J., BREURE, A.M., VAN ANDEL, J.G. (1996). Reversibility of Adsorption of Aromatic Compounds onto Powdered Activated Carbon (PAC). In: *Water Research*, 30(4), 883–892.
- DE JONGE, R.J., BREURE, A.M., VAN ANDEL, J.G. (1996). Bioregeneration of Powdered Activated Carbon (PAC) Loaded with Aromatic Compound. In: *Water Research*, 30(4), 875–882.
- JUNG, C. *et al.* (2013). Adsorption of Selected Endocrine Disrupting Compounds and Pharmaceuticals on Activated Biochars. In: *Journal of Hazardous Materials*, 263, 702–710.
- KEW, S.-L., ADNAN, R., LIM, P.-E., SENG, C.E. (2016). Bioregeneration of Cresol-Loaded Granular Activated Carbon Using Immobilized Biomass: Effects of Operational Factors and Chemical Structure of Cresol Isomers. In: *Journal of the Taiwan Institute of Chemical Engineers*, 63, 386–395.
- KHIEWWIJIT, R., KEESMAN, K.J., RIJNAARTS, H., TEMMINK, H. (2015). Volatile Fatty Acids Production from Sewage Organic Matter by Combined Bioflocculation and Anaerobic Fermentation. In: *Bioresource Technology*, 193, 150–155.
- KLIMENKO, N.A. *et al.* (2003). Bioregeneration of Activated Carbons by Bacterial Degradation after Adsorption of Surfactants from Aqueous Solutions. In: *Colloids and Surfaces A: Physicochemical and Engineering Aspects*, 230(1–3), 141–158.
- KLIMENKO, N.A. *et al.* (2002). Biosorption Processes for Natural and Wastewater Treatment – Part 1: Literature Review. In: *Engineering in Life Sciences*, 2(10), 317–324.
- KNEZEV, A. (2015). *Microbial Activity in Granular Activated Carbon Filters in Drinking Water Treatment*. Wageningen, WUR.
- KOROTTA-GAMAGE, S.M., SATHASIVAN, A. (2017). A Review: Potential and Challenges of Biologically Activated Carbon to Remove Natural Organic Matter in Drinking Water Purification Process. In: *Chemosphere*, 167, 120–138.
- KWON, K., BAE, W., OH, J., SHIM, H. (2015). Enhancing Bioregeneration of TCE-Sorbed Biological Powdered Activated Carbon by Dosing Toluene as Primary Substrate and Competitive Adsorbate. In: *KSCE Journal of Civil Engineering*, 19(3), 550–557.
- LAI, B., ZHOU, Y., YANG, P. (2013). Treatment of Wastewater from Acrylonitrile-Butadiene-Styrene (ABS) Resin Manufacturing by Biological Activated Carbon (BAC). In: *Journal of Chemical Technology & Biotechnology*, 88(3), 474–482.
- LAURENT, P., KIHN, A., ANDERSSON, A., SERVAIS, P. (2003). Impact of Backwashing on Nitrification in the Biological Activated Carbon Filters Used in Drinking Water Treatment. *Environmental Technology*, 24(3), 277–287.
- LEE, K.M., LIM, P.E. (2005). Bioregeneration of Powdered Activated Carbon in the Treatment of Alkyl-Substituted Phenolic Compounds in Simultaneous Adsorption and Biodegradation Processes. In: *Chemosphere*, 58(4), 407–416.
- LI, Z., DVORAK, B., LI, X. (2012). Removing 17 β -Estradiol from Drinking Water in a Biologically Active Carbon (BAC) Reactor Modified from a Granular Activated Carbon (GAC) Reactor. In: *Water Research*, 46(9), 2828–2836.
- LILLO-RODENAS, M.A., CAZORLA-AMOROS, D., LINARES-SOLANO, A. (2005). Behaviour of Activated Carbons with Different Pore Size Distributions and Surface Oxygen Groups for Benzene and Toluene Adsorption at Low Concentrations. In: *Carbon*, 43(8), 1758–1767.
- LINDH, M.V., FIGUEROA, D., SJÖSTEDT, J. (2015). Transplant Experiments Uncover Baltic Sea Basin-Specific Responses in Bacterioplankton Community Composition and Metabolic Activities. In: *Frontiers in Microbiology*, 6, 223.

- LIU, H. *et al.* (2015). Effect on Physical and Chemical Characteristics of Activated Carbon on Adsorption of Trimethoprim: Mechanisms Study. In: *RSC Adv.*, 5(104), 85187–85195.
- LULI, G.W., STROHL, W.R. (1990). Comparison of Growth, Acetate Production, and Acetate Inhibition of *Escherichia Coli* Strains in Batch and Fed-Batch Fermentations. In: *Applied and Environmental Microbiology*, 56(4), 1004–1011.
- VAN DER MAAS, P., MAJOUR, E., SCHIPPERS, J.C. (2009). Biofouling Control by Biological Activated Carbon Filtration: A Promising Method for WWTP Effluent Reuse. In: *IWA Membrane Technology Conference*, 1–8.
- MARCHAL, G. *et al.* (2013). Comparing the Desorption and Biodegradation of Low Concentrations of Phenanthrene Sorbed to Activated Carbon, Biochar and Compost. In: *Chemosphere*, 90(6), 1767–1778.
- MARGOT, J., ROSSI, L., BARRY, D.A., HOLLIGER, C. (2015). A Review of the Fate of Micropollutants in Wastewater Treatment Plants. In: *Wiley Interdisciplinary Reviews: Water*, 2(5), 457–487.
- MARKOVIĆ, D.D. *et al.* (2014). A New Approach in Regression Analysis for Modeling Adsorption Isotherms. In: *The Scientific World Journal*, 2014, 930879.
- MARQUEZ, M.C., COSTA, C. (1996). Biomass Concentration in Pact Process. In: *Water Research*, 30(9), 2079–2085.
- MASSOL-DEY, A.A., WHALLON, J., HICKEY, R.F., TIEDJE, J.M. (1995). Channel Structures in Aerobic Biofilms of Fixed-Film Reactors Treating Contaminated Groundwater. In: *Applied and Environmental Microbiology*, 61(2), 769–777.
- MATOVIC, M.D. (2013). *Biomass Now – Cultivation and Utilization*. Rijeka, Croatia, InTech.
- MECHATI, F. *et al.* (2015). Effect of Hard and Soft Structure of Different Biomasses on the Porosity Development of Activated Carbon Prepared under N₂/Microwave Radiations. In: *Journal of Environmental Chemical Engineering*, 3(3), 1928–1938.
- MEIDL, J.A. (1997). Responding to Changing Conditions: How Powdered Activated Carbon Systems Can Provide the Operational Flexibility Necessary to Treat Contaminated Groundwater and Industrial Wastes. In: *Carbon*, 35(9), 1207–1216.
- MUTAMIM, N.S.A., NOOR, Z.Z., ABU HASSAN, M.A., OLSSON, G. (2012). Application of Membrane Bioreactor Technology in Treating High Strength Industrial Wastewater: A Performance Review. In: *Desalination*, 305, 1–11.
- NAIDU, G., JEONG, S., VIGNESWARAN, S., RICE, S.A. (2013). Microbial Activity in Biofilter Used as a Pretreatment for Seawater Desalination. In: *Desalination*, 309, 254–260.
- OH, W.-D. *et al.* (2016). Bioregeneration of Granular Activated Carbon Loaded with Binary Mixture of Phenol and 4-Chlorophenol. In: *Desalination and Water Treatment*, 57(43), 20476–20482.
- OH, W.-D., LIM, P.-E., SENG, C.-E., SUJARI, A.N.A. (2012). Kinetic Modeling of Bioregeneration of Chlorophenol-Loaded Granular Activated Carbon in Simultaneous Adsorption and Biodegradation Processes. In: *Bioresource Technology*, 114, 179–187.
- ORLANDINI, E. (1999). *Pesticide Removal by Combined Ozonation and Granular Activated Carbon Filtration*. Rotterdam, Netherlands, A.A. Balkema.
- PERCIVAL, S.L., KNAPP, J.S., WALES, D.S. EDYVEAN, R.G.J. (1999). The Effect of Turbulent Flow and Surface Roughness on Biofilm Formation in Drinking Water. In: *Journal of Industrial Microbiology and Biotechnology*, 22(3), 152–159.
- PIETRANSKI, F. (2012). Mechanical Agitator Power Requirements for Liquid Batches. Fairfax, USA, PDH Online, 103:23.
- PURKHOLD, U. *et al.* (2000). Phylogeny of All Recognized Species of Ammonia Oxidizers Based on Comparative 16S rRNA and amoA Sequence Analysis: Implications for Molecular Diversity Surveys. In: *Applied and Environmental Microbiology*, 66(12), 5368–5382.
- PUTZ, A.R.H., LOSH, D.E., SPEITEL, G.E. (2005). Removal of Nonbiodegradable Chemicals from Mixtures during Granular Activated Carbon Bioregeneration. In: *Journal of Environmental Engineering*, 131(2), 196–205.
- QUAST, C. *et al.* (2013). The SILVA Ribosomal RNA Gene Database Project: Improved Data Processing and Web-Based Tools. In: *Nucleic Acids Research*, 41(D1), 590–596.
- QUINLIVAN, P.A., LI, L., KNAPPE, D.R.U. (2005). Effects of Activated Carbon Characteristics on the Simultaneous Adsorption of Aqueous Organic Micropollutants and Natural Organic Matter. In:

- Water Research*, 39(8), 1663–1673.
- RACYTE, J. *et al.* (2014). Alternating Electric Field Fluidized Bed Disinfection Performance with Different Types of Granular Activated Carbon. In: *Separation and Purification Technology*, 132, 70–76.
- RAHIM, A.A., GARBA, N.Z. (2016). Efficient Adsorption of 4-Chloroguaiacol from Aqueous Solution Using Optimal Activated Carbon: Equilibrium Isotherms and Kinetics Modeling. In: *Journal of the Association of Arab Universities for Basic and Applied Sciences*, 21, 17–23.
- RATTIER, M., REUNGOAT, J., GERNJAK, W., KELLER, J. (2012). *Organic Micropollutant Removal by Biological Activated Carbon Filtration: A Review*. Queensland, Australia, University of Queensland. Urban Water Security Alliance, Technical Report No. 53.
- REUNGOAT, J. *et al.* (2012). Ozonation and Biological Activated Carbon Filtration of Wastewater Treatment Plant Effluents. In: *Water Research*, 46(3), 863–872.
- REUNGOAT, J. *et al.* (2010). Removal of Micropollutants and Reduction of Biological Activity in a Full Scale Reclamation Plant Using Ozonation and Activated Carbon Filtration. In: *Water Research*, 44(2), 625–637.
- RITTMANN, B.E., MCCARTY, P.L. (2001). *Environmental Biotechnology: Principles and Applications*. McGraw-Hill Education, Columbus, USA.
- ROBERTSON, C.E. *et al.* (2013). Explicet: Graphical User Interface Software for Metadata-Driven Management, Analysis and Visualization of Microbiome Data. In: *Bioinformatics*, 29(23), 3100–3101.
- ROCHEX, A., GODON, J.-J., BERNET, N., ESCUDIE, R. (2008). Role of Shear Stress on Composition, Diversity and Dynamics of Biofilm Bacterial Communities. In: *Water Research*, 42(20), 4915–4922.
- ROMÁN, S. *et al.* (2017). Dependence of the Microporosity of Activated Carbons on the Lignocellulosic Composition of the Precursors. In: *Energies*, 10(4), 542.
- RUBIROLA, A. *et al.* (2014). Characterization of Metoprolol Biodegradation and Its Transformation Products Generated in Activated Sludge Batch Experiments and in Full Scale WWTPs. In: *Water Research*, 63, 21–32.
- RUTHVEN, D.M. (1984). *Principles of Adsorption and Adsorption Processes*. New Jersey, USA, Wiley-Interscience.
- SALVADOR, F. *et al.* (2015). Regeneration of Carbonaceous Adsorbents. Part II: Chemical, Microbiological and Vacuum Regeneration. In: *Microporous and Mesoporous Materials*, 202, 277–296.
- SHEN, L., LU, Y., LIU, Y. (2012). Mathematical Modeling of Biofilm-Covered Granular Activated Carbon: A Review. In: *Journal of Chemical Technology & Biotechnology*, 87(11), 1513–1520.
- SIMPSON, D.R. (2008). Biofilm Processes in Biologically Active Carbon Water Purification. In: *Water Research*, 42(12), 2839–2848.
- SIROTKIN, A.S., KOSHKINA, L.Y., IPPOLITOV, K.G. (2001). The BAC-Process for Treatment of Waste Water Containing Non-Ionogenic Synthetic Surfactants. In: *Water Research*, 35(13), 3265–3271.
- SKOUTERIS, G. *et al.* (2015). The Effect of Activated Carbon Addition on Membrane Bioreactor Processes for Wastewater Treatment and Reclamation – A Critical Review. In: *Bioresource Technology*, 185, 399–410.
- SODHA, K., PANCHANI, S.C., NATH, K. (2013). Feasibility Study of Microbial Regeneration of Spent Activated Carbon Sorbed with Phenol Using Mixed Bacterial Culture. In: *Indian Journal of Chemical Technology*, 20(1), 33–39.
- SONTHEIMER, H., CRITTENDEN, J.C., SCOTT SUMMERS, R. (1988). *Activated Carbon for Water Treatment*. Karlsruhe: DVGW-Forschungsstelle, Engler-Bunte-Institut, Universität Karlsruhe (TH).
- SOTELO, J.L. *et al.* (2014). Competitive Adsorption Studies of Caffeine and Diclofenac Aqueous Solutions by Activated Carbon. In: *Chemical Engineering Journal*, 240, 443–453.
- STOQUART, C., BARBEAU, B., SERVAIS, P., VAZQUEZ-RODRIGUEZ, G.A. (2014). Quantifying Bacterial Biomass Fixed onto Biological Activated Carbon (PAC and GAC) Used in Drinking Water Treatment. In: *Journal of Water Supply: Research and Technology –AQUA*, 63(1), 1–11.
- SUZUKI, M. (1990). *Adsorption Engineering*. Tokyo, Japan, Kodansha LTD.

- TAN, I.A.W., AHMAD, A.L., HAMEED, B.H. (2009). Adsorption Isotherms, Kinetics, Thermodynamics and Desorption Studies of 2,4,6-Trichlorophenol on Oil Palm Empty Fruit Bunch-Based Activated Carbon. In: *Journal of Hazardous Materials*, 164(2), 473–482.
- THOMAS, W.J., CRITTENDEN, B.D. (1998). *Adsorption Technology and Design*. Oxford, United Kingdom, Butterworth-Heinemann.
- ULLHYAN, A., GHOSH, U.K. (2012). Biodegradation of Phenol with Immobilized Pseudomonas Putida Activated Carbon Packed Bio-Filter Tower. In: *African Journal of Biotechnology*, 11(85), 15160–15167.
- VIENO, N., TUHKANEN, T., KRONBERG, L. (2007). Elimination of Pharmaceuticals in Sewage Treatment Plants in Finland. In: *Water Research*, 41(5), 1001–1012.
- VINITNANTHARAT, S., BARAL, A., ISHIBASHI, Y., HA, S.R. (2001). Quantitative Bioregeneration of Granular Activated Carbon Loaded with Phenol and 2,4-Dichlorophenol. In: *Environmental Technology*, 22(3), 339–344.
- WANG, Z.-B., MIAO, M.-S., KONG, Q., NI, S.-Q. (2016). Evaluation of Microbial Diversity of Activated Sludge in a Municipal Wastewater Treatment Plant of Northern China by High-Throughput Sequencing Technology. In: *Desalination and Water Treatment*, 57(50), 23516–23521.
- WATERZUIVERING, B. (2012). *Beheers – En Bedrijfsresultaten Zuiveringstechnische Werken*.
- WEI, X.-Y. *et al.* (2009). The Effects of LMWOAs on Biodegradation of Multi-Component PAHs in Aqueous Solution Using Dual-Wavelength Fluorimetry. In: *Environmental Pollution*, 157(11), 3150–3157.
- WEILIN, H., WEBER, W.J. JR. (1997). A Distributed Reactivity Model for Sorption by Soils and Sediments. 10. Relationships between Desorption, Hysteresis, and the Chemical Characteristics of Organic Domains. In: *Environmental Science and Technology*, 31(9), 2562–2569.
- WORCH, E. (2008). Fixed-Bed Adsorption in Drinking Water Treatment: A Critical Review on Models and Parameter Estimation. In: *Journal of Water Supply: Research and Technology – Aqua*, 57(3), 171–183.
- WORSCH, E. (2012). *Adsorption Technology in Water Treatment: Fundamentals, Processes, and Modeling*. Berlin, Boston: De Gruyter.
- WU, F.-C., TSENG, R.L., JUANG, R.S. (2005). Comparisons of Porous and Adsorption Properties of Carbons Activated by Steam and KOH. In: *Journal of Colloid and Interface Science*, 283(1), 49–56.
- XIAOJIAN, Z., ZHANSHENG, W., XIASHENG, G. (1991). Simple Combination of Biodegradation and Carbon Adsorption – the Mechanism of the Biological Activated Carbon Process. In: *Water Research*, 25(2), 165–172.
- XIE, S., LIU, J., LI, L., QIAO, C. (2009). Biodegradation of Malathion by Acinetobacter Johnsonii MA19 and Optimization of Cometabolism Substrates. In: *Journal of Environmental Sciences*, 21(1), 76–82.
- YAN, D., GANG, D.D., ZHANG, N., LIN, L.S. (2013). Adsorptive Selenite Removal Using Iron-Coated GAC: Modeling Selenite Breakthrough with the Pore Surface Diffusion Model. In: *Journal of Environmental Engineering*, 139(2), 213–219.
- YING, C.P. (2015). *Bioregeneration of Granular Activated Carbon Loaded with Phenol and P-Nitrophenol: Effects of Physico-Chemical and Biological Factors*. University of Malaysia, Thesis for the degree of Doctor of Philosophy
- YONGE, D.R., KEINATH, T.M., POZNANSKA, K., JIANG, Z.P. (1985). Single-Solute Irreversible Adsorption on Granular Activated Carbon. In: *Environmental Science & Technology*, 19(8), 690–694.
- Zhang, H., Wang, S. (2017). Modeling Bisolute Adsorption of Aromatic Compounds Based on Adsorbed Solution Theories. In: *Environmental Science & Technology*, 51(10), 5552–5562.
- ZHANG, J., HE, M. (2013). Effect of Dissolved Organic Matter on Sorption and Desorption of Phenanthrene onto Black Carbon. In: *Journal of Environmental Sciences*, 25(12), 2378–2383.
- ZHAO, Q. *et al.* (2015). Adsorption and Bioregeneration in the Treatment of Phenol, Indole, and Mixture with Activated Carbon. In: *Desalination and Water Treatment*, 55(7), 1876–1884.

Publications

Publications in International Peer-Reviewed Scientific Journals

1. **ABROMAITIS, V.**, RACYS, V., VAN DER MAREL, P., NI, G., DOPSON, M., WOLTHUIZEN, A.L., MEULEPAS, R.J.W. (2017). Effect of Shear Stress and Carbon Surface Roughness on Bioregeneration and Performance of Suspended Versus Attached Biomass in Metoprolol-Loaded Biological Activated Carbon Systems. In: *Chemical Engineering Journal*, 317, pp. 503–511.
2. **ABROMAITIS, V.**, RACYS, V., VAN DER MAREL, P., MEULEPAS, R.J.W. (2016). Biodegradation of Persistent Organics Can Overcome Adsorption-Desorption Hysteresis in Biological Activated Carbon Systems. In: *Chemosphere*, 149, pp. 183–189.

Poster Presentations

1. RUMSKAITĖ, I., **ABROMAITIS, V.** (2014). *Adsorption of Target Organic Compounds on Activated Carbon*. March 19–21, 2014. 57th Scientific Conference for Students of Physics and Natural Sciences, Vilnius, Lithuania: Vilnius University. ISSN 2029-4425, p. 191.
2. **ABROMAITIS, V.** (2013). *Modification of Experimental Set-Up Designed for the Treatment of BTEX Polluted Wastewater with Biological Activated Carbon (BAC) System*. October 2–4, 2013. 3rd IWA BeNeLux Young Water Professional Regional Conference, Belval, Luxemburg p. 1–2.

Oral Presentations

1. **ABROMAITIS, V.**, RACYS, V., MEULEPAS, R. (2016). *Biological Activated Carbon: Effective Technology to Remove Slowly Biodegradable Micropollutants from Wastewater*. Water, Waste and Energy Management: 3rd International Congress, ScienceKNOW Conferences, ISBN 9788494431159. pp. 1–4.
2. **ABROMAITIS, V.**, MEULEPAS, R., RACYS, V. (2014). *The Effect of Easy Biodegradable Organic Carbon for Metoprolol Biodegradation*. April 25, 2014. Chemistry and Chemical Technology: Proceedings of the International Conference. Kaunas, Lithuania. Kaunas University of Technology. Kaunas: Technologija, ISSN 2351-5643, pp. 10–13.
3. RACYS, V., **ABROMAITIS, V.**, MEULEPAS, R. (2013). *Set-Up for Process Development of Biological Activated Carbon*. April 25, 2013. Conference “Chemija ir cheminė technologija”. Kaunas, Lithuania, pp. 6–10.
4. **ABROMAITIS, V.**, RAČYS, V., MEULEPAS, R. *Fundamentals and Application of Biological Activated Carbon*. November 17, 2015. “Internal Wetsus Congress”. Leeuwarden, the Netherlands.

Publications not Related to the Topic of the Doctoral Thesis

1. STASIULAITIENĖ, I., MARTUZEVIČIUS, D., ABROMAITIS, V., TICHONOVAS, M., BALTRUŠAITIS, J., BRANDENBURG, R., PAWELEC, A., SCHWOCK, A. (2016). Comparative Life Cycle Assessment of Plasma-Based and Traditional Exhaust Gas Treatment Technologies. In: *Journal of Cleaner Production*, 2016, 112, pp. 1804–1812.

Courses Attended by the Author of the Thesis

1. *Advanced Course on Environmental Biotechnology*. July 1–11, 2014. Delft University of Technology, the Netherlands (3 ECTS).
2. *Techniques for Writing and Presenting a Scientific Paper*. February 11–14, 2014. Wageningen University, the Netherlands (1.2 ECTS).
3. *Training Presentation Skills*. November 15, 2013. Wetsus – European centre of Excellence for Sustainable Water Technology, the Netherlands.

SL344. 2017–12–12, 14,25 leidyb. apsk. 1. Tiražas 212 egz. Užsakymas 382.
Išleido Kauno technologijos universitetas, K. Donelaičio g. 73, 44249 Kaunas
Spausdino leidyklos „Technologija“ spaustuvė, Studentų g. 54, 51424 Kaunas

Appendices

Appendix 1. Impeller tip speed and velocity gradient calculation

The mixing intensity inside the reactors was calculated as velocity gradient G (s^{-1}) (J. C. Crittenden and Harza M. W. 2012):

$$G = \left(\frac{P}{V \cdot \mu} \right)^{1/2} \quad (A1.1)$$

where: P denotes the power applied for stirring, $kg \cdot m^2/s^2$;
 V stands for the liquid volume in the mixing tank, m^3 ;
 μ is the liquid dynamic viscosity, $N \cdot s/m^2$.

The power applied for stirring when the mixing is turbulent ($Re > 10000$) can be calculated by employing the equation below:

$$P = N_p \cdot \rho \cdot n^3 \cdot d^5 \quad (A1.2)$$

where: N_p is the power number of the impeller (depends on the impeller type; $N_p=1.8$ was chosen from a manual for the flat blade impeller when $Re > 10000$) (Pietranski 2012).

ρ denotes the liquid density, kg/m^3 ;
 n is the impeller speed, revolutions per second (rps);
 d stands for the impeller diameter, m.

Having obtained the velocity gradient, the impeller tip speed was calculated:

$$v = \pi \cdot D \cdot N \quad (A1.3)$$

where: D is the impeller diameter, m;
 N denotes the impeller speed, rpm.

The velocity gradient and impeller tip speed values were calculated in low and high shear reactors:

Table A1.1. Velocity gradient and impeller tip speed values

	Velocity gradient G , s^{-1}	Impeller tip speed v , m/s
Low shear reactors	8.8	0.52
High shear reactors	25	1.03

Appendix 2. Specifications of virgin Norit carbon (standard deviation)

Granular size (mm)	BET Surface area (m^2/g)	Micropore area (m^2/g)	External surface area (m^2/g)	Pore volume, cm^3/g		Sample size, N
				Micropores	Meso & Macropores	
0.3–0.8	986 (4)	863 (3)	45 (1)	0.36 (0.01)	0.14 (0.02)	3

Appendix 3. COD consumption, O₂ consumption, CO₂ production and the total available O₂ during triplicate metoprolol biodegradation experiments with and without acetate (standard deviation)

	Start of experiment COD, mg/L	End of experiment COD, mg/L	O ₂ consumption per litre of suspension, mg/L	CO ₂ production per litre of suspension, mg/L	Available O ₂ per litre of suspension, mg/L
Metoprolol biodegradation without acetate	17.8 (3)	27.1 (0.3)	100 (4)	0	1270 (32)
Metoprolol biodegradation when acetate was added at day 0	986 (13)	33.1 (2)	2070 (70)	990 (80)	3560 (84)
Metoprolol biodegradation when metoprolol was added at day 7 after acetate depletion	968 (5)	37.9 (0.4)	1910 (40)	890 (40)	3410 (124)

Appendix 4. Physical properties of spherical Mast AC granules, standard Mast AC granules and carbonized Mast granules

Carbon	BET, m ² /g	Micropore volume, cm ³ /g	Mesopore volume, cm ³ /g	Micropore area, m ² /g	Mesopore area, m ² /g	Average pore diameter, nm
S0.25+	782	0.26	0.37	730	47	15.8
S0.25++	1250	0.45	0.45	1161	59	13.6
S0.25+++	1832	0.67	0.64	1469	103	11.4
S0.5+	823	0.29	0.40	839	51	15.6
S0.5++	1295	0.47	0.60	1177	72	15.5
S0.5+++	1833	0.66	0.70	1485	98	12.6
S1+	867	0.31	0.38	849	48	15.2
S1++	1181	0.43	0.49	1149	60	15.0
S1+++	1619	0.59	0.67	1411	89	13.7
0.25C-1	600	0.21	0.71	569	82	21.3
0.25C	650	0.23	0.36	656	50	14.5
0.25A-1	1319	0.49	0.99	1222	115	19.0
0.25A	1286	0.50	0.36	1295	66	17.5

Appendix 5. Physical properties of Norit AC granules

Carbon	BET, m ² /g	Micropore volume, cm ³ /g	Mesopore volume, cm ³ /g	Micropore area, m ² /g	Mesopore area, m ² /g	Average pore diameter, nm
N1	1112	0.42	0.01	1090	3	2.7
N1+	1097	0.42	0.01	1068	5	2.9
N2	897	0.34	0.07	842	28	4.1
N2+	986	0.36	0.14	863	45	5.1
N3	1475	0.47	0.61	894	234	4.6
N4	782	0.28	0.20	707	74	4.9
N5	584	0.19	0.32	452	92	6.9

Appendix 6. Langmuir constants obtained from metoprolol adsorption equilibrium experiments with spherical Mast AC granules, standard Mast AC granules and carbonized Mast granules

Carbon	Q _{exp.} (mg/g)	Q _m (mg/g)	K _L (L/mg)	R _L	R ²
S0.25+	155	172	0.2	0.03÷0.47	0.98
S0.25++	283	284	0.6	0.01÷0.40	0.99
S0.25+++	310	307	6.3	0.01÷0.13	1.00
S0.5+	202	214	0.2	0.02÷0.46	0.98
S0.5++	286	286	0.8	0.01÷0.37	1.00
S0.5+++	311	310	1.9	0.01÷0.27	1.00
S1+	195	185	1.5	0.01÷0.30	1.00
S1++	244	241	7.0	0.01÷0.12	1.00
S1+++	295	297	1.5	0.01÷0.30	1.00
0.25C-1	95	99	0.3	0.02÷0.42	0.97
0.25C	107	103	3.6	0.01÷0.15	1.00
0.25A-1	273	270	1.7	0.01÷0.23	1.00
0.25A	310	291	19	0.01÷0.04	1.00

Appendix 7. Langmuir constants obtained from metoprolol adsorption equilibrium experiments with Norit AC granules

Carbon	Q _{exp.} (mg/g)	Q _m (mg/g)	K _L (L/mg)	R _L	R ²
N1	222	243	0.3	0.01÷0.44	0.98
N1+	211	212	0.9	0.01÷0.36	0.99
N2	192	192	1.9	0.01÷0.23	0.99
N2+	204	202	1.1	0.01÷0.34	1.00
N3	199	211	0.4	0.01÷0.42	1.00
N4	172	169	5.7	0.01÷0.14	0.99
N5	121	124	1.3	0.01÷0.27	1.00

Appendix 8. Langmuir constants obtained from desorption equilibrium experiments with loaded spherical Mast AC granules, standard Mast AC granules, carbonized Mast granules and Norit AC granules

Carbon	Q _m (mg/g)	K _L (L/mg)	R ²	Carbon	Q _m (mg/g)	K _L (L/mg)	R ²
S0.25+	164	3.8	0.96	0.25C	99	44	1.00
S0.25++	253	13	0.99	0.25A-1	236	12	1.00
S0.25+++	288	27	1.00	0.25A	270	62	1.00
S0.5+	193	7.2	0.97	N1	229	3.9	0.98
S0.5++	260	11	1.00	N1+	203	6.4	0.99
S0.5+++	283	6.3	1.00	N2	171	27	0.98
S1+	161	17	0.99	N2+	182	13	1.00
S1++	223	9.6	1.00	N3	183	5.4	0.99
S1+++	271	12	1.00	N4	152	18	0.99
0.25C-1	83	18	0.96	N5	107	19	1.00

Appendix 9. Pseudo first order kinetic rates obtained from metoprolol adsorption kinetic experiments with spherical Mast AC granules, standard Mast AC granules, carbonized Mast granules and Norit AC granules

Carbon	k ₁ (g/mg h) × 10 ⁻²	q _e (mg/g)	R ²	Carbon	k ₁ (g/mg h) × 10 ⁻²	q _e (mg/g)	R ²
S0.25+	0.6	42	0.51	0.25C	1.4	83	0.76
S0.25++	0.9	105	0.88	0.25A-1	1.5	109	0.94
S0.25+++	1.0	34	0.63	0.25A	1.7	72	0.87
S0.5+	0.5	86	0.73	N1	0.8	123	0.97
S0.5++	0.8	151	0.96	N1+	0.8	118	0.97
S0.5+++	0.9	69	0.88	N2	0.9	148	0.98
S1+	0.4	151	0.96	N2+	1.3	107	0.97
S1++	0.7	132	0.96	N3	1.2	78	0.91
S1+++	0.8	98	0.92	N4	1.9	76	0.94
0.25C-1	0.7	94	0.73	N5	1.1	82	0.90

Appendix 10. Pseudo second order kinetic rates, obtained from metoprolol adsorption kinetic experiments with spherical Mast AC granules, standard Mast AC granules and carbonized Mast granules

Carbon	$q_{exp.}$ (mg/g)	k_2 (g/mg h) $\times 10^{-3}$	q_e (mg/g)	R^2
S0.25+	107	0.68	106	0.99
S0.25++	210	0.26	216	1.00
S0.25+++	214	1.58	215	1.00
S0.5+	168	0.8	168	1.00
S0.5++	208	0.10	223	1.00
S0.5+++	227	0.56	229	1.00
S1+	183	0.25	186	1.00
S1++	220	0.13	230	1.00
S1+++	226	0.27	232	1.00
0.25C-1	102	0.49	96	0.98
0.25C	111	0.45	108	0.99
0.25A-1	218	0.58	221	1.00
0.25A	228	1.16	229	1.00

Appendix 11. Pseudo second order kinetic rates obtained from metoprolol adsorption kinetic experiments with Norit AC granules

Carbon	$q_{exp.}$ (mg/g)	k_2 (g/mg h) $\times 10^{-3}$	q_e (mg/g)	R^2
N1	159	0.19	163	0.99
N1+	161	0.22	164	0.99
N2	182	0.16	189	1.00
N2+	175	0.45	179	1.00
N3	160	0.69	162	1.00
N4	146	0.96	148	1.00
N5	126	0.43	125	1.00

Appendix 12. Intraparticle diffusion constants obtained from metoprolol adsorption kinetic experiments with spherical Mast AC granules, standard Mast AC granules and carbonized Mast granules

Carbon	k_{d1} (g/mg h ^{1/2}) $\times 10^{-2}$	L_{d1}	k_{d2} (g/mg h ^{1/2}) $\times 10^{-2}$	L_{d2}	k_{d3} (g/mg h ^{1/2}) $\times 10^{-2}$	L_{d3}
S0.25+	19	1.2	2.3	60.0	1.4	73
S0.25++	29	0.4	5.1	128	1.0	186
S0.25+++	67	0.8	4.0	170	0.1	212
S0.5+	21	0.3	4.5	87	1.1	137
S0.5++	19	1.6	10.4	47	3.3	133
S0.5+++	38	1.0	2.6	186	1.0	203
S1+	21	0.9	9.6	45	1.2	152
S1++	25	1.9	6.0	102	0.8	198
S1+++	29	1.2	9.6	93	0.9	205
0.25C-1	19	1.6	1.7	58	2.0	53
0.25C	19	4.1	4.4	47	2.1	62
0.25A-1	42	4.7	10.1	112	0.6	204
0.25A	62	6.8	6.4	164	0.2	224

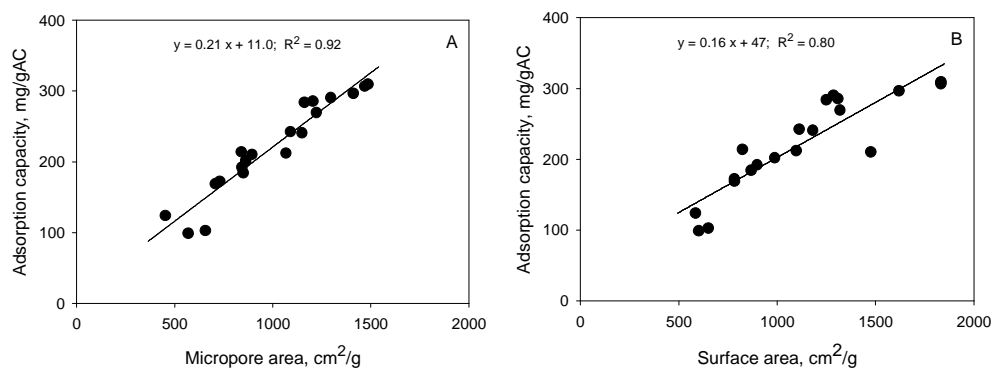
Appendix 13. Intraparticle diffusion constants obtained from metoprolol adsorption kinetic experiments with Norit AC granules

Carbon	$k_{d1} \text{ (g/mg h}^{1/2}) \times 10^{-2}$	L_{d1}	$k_{d2} \text{ (g/mg h}^{1/2}) \times 10^{-2}$	L_{d2}	$k_{d3} \text{ (g/mg h}^{1/2}) \times 10^{-2}$	L_{d3}
N1	16	0.9	9.8	19	4.1	72
N1+	18	1.5	8.6	33	3.0	95
N2	24	2.8	9.5	38	3.3	109
N2+	28	2.4	15	32	1.9	137
N3	30	1.1	13.2	49	1.5	130
N4	29	1.5	9.0	67	0.9	129

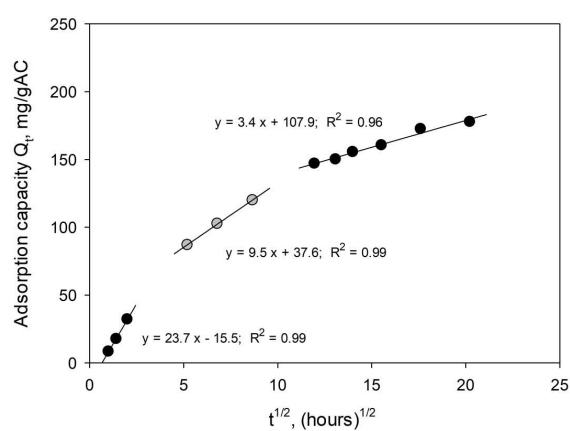
Appendix 14. Metoprolol adsorption and desorption isotherm models used to calculate hysteresis indexes (HI) for spherical Mast AC granules, standard Mast AC granules, carbonized Mast granules and Norit AC granules. Isotherms were modelled by using natural logarithm equations

Carbon	Adsorption	Desorption
S0.25+	$q_e = 13.1 \ln c_e + 85$	$q_e = 12.4 \ln c_e + 123$
S0.25++	$q_e = 22.1 \ln c_e + 172$	$q_e = 21.0 \ln c_e + 209$
S0.25+++	$q_e = 26.4 \ln c_e + 207$	$q_e = 22.9 \ln c_e + 237$
S0.5+	$q_e = 16.5 \ln c_e + 118$	$q_e = 15.5 \ln c_e + 158$
S0.5++	$q_e = 21.3 \ln c_e + 180$	$q_e = 21.4 \ln c_e + 216$
S0.5+++	$q_e = 23.1 \ln c_e + 199$	$q_e = 24.4 \ln c_e + 212$
S1+	$q_e = 16.1 \ln c_e + 114$	$q_e = 19.2 \ln c_e + 127$
S1++	$q_e = 17.0 \ln c_e + 159$	$q_e = 20.9 \ln c_e + 173$
S1+++	$q_e = 20.9 \ln c_e + 195$	$q_e = 23.9 \ln c_e + 216$
0.25C-1	$q_e = 6.3 \ln c_e + 61$	$q_e = 8.3 \ln c_e + 71$
0.25C	$q_e = 6.8 \ln c_e + 72$	$q_e = 10.4 \ln c_e + 88$
0.25A-1	$q_e = 18.8 \ln c_e + 179$	$q_e = 21.6 \ln c_e + 185$
0.25A	$q_e = 20.8 \ln c_e + 208$	$q_e = 25.1 \ln c_e + 231$
N1	$q_e = 18.5 \ln c_e + 129$	$q_e = 19.8 \ln c_e + 168$
N1+	$q_e = 17.4 \ln c_e + 123$	$q_e = 20.2 \ln c_e + 156$
N2	$q_e = 13.2 \ln c_e + 126$	$q_e = 17.9 \ln c_e + 138$
N2+	$q_e = 16.9 \ln c_e + 120$	$q_e = 16.7 \ln c_e + 146$
N3	$q_e = 17.1 \ln c_e + 113$	$q_e = 17.7 \ln c_e + 135$
N4	$q_e = 13.7 \ln c_e + 101$	$q_e = 14.1 \ln c_e + 122$
N5	$q_e = 8.7 \ln c_e + 75$	$q_e = 9.5 \ln c_e + 83$

Appendix 15. Relationships between adsorption capacity versus micropore surface area (A) and total surface area (B) obtained from metoprolol adsorption equilibrium experiments with spherical Mast AC granules, standard Mast AC granules, carbonized Mast granules and Norit AC granules



Appendix 16. Intraparticle diffusion model graph for spherical Mast AC granules



Appendix 17. Estimated metoprolol adsorption and biodegradation rates obtained immediately after a peak load for BAC reactor at shear stress of $G=8.8 \text{ s}^{-1}$ with smooth ($R_a=1.6 \text{ }\mu\text{m}$) Mast AC granules (R1), the BAC reactor at shear stress of $G=8.8 \text{ s}^{-1}$ with rough ($R_a=13 \text{ }\mu\text{m}$) Norit AC granules (R2), and BAC reactor at shear stress of $G=25 \text{ s}^{-1}$ with rough ($R_a=13 \text{ }\mu\text{m}$) Norit AC granules (R3)

Reactor	Biomass conc., $\text{mg}_{\text{total-N}}/\text{L}$	Volumetric adsorption rate, $\text{mg}/(\text{L}\cdot\text{h})$	Volumetric biodegradation rate, $\text{mg}/(\text{L}\cdot\text{h})$	Specific adsorption rate, $\mu\text{g}/(\text{mg}_{\text{total-N}}\cdot\text{h})$	Specific biodegradation rate, $\mu\text{g}/(\text{mg}_{\text{total-N}}\cdot\text{h})$	Metoprolol load during the prior reactor run, $\text{mg}_{\text{MET}}/\text{mg}_{\text{total-N}}$
R1	61	5.3	2.2	86	36	1.5
R2	76	4.9	2.2	64	29	1.2
R3	40	4.1	1.9	103	48	2.2

Appendix 18. Metoprolol biodegradation rates of the biomass separated from the AC granules from BAC reactor at shear stress of $G=8.8 \text{ s}^{-1}$ and with smooth ($R_a=1.6 \text{ }\mu\text{m}$) Mast AC granules (R1), BAC reactor at shear stress of $G=8.8 \text{ s}^{-1}$ and with rough ($R_a=13 \text{ }\mu\text{m}$) Norit AC granules (R2), and BAC reactor at shear stress of $G=25 \text{ s}^{-1}$ and with rough ($R_a=13 \text{ }\mu\text{m}$) Norit AC granules (R3)

Reactor	Biomass concentration, $\text{mg}_{\text{total-N}}/\text{L}$	Volumetric rate, $\text{mg}/(\text{L}\cdot\text{h})$	Specific biodegradation rate, $\mu\text{g}/(\text{mg}_{\text{total-N}}\cdot\text{h})$	Metoprolol load during the prior reactor run, $\text{mg}_{\text{MET}}/\text{mg}_{\text{total-N}}$
R1	30	0.99	32	3.1
R2	41	0.95	23	2.1
R3	16	1.53	97	5.9